Pairing Matrix Elements and Pairing Gaps with Bare, Effective and Induced Interactions

F. Barranco

Sevilla University

R.A. Broglia

Milano University and The Niels Bohr Institute, Copenhagen

E. Vigezzi

INFN Milano

A. Idini

Surrey Univ.

Xavier Viñas celebration 2017 workshop at Milano
"Nuclear Structure and Astrophysical Applications"

Milano (during the last 20 years)

R.A. Broglia, P.F.Bortignon, G.L. Coló, E. Vigezzi,

J.Terasaki, G. Gori, N. Giovanardi
L. Viverit, A.Pastore, ,S. Baroni, F. Raimondi
P. Avogadro, A. Idini, G.Potel

"External" collaborations with

H. Esbensen, P.Schuck, X. Viñas

OUTLINE

-Introduction

- Putting together the Bare Pairing Interaction and
  The Interaction Induced from the Exchange of Surface Modes

V_{bare}, V_{ind}

- Including Exchange of (volume) Spin Modes,
  Application to the proton-neutron (T=0) pairing.

-Including Fragmentation

-Evidences from data

.

Commonly used mean-field approach:
HFB theory with Gogny force

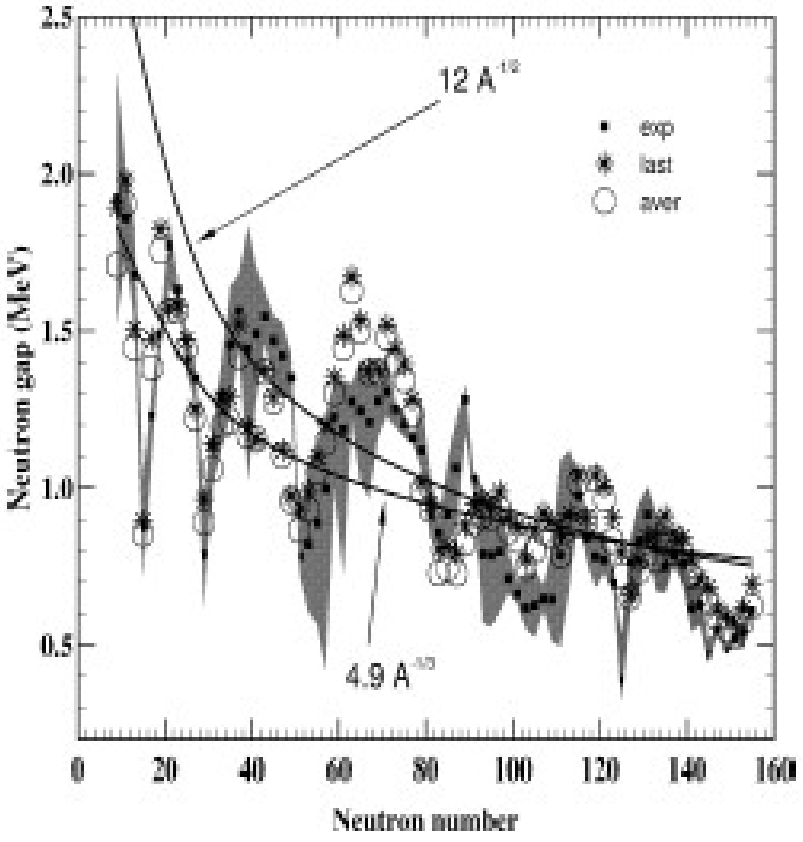

Overall agreement with
'experimental' $^1S_0$ pairing gaps, but
many open questions remain.
Among them:
connection with the bare force
many-body effects
detailed isotopic dependence
spectroscopic factors

Hilaire et al., Phys. Lett B 531(2002)61

Contact interaction

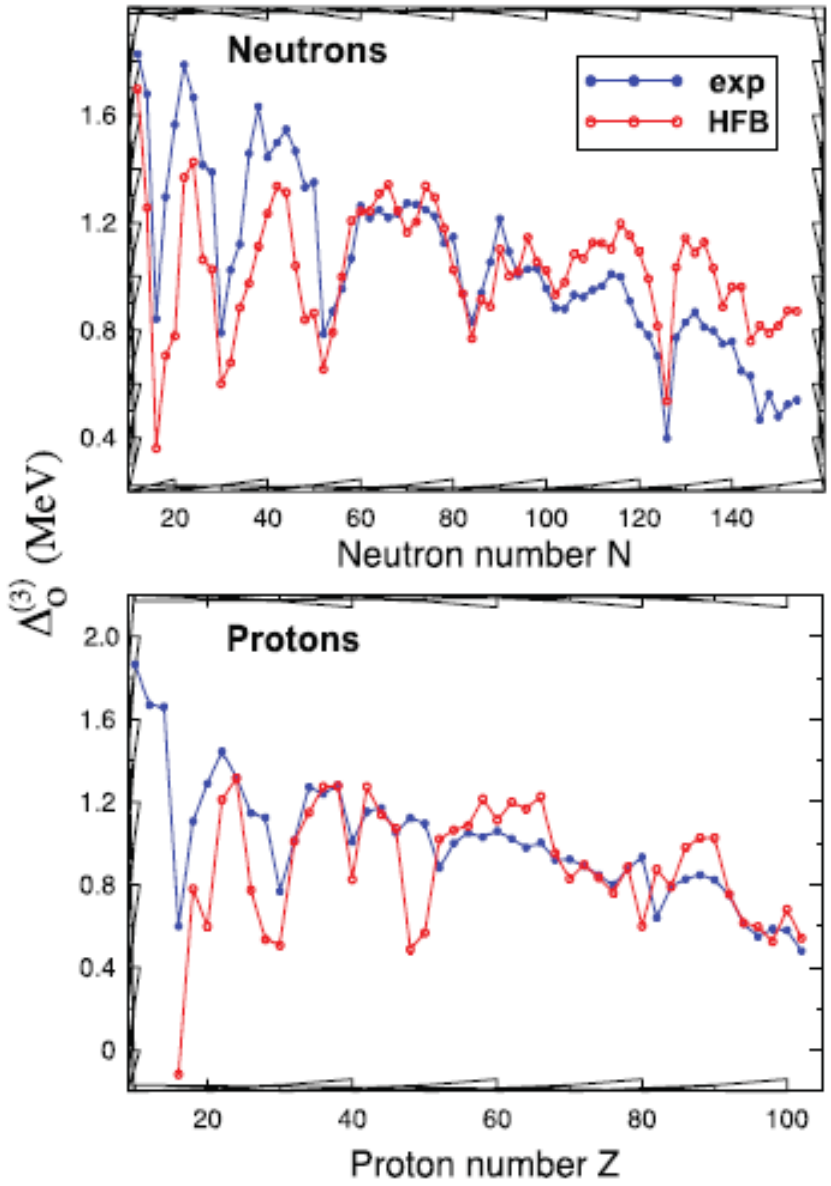

Survey of OES: G.F. Bertsch et al. Phys. Rev. C 79, 034306 (2009)

$$V(r-r') = V_c(1-\eta^*\rho(r)/\rho_0)\,\delta^3(r-r')$$

η=0; 0.5 and 1.0 (vol.; mix.; surf.)

(Ecut=60MeV);

TABLE IV: RMS residuals of $\Delta_o^{(3)}$ obtained in various models. All energies are in MeV. The last column shows the ratio of proton and neutron effective pairing strengths obtained through the optimization procedure. The mass predictions of the HFB-14 model [16] were taken from [51].

Theory	pairing	residual neutrons	residual protons	$V_0^{\rm eff}(p)/V_0^{\rm eff}(n)$
Constant		0.31	0.27	
c/A^α		0.24	0.22	
HF+BCS	volume	0.31	0.38	1.05
HF+BCS	mixed	0.30	0.36	1.08
HF+BCS	surface	0.27	0.35	1.12
HFB	mixed	0.27	0.32	1.11
HFB+LN	mixed	0.23	0.28	1.11
HFB-14		0.46	0.44	1.10

Various effective forces in the pairing channel have been proposed, with different features (finite/zero range, density dependence...)
Unfortunately it is difficult to to discriminate among them comparing with available data.

We want to follow a different strategy:

Start from an Hartree-Fock calculation with a 'reasonable' interaction. Then solve the pairing problem with a bare interaction in the $^1S_0$ channel. And finally add correlations beyond mean field.
We know that these correlations strongly renormalize the density of single-particle levels (effective mass) and their occupation factors (fragmentation), and we expect that they can have a large effect on pairing properties.

Putting together bare and Induced Interaction

PHYSICAL REVIEW C **72**, 054314 (2005)

Pairing matrix elements and pairing gaps with bare, effective, and induced interactions

F. Barranco,[1] P. F. Bortignon,[2,3] R. A. Broglia,[2,3,4] G. Colò,[2,3] P. Schuck,[5] E. Vigezzi,[3] and X. Viñas[6]

[1]*Departamento de Fisica Aplicada III, Escuela Superior de Ingenieros, Universidad de Sevilla, Camino de los Descubrimientos s/n, E-41092 Sevilla, Spain*

[2]*Dipartimento di Fisica, Università degli Studi, via Celoria 16, I-20133 Milano, Italy*

[3]*INFN Sezione di Milano, via Celoria 16, I-20133 Milano, Italy*

[4]*The Niels Bohr Institute, University of Copenhagen, Blegdamsvej 17, DK-20100 Copenhagen Ø, Denmark*

[5]*Institut de Physique Nucléaire, 15 rue Georges Clémenceau, F-91406 Orsay Cedex, France*

[6]*Departament d'Estructura i Constituents de la Matèria, Facultat de Fìsica, Universitat de Barcelona, Diagonal 647, E-08028 Barcelona, Spain*

(Received 24 February 2005; published 21 November 2005)

Bare Pairing interaction: V-14 Argonne $^1S_0$

$$\begin{pmatrix} \epsilon - \epsilon_F & \Delta \\ -\Delta & -(\epsilon - \epsilon_F) \end{pmatrix} \begin{pmatrix} U^i \\ V^i \end{pmatrix} = E_i \begin{pmatrix} U^i \\ V^i \end{pmatrix}, \qquad (1)$$

$$\Delta_{a_1 a_2} = -\tfrac{1}{2} \sum_{b_1 b_2} \sum_i U^i_{b_1} V^i_{b_2} \langle a_1 \tilde{a}_2 | v(12) | b_1 \tilde{b}_2 \rangle. \qquad (2)$$

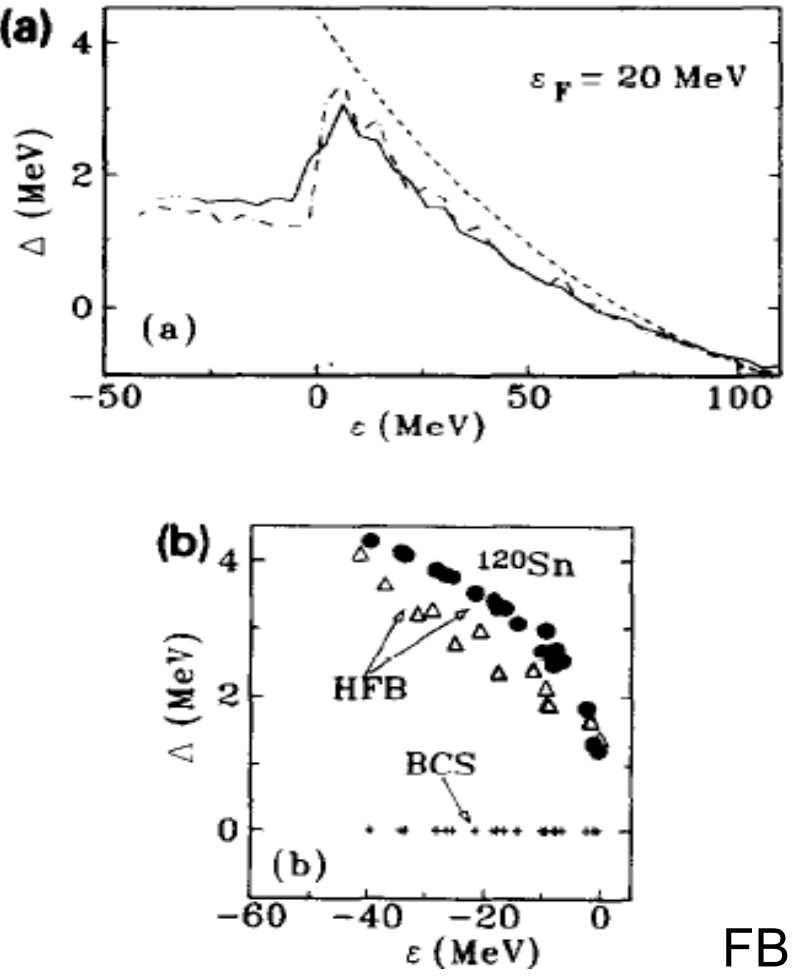

Fig. 1. (a) The pairing gaps obtained in a Wigner-Seitz cell of radius equal to 15 fm, and ϵ_F = 20 MeV, containing the nucleus Sn whose bound states are described in terms of a Woods-Saxon potential with a radius of 6.26 fm and a depth of 45.5 MeV, are shown by a solid and dash-dotted curve, respectively for a diffusivity a = 0.67 fm and a = 0 fm. The gaps obtained for the discrete states have been averaged over 4 MeV. The gaps obtained for uniform neutron matter are shown by the dashed line. (b) The pairing gaps obtained for the bound states in the potential used already in connection with Fig. (a) with the diffusivities a = 0.67 fm and 0 fm are shown by filled circles and by open triangles respectively. The Fermi energy has been set at the values ϵ_F = −7.2 MeV (for a= 0.67 fm) and ϵ_F = −10.5 MeV (for a= 0 fm), appropriate for the nucleus ^{120}Sn. Also shown is the BCS result (small crosses).

FB,Vigezzi,Broglia, Esbensen PLB 390(1997)13

$$\Delta_k = -\frac{1}{2\pi^2}\int_0^\infty dk' k'^2 V_{kk'} \frac{\Delta_{k'}}{2E_{k'}} \longrightarrow = U_k V_k$$

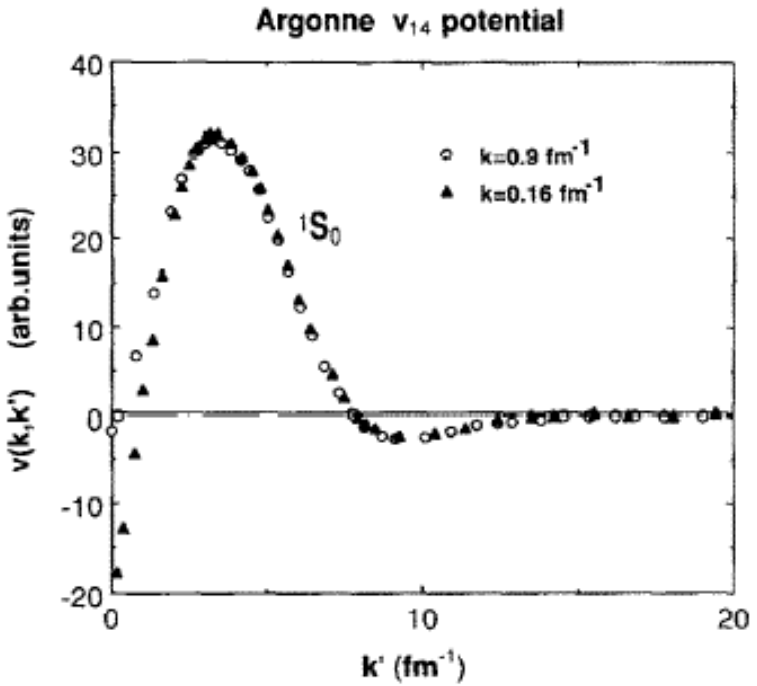

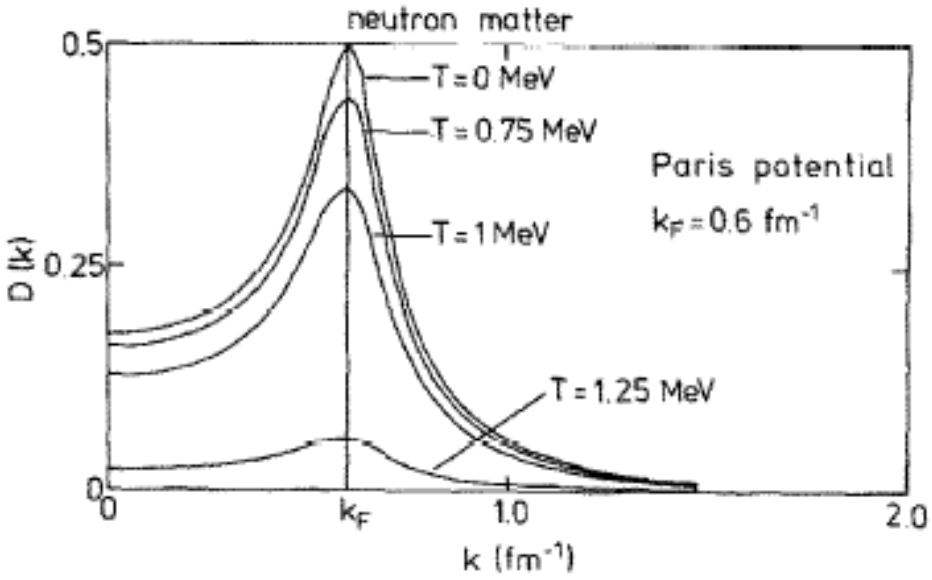

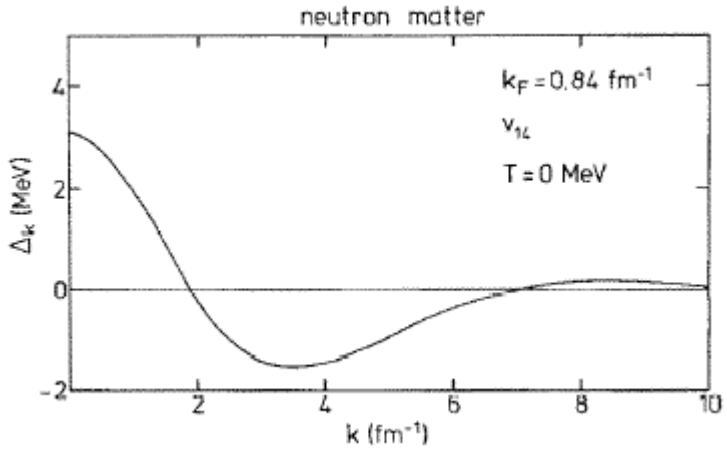

M .Baldo, J. Cugnon,
A. Lejeune, U. Lombardo,
NPA 515(1990) 409

Effective forces: $V_{low\text{-}k}$ vs. Gogny

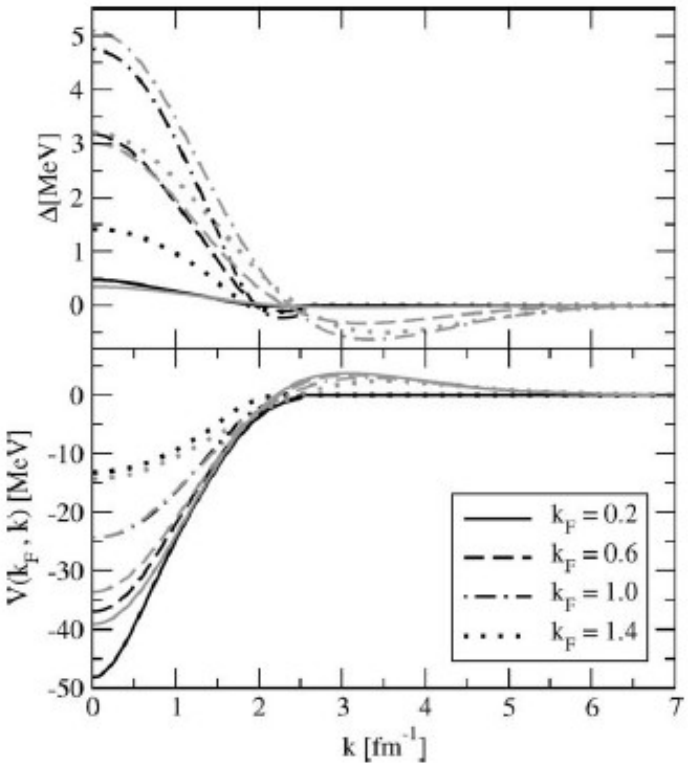

Fig. 1. The pairing gaps in the $^1S_0$ channel and the corresponding pairing potentials $V(k_F, k)$ as functions of the momentum k for several fixed Fermi-momenta k_F. The black and grey lines refer to the $V_{low\text{-}k}$ and the Gogny interaction, respectively. The solid, dashed, dashed-dotted and dotted lines correspond to the values of k_F equal 0.2, 0.6, 1.0 and 1.4 fm^{-1}.

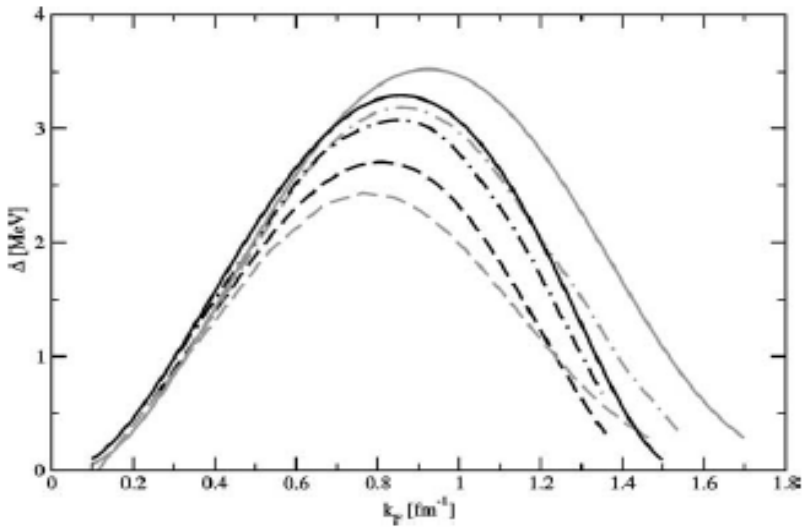

Fig. 2. The pairing gaps in the $^1S_0$ channel as functions of Fermi-momentum (density) of the matter for two effective interactions. The heavy and light lines refer to the $V_{low\text{-}k}$ and the Gogny interaction, respectively. The solid lines correspond to the non-interacting single-particle spectrum, the dashed and dashed-dotted lines—to renormalized single particle spectrum in symmetric nuclear matter and neutron matter, respectively. The single particle spectra are computed in the Hartree–Fock theory for the Gogny interaction and the Brueckner–Hartree–Fock theory for the $V_{low\text{-}k}$ interaction.

A. Sedrakian, T.T.S. Kuo, H. Muther, P. Schuck, Phys. Lett. B576(2003)68

Induced Pairing Interaction

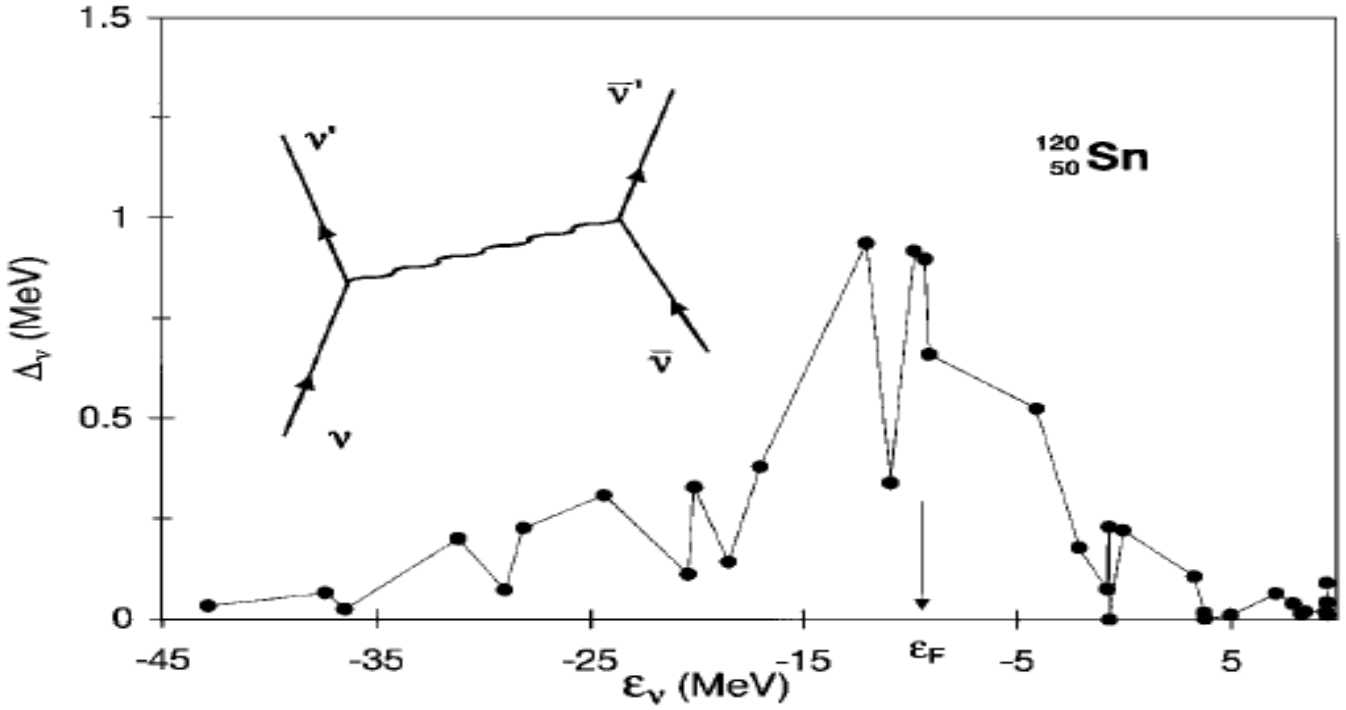

FIG. 1. State dependent pairing gap Δ_ν [cf. Eq. (3)] for the nucleus ^{120}Sn, calculated making use of the induced interaction defined in Eq. (2) (cf. inset, where particles are represented by arrowed lines and phonons by a wavy line).

PRL83(1999)2147

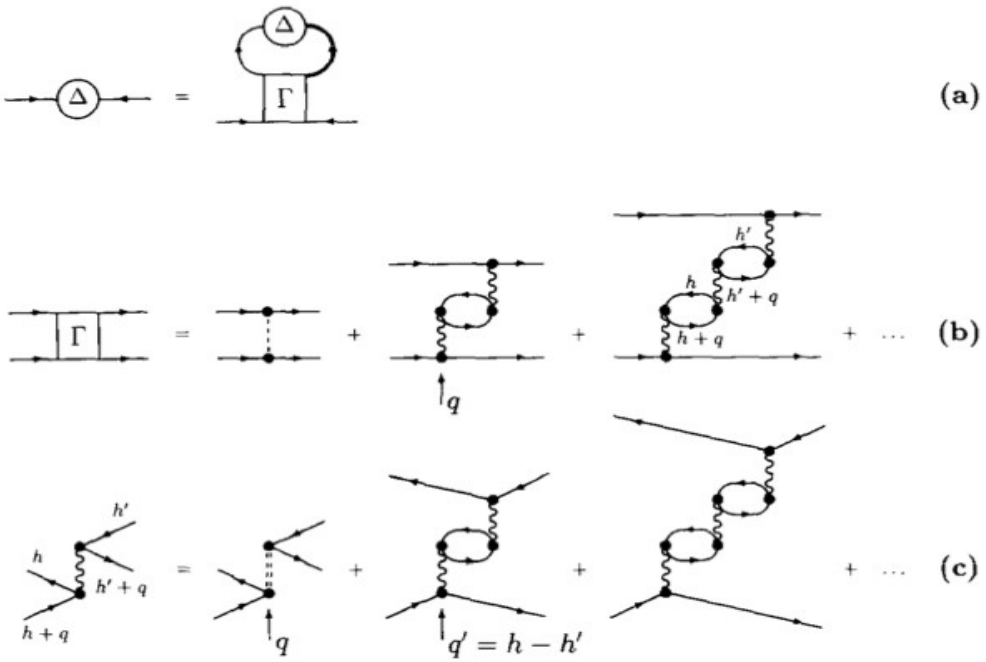

H.J. Schulze et al., Phys. Lett. 375B (1996) 1

In the box: finite nucleus, neutron star, infinite matter

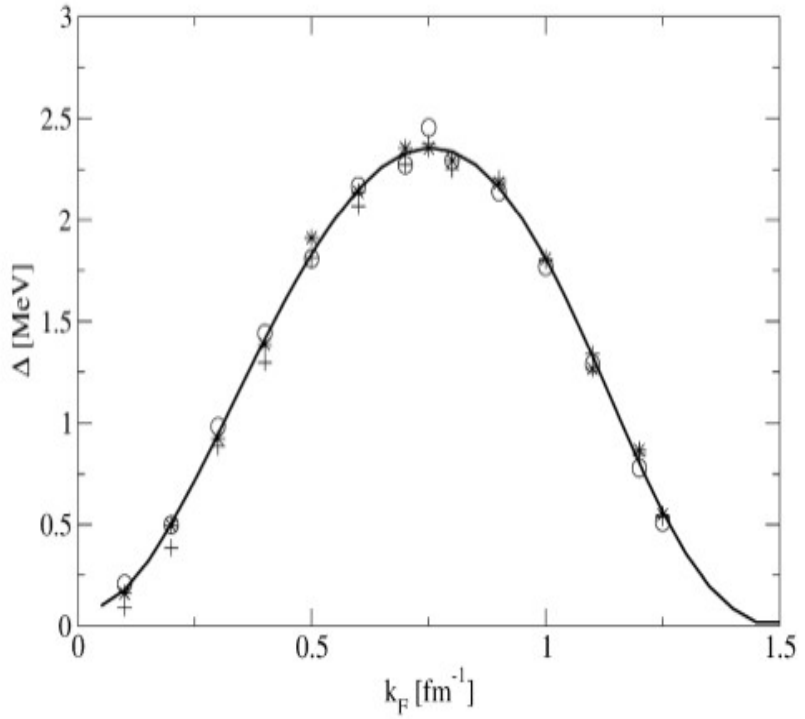

Fig. 30. Comparison between the gap obtained requiring that the radial single-particle wavefunctions $u_L(r)$ vanish at the edge of the spherical box for all orbital angular momenta L (crosses), or that $u_L(R)$ (for L even) and du_L/dR (L odd) vanish at the edge of the box (stars), or that $u_L(R)$ (for L odd) and du_L/dR (L even) vanish at the edge of the box (circles). The solid curve shows the pairing gap calculated in infinite neutron matter.

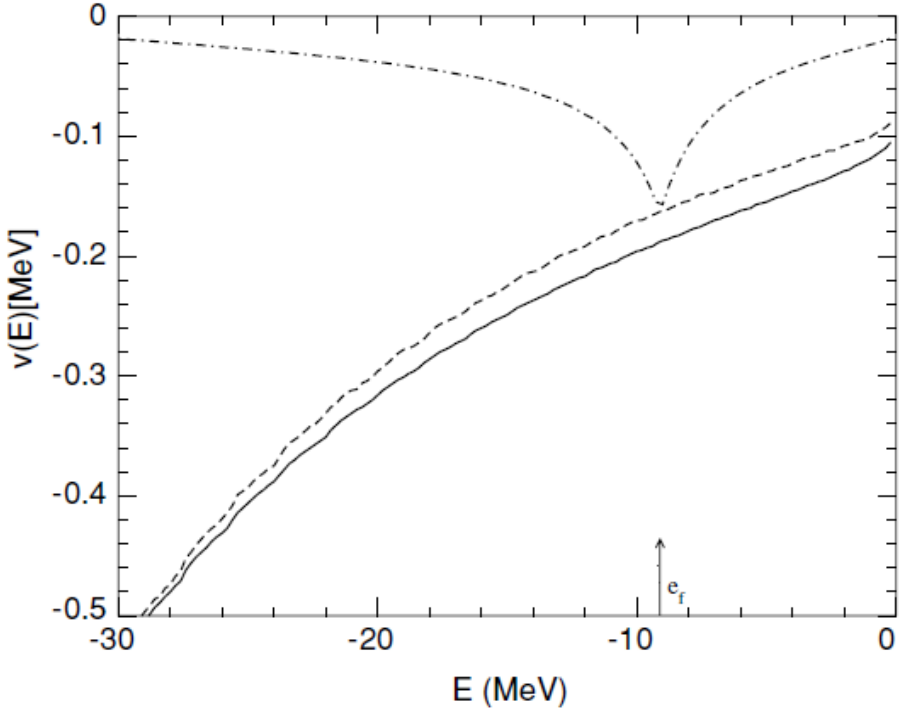

FIG. 5. The nucleus ^{120}Sn. The semiclassical matrix elements of the induced interaction, calculated according to Eq. (11) (dash-dotted curve), are compared with the matrix elements of the Gogny force (solid curve, cf. Fig. 3) and with those of the $v_{\text{low-}k}$ interaction (dashed curve). Calculations are performed with $m_k = m$ and with the same Woods-Saxon potential used in Figs. 1 and 3.

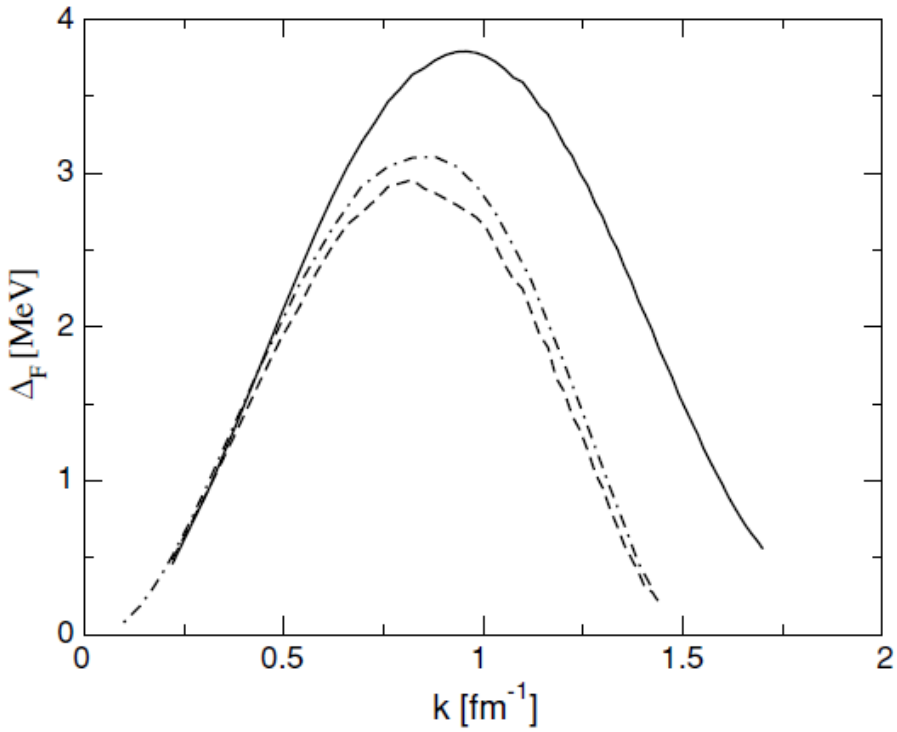

FIG. 7. Pairing gaps calculated in neutron matter as a function of the Fermi momentum, obtained with the Gogny interaction (solid line), the Argonne v_{14} potential (dash-dotted line), and the $v_{\text{low-}k}$ potential (dashed line). The bare effective mass has been used in the calculation.

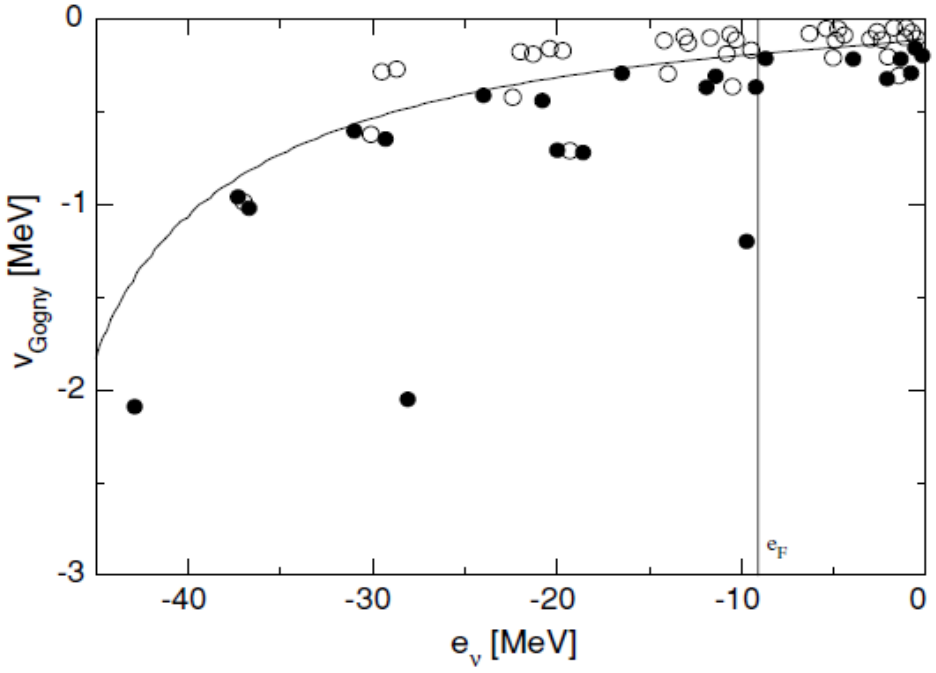

FIG. 3. The nucleus ^{120}Sn. The same as Fig. 2 (i.e., also with $m_k = m$) but for the fact that the single-particle wave functions have been calculated making use of the Woods-Saxon potential including the spin-orbit term already used for Fig. 1, where the diagonal matrix elements have already been shown. The nondiagonal matrix elements are plotted here at an energy e_ν, which is the average between the energies of the initial and final states.

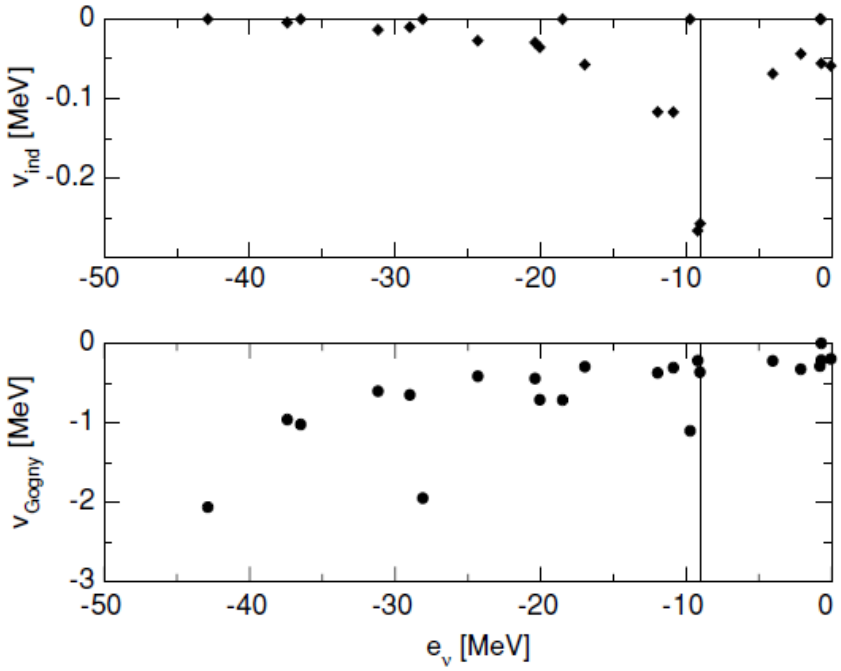

FIG. 1. The nucleus ^{120}Sn. Diagonal pairing matrix elements of the induced interaction (upper panel, solid diamonds) and of the Gogny force (lower panel, solid circles), displayed as a function of the single-particle energy, e_ν, of the state ν calculated using the bare nucleon mass and the single-particle wave functions of a Woods-Saxon potential with standard parameters (depth $V_0 = -49$ MeV, diffusivity $a = 0.65$ fm, and radius $R_0 = 6.16$ fm), including the spin-orbit term, parametrized according to Ref. [21]. Also shown by means of vertical lines is the position of the Fermi energy, $e_F = -9.1$ MeV. Note the different scale in the two figures.

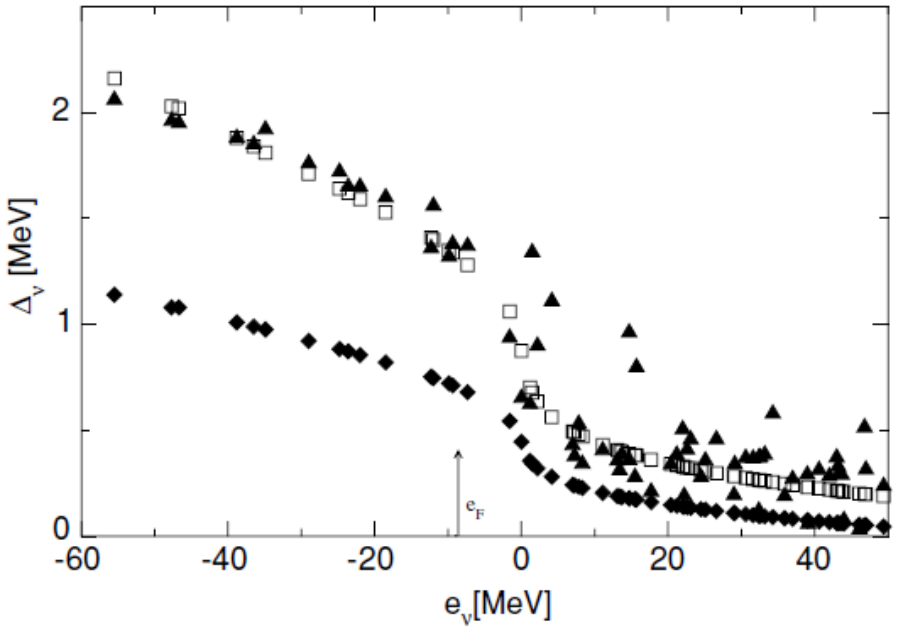

FIG. 8. State-dependent pairing gaps of ^{120}Sn calculated with a Woods-Saxon potential (with depth $V_0 = -64$ MeV, diffusivity $a = 0.65$ fm, and radius $R_0 = 6.17$ fm) as a function of the single-particle energy. The k-mass m_k was set equal to 0.7 m. The Fermi energy is $e_F = -8.6$ MeV. Solid triangles (open squares) display the results of a HFB calculation with the Gogny interaction, with quantal (semiclassical) matrix elements. The solid diamonds refer instead to a HFB calculation using the semiclassical matrix elements of the $v_{\text{low-}k}$ potential.

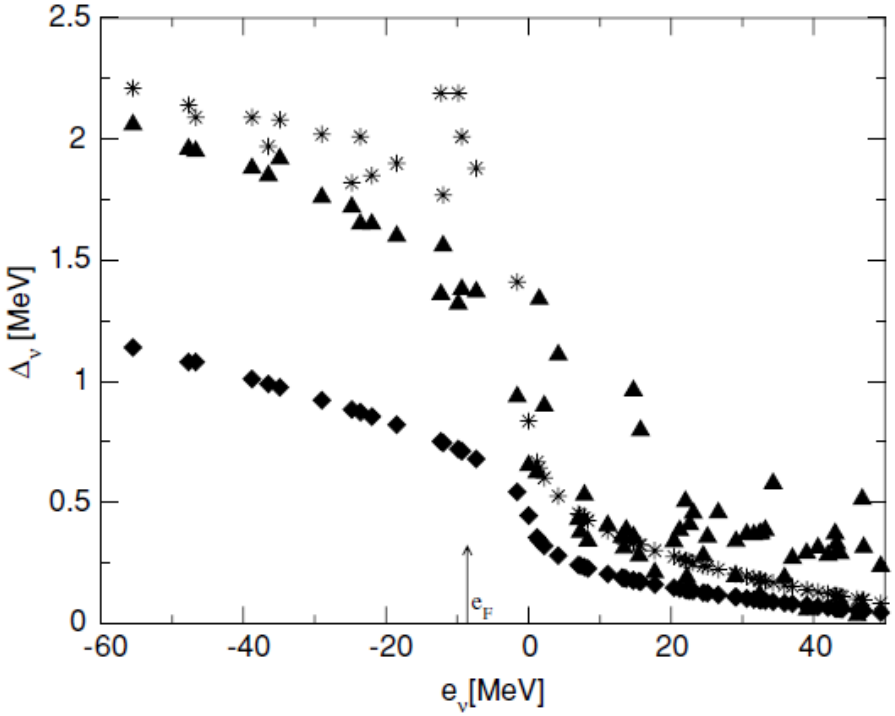

FIG. 9. State-dependent pairing gap of ^{120}Sn obtained making use of the Woods-Saxon potential used in calculating the results displayed in Fig. 8 (i.e., with $m_k = 0.7\ m$) and different interactions. Diamonds and triangles show again the gaps obtained with the $v_{\text{low-}k}$ and v_{Gogny} interactions, respectively. Stars show the gap associated with the matrix elements obtained, summing the matrix elements of $v_{\text{low-}k}$ and v_{ind}. The latter have been evaluated using Eq. (1).

No fragmentation
Only surface (density) modes exchanged

Repulsive Vind by S=1 modes exchange

Well known from Neutron Matter studies.

Microscopic calculation of the matrix elements of the induced interaction in spherical open-shell nuclei including spin modes

Vibrations are calculated with QRPA and SKM* interaction

Particle-hole interaction:

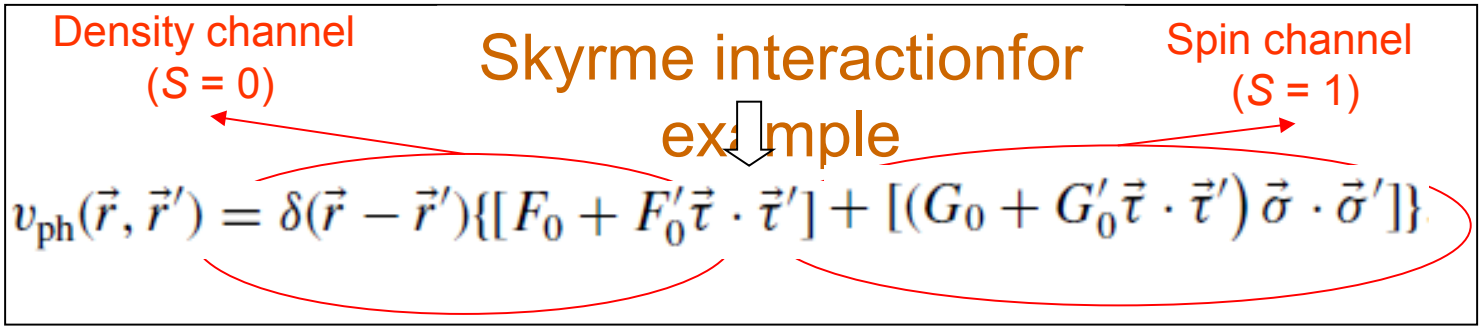

G. Gori et al., Phys. Rev. C72(2005)11302

$$v_{\rm ph}(\vec{r},\vec{r}') = \delta(\vec{r}-\vec{r}')\{[F_0 + F_0'\vec{\tau}\cdot\vec{\tau}'] + [(G_0 + G_0'\vec{\tau}\cdot\vec{\tau}')\,\vec{\sigma}\cdot\vec{\sigma}']\}$$

$$\langle \nu' m' \nu' \bar{m}' | v_{\rm ind} | \nu m \nu \bar{m}\rangle = \sum_{J^\pi M i} \frac{2(f+g)^{\nu' m'}_{\nu m; J^\pi M i}(f-g)^{\nu' m'}_{\nu m; J^\pi M i}}{E_0 - E_{\rm int}}$$

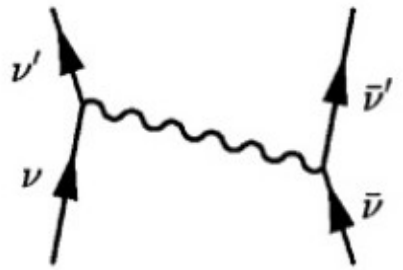

(a)

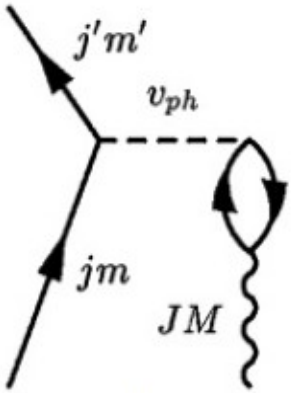

(b)

$$f^{\nu' m'}_{\nu m; J^\pi M i} = i^{l-l'}\langle j' m' | (i)^J Y_{JM} | j m\rangle \times \int dr \varphi_{\nu'}\left[(F_0 + F_0')\delta\rho^i_{J^\pi n} + (F_0 - F_0')\delta\rho^i_{J^\pi p}\right]\varphi_\nu$$

$$g^{\nu' m'}_{\nu m J^\pi M i} = \sum_{L=J-1}^{J+1} i^{l-l'}\langle j' m' | (i)^L [Y_L \times \sigma]_{JM} | j m\rangle \times \int dr \varphi_{\nu'}\left[(G_0 + G_0')\delta\rho^i_{J^\pi L n} + (G_0 - G_0')\delta\rho^i_{J^\pi L p}\right]\varphi_\nu$$

Microscopic calculation of the matrix elements of the induced interaction

S=0 (attractive)

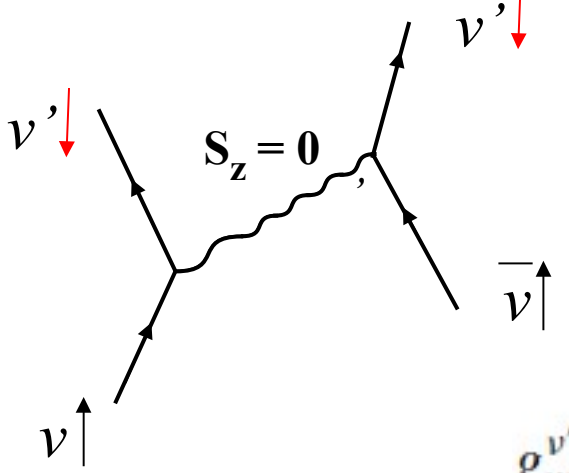

$$f^{\nu'm'}_{\nu m;J^\pi Mi} = i^{l-l'}\langle j'm'|(i)^J Y_{JM}|jm\rangle \times \int dr\varphi_{\nu'}\left[(F_0+F_0')\delta\rho^i_{J^\pi n}+(F_0-F_0')\delta\rho^i_{J^\pi p}\right]\varphi_\nu$$

S=1 (repulsive)

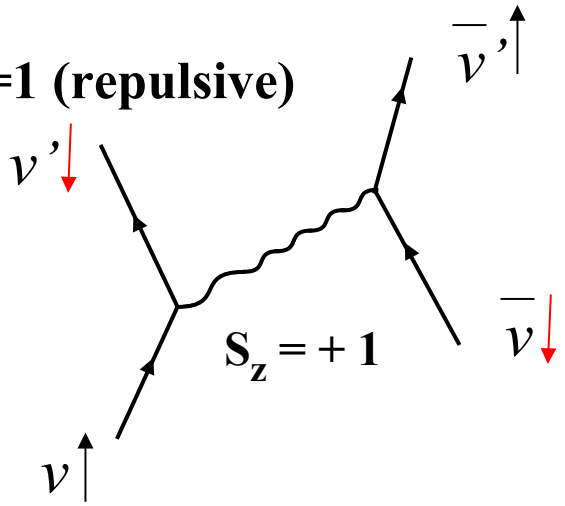

$$g^{\nu'm'}_{\nu m J^\pi Mi} = \sum_{L=J-1}^{J+1} i^{l-l'}\langle j'm'|(i)^L[Y_L\times\sigma]_{JM}|jm\rangle \times \int dr\varphi_{\nu'}\left[(G_0+G_0')\delta\rho^i_{J^\pi Ln} + (G_0-G_0')\delta\rho^i_{J^\pi Lp}\right]\varphi_\nu$$

FINITE NUCLEI (^{120}Sn):

The induced interaction arising from the coupling to surface and spin modes is attractive and leads to a pairing gap of about 0.7 MeV (50 % of the experimental value). Excluding the coupling to spin modes, the gap increases to about 1.1 MeV.

One must then add the bare interaction.

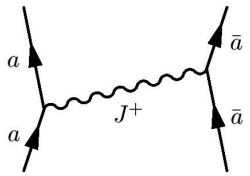

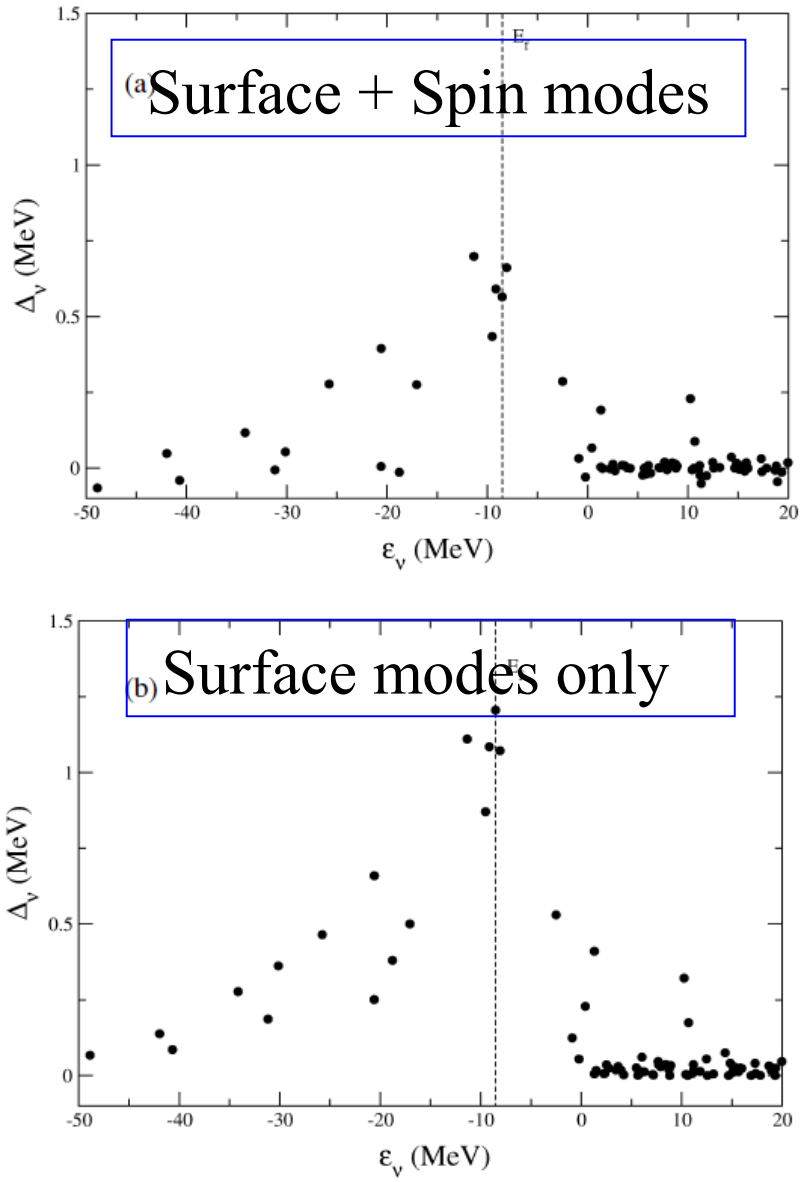

FIG. 4. (a) The state-dependent pairing gap as a function of the single-particle energies obtained by solving the BCS equations associated with the total induced interaction matrix elements; (b) same as (a) but for the matrix elements associated with the spin-independent part of the particle-hole interaction.

T=0 pairing

T=0 (attractive)

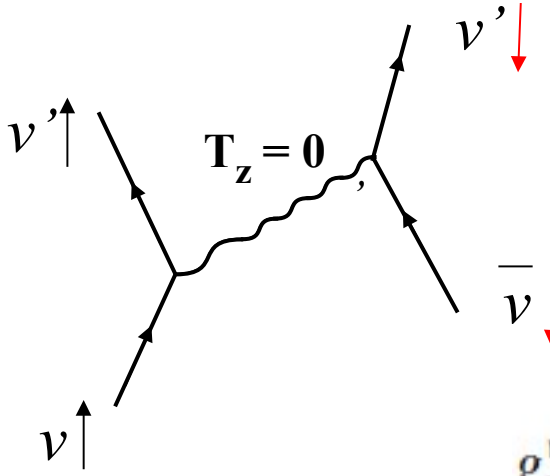

$$f^{\nu' m'}_{\nu m; J^\pi M i} = i^{l-l'} \langle j' m' | (i)^J Y_{JM} | j m \rangle$$

$$\times \int dr \varphi_{\nu'} \left[(F_0 + F_0') \delta\rho^i_{J^\pi n} + (F_0 - F_0') \delta\rho^i_{J^\pi p} \right] \varphi_\nu$$

]T=0;Sz=+1

T=1 (repulsive)

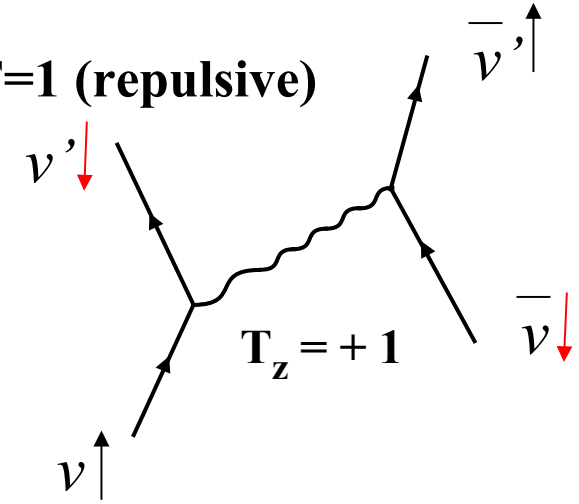

$$g^{\nu' m'}_{\nu m J^\pi M i} = \sum_{L=J-1}^{J+1} i^{l-l'} \langle j' m' | (i)^L [Y_L \times \sigma]_{JM} | j m \rangle$$

$$\times \int dr \varphi_{\nu'} \left[(G_0 + G_0') \delta\rho^i_{J^\pi Ln} + (G_0 - G_0') \delta\rho^i_{J^\pi Lp} \right] \varphi_\nu$$

T=0 pairing problem

Alm et al. Z.Phys.A337,355 (1990)
Vonderfecht et al. PLB253,1 (1991)
Baldo et al. PLB283, 8 (1992)

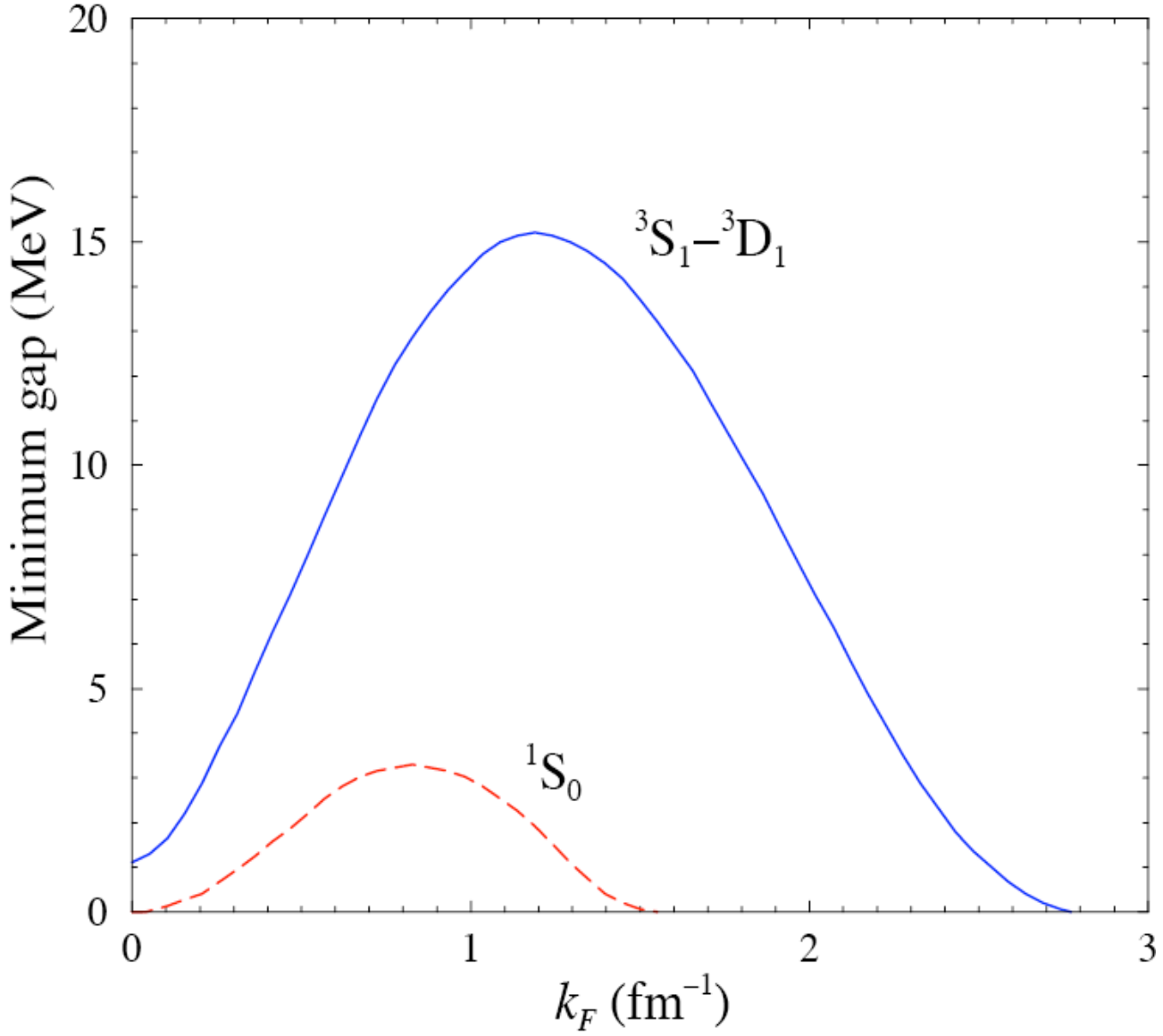

Proton-neutron pairing in symmetric nuclear matter 3S1-3D1

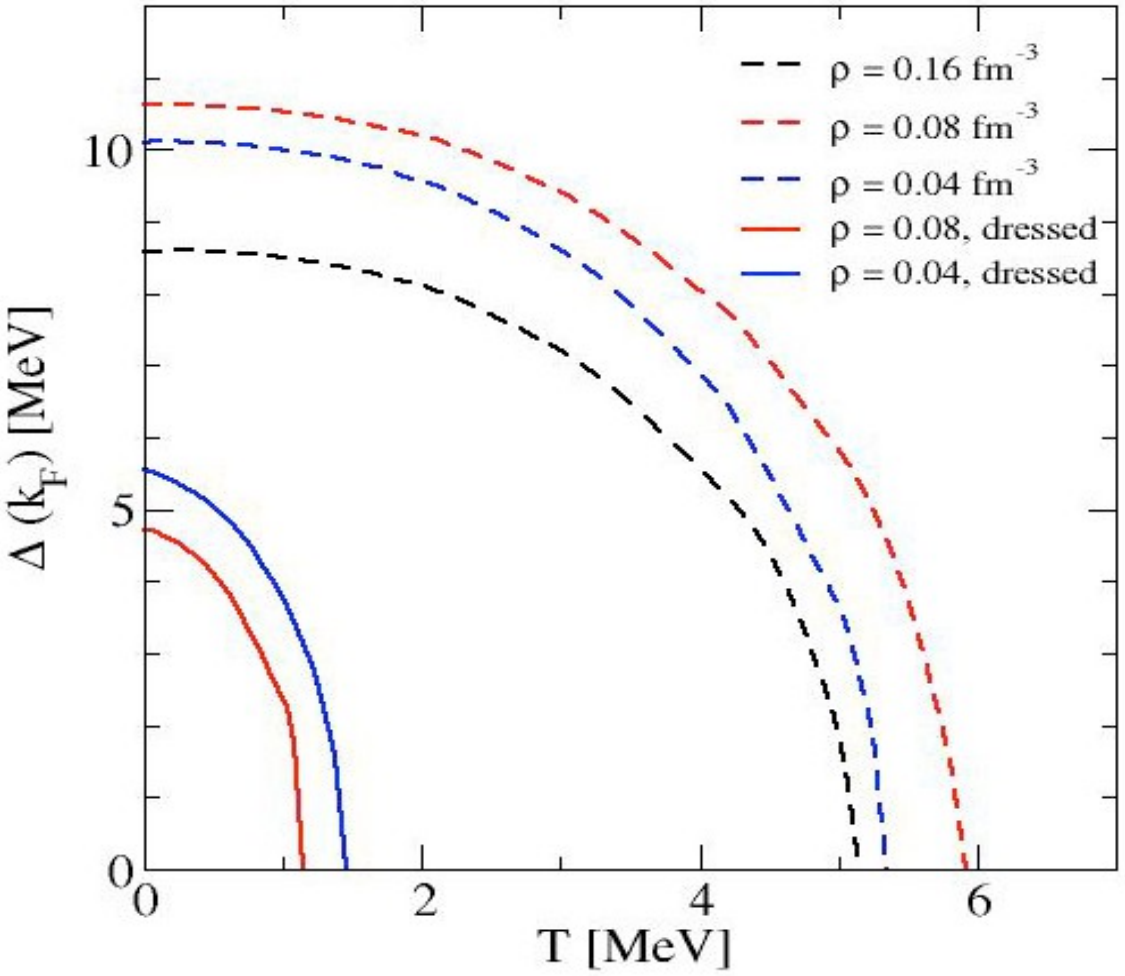

Using CDBonn

Dashed lines:
quasiparticle poles

Solid lines:
dressed nucleons

No pairing at saturation density!!!!

Dickhoff PRC72(2005)054313

Lombardo preliminary results: No SD pairing at about 0.14fm^-3

Strength of T=0 pairing interaction can have a large effect on beta-decay lifetimes

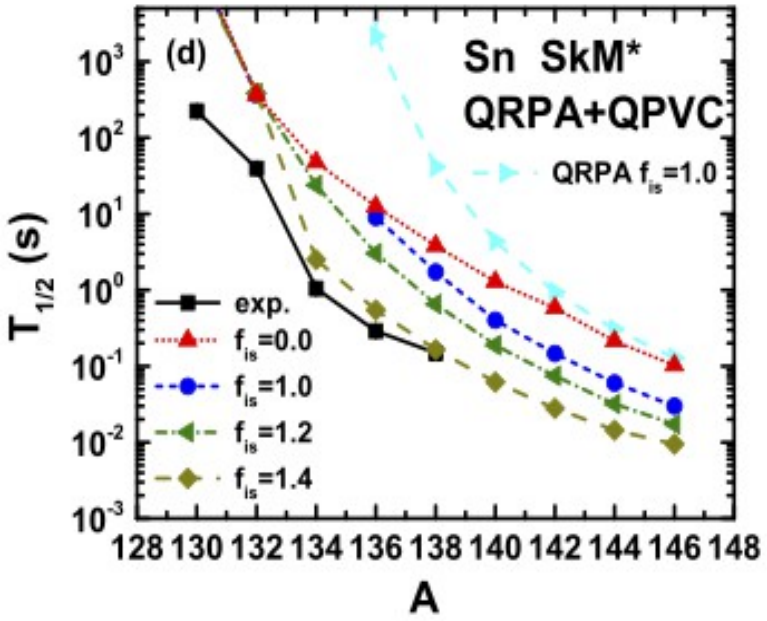

Y.F.Niu et al.,
PRC 94 (2016) 064328 and
to be published

PHYSICAL REVIEW C **78**, 024315 (2008)

Microscopic calculation and local approximation of the spatial dependence of the pairing field with bare and induced interactions

A. Pastore,[1,2] F. Barranco,[3] R. A. Broglia,[1,2,4] and E. Vigezzi[2]

[1]*Dipartimento di Fisica, Università degli Studi di Milano, via Celoria 16, I-20133 Milano, Italy*

[2]*INFN, Sezione di Milano, via Celoria 16, I-20133 Milano, Italy*

[3]*Departamento de Fisica Aplicada III, Escuela Superior de Ingenieros, Camino de los Descubrimientos s/n, E-41092 Sevilla, Spain*

[4]*The Niels Bohr Institute, University of Copenhagen, Blegdamsvej 17, DK-2100 Copenhagen Ø, Denmark*

(Received 6 December 2007; revised manuscript received 4 June 2008; published 28 August 2008)

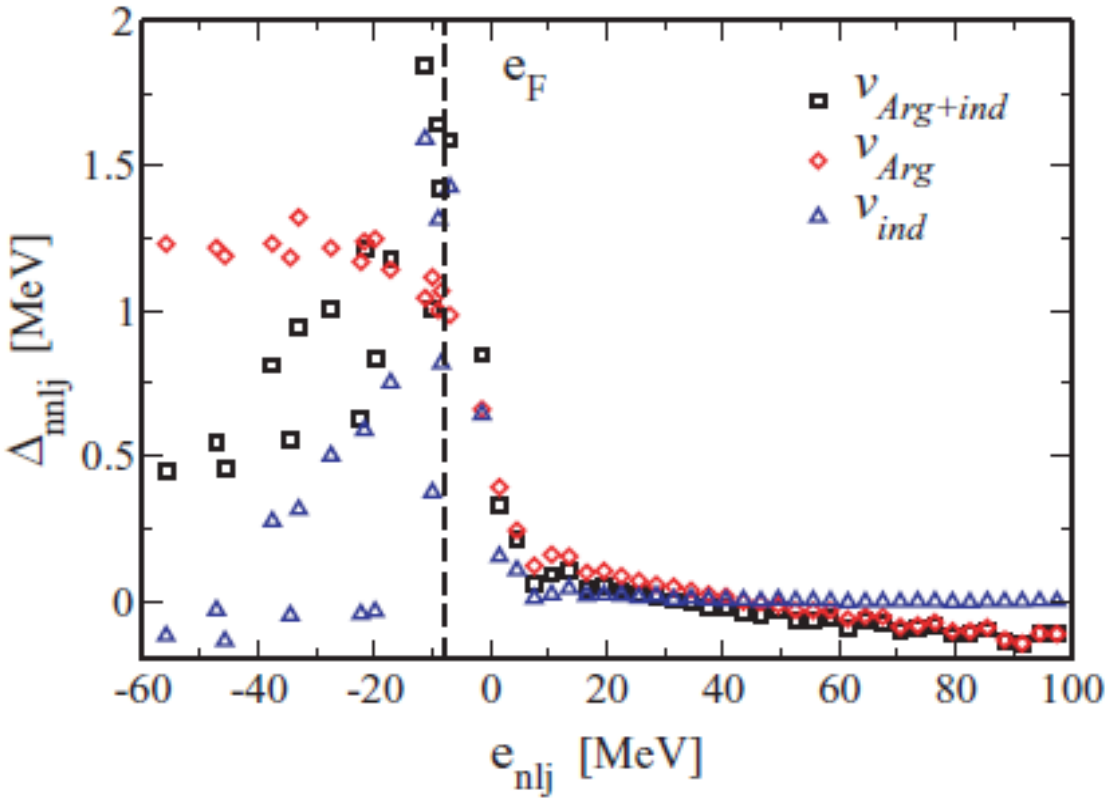

$$v^{\delta}(\vec{r}_1,\vec{r}_2) = v_0\left[1-\eta\left(\frac{\rho\left(\frac{\vec{r}_1+\vec{r}_2}{2}\right)}{\rho_0}\right)^{\alpha}\right]\delta(\vec{r}_1-\vec{r}_2)$$

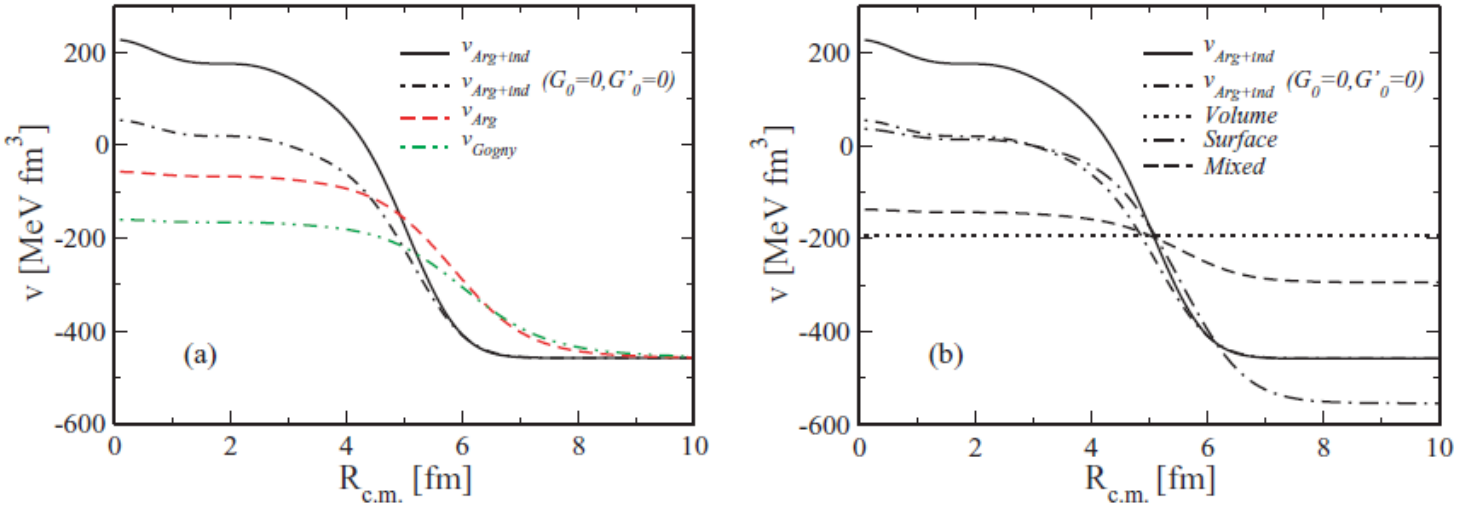

FIG. 11. (Color online) (a) Spatial dependence of the different local pairing interactions introduced in this work to simulate the local pairing gaps [cf. Eq. (19)] obtained with the corresponding microscopic, nonlocal interactions: bare+induced interaction $v_{\rm Arg+ind}$ (corresponding to the parameters $\alpha = 2.0$, $\eta = 1.32$; cf. Table II); bare+induced interaction neglecting the spin-dependent part ($v_{\rm Arg+ind}$, $G_0 = 0$, $G'_0 = 0$), ($\alpha = 1.79$, $\eta = 1.0$; cf. Table V in Appendix B); bare v_{14} interaction $v_{\rm Arg}$($\alpha = 0.66$, $\eta = 0.84$; cf. Table II); Gogny interaction $v_{\rm Gogny}$ ($\alpha = 0.51$, $\eta = 0.63$; cf. Table IV in Appendix A). (b) The spatial dependence of the bare+induced interaction with and without the spin-dependent part of the induced interaction, already shown in (a), compared with the volume, surface, and mixed interaction of Ref. [26] (see text).

$$v^G_{\rm attr}(R_{\rm c.m.}, r_{12}) = -b_{\rm attr} \cdot \exp\{-[(r_{12} - c)/a_{\rm attr}]^2\}$$

$$c = 2|R_{\rm nucl} - R_{\rm c.m.}|$$

$$a_{\rm attr} = 2 \text{ fm}$$

$$v^G_{\rm rep}(R_{\rm c.m.}, r_{12}) = b_{\rm rep} \cdot \exp[-(r_{12}/a_{\rm rep})^2]\Theta(R_{\rm c.m.} - R_0)$$

$$a_{\rm rep} = 3.5 \text{ fm}$$

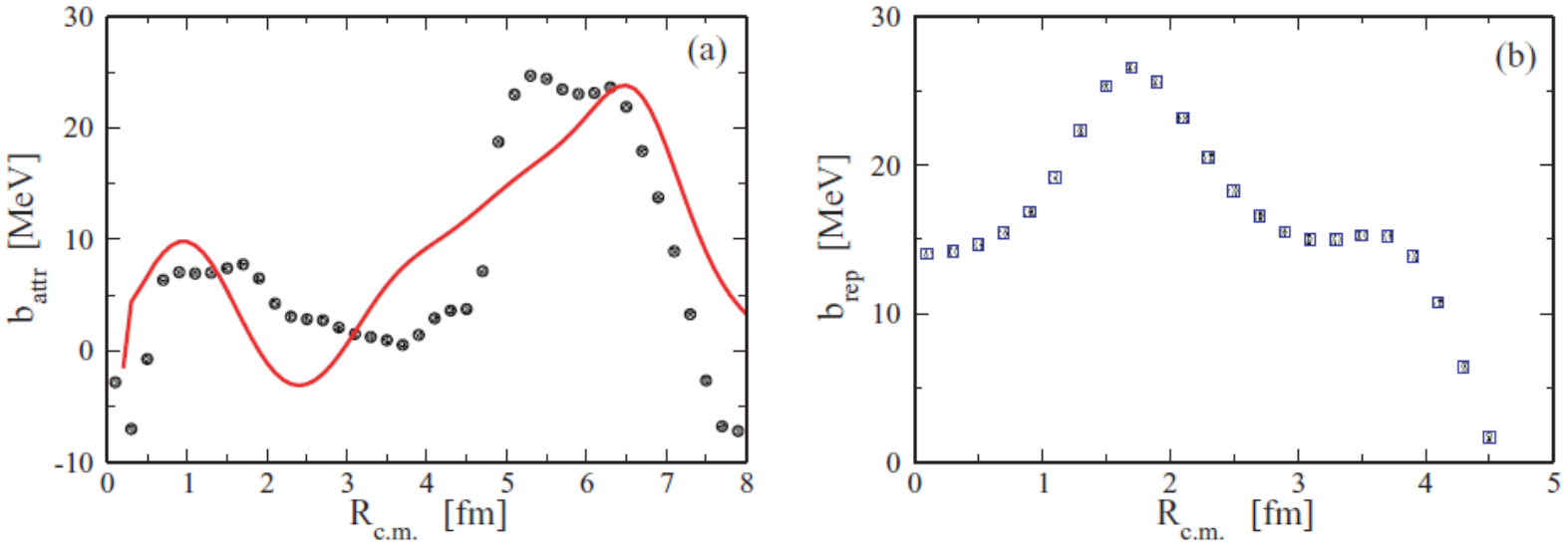

FIG. 12. (Color online) (a) The values of the parameter $b_{\rm attr}$, obtained by fitting the Gaussian interaction [Eq. (23)], shown as a function of the center of mass $R_{\rm c.m.}$ (filled dots) and compared with the function $0.14 R_{\rm nucl} \frac{dU(r)}{dR_{\rm c.m.}}$ (solid line). (b) The values of the parameter $b_{\rm rep}$, obtained by fitting the Gaussian interaction [Eq. (23)], also shown as a function of the center of mass $R_{\rm c.m.}$ (filled squares).

Medium polarization and finite size effects on the superfluidity of the inner crust of neutron stars

S.Baroni[a,b,c], F. Raimondi[a,b], F.Barranco[d], R.A.Broglia[a,b,e], A. Pastore[a,b], and E.Vigezzi[b]

[a] *Dipartimento di Fisica, Università degli Studi di Milano,via Celoria 16, 20133 Milano, Italy.*

[b] *INFN, Sezione di Milano, via Celoria 16, 20133 Milano, Italy.*

[c] *TRIUMF, 4004 Wesbrook Mall, Vancouver, B.C. V6T 2A3, Canada*

[d] *Departamento de Fisica Aplicada III, Escuela Tecnica Superior de Ingenieros, Camino de los Descubrimientos s/n, 41029 Sevilla, Spain.*

[e] *The Niels Bohr Institute, University of Copenhagen, Blegdamsvej 17, 2100 Copenhagen Ø, Denmark.*

(Dated: July 6, 2017)

The $^1S_0$ pairing gap Δ associated with the inner crust of a neutron star is calculated, taking into account the coexistence of the nuclear lattice with the sea of free neutrons (finite size effects), as well as medium polarization effects associated with the exchange of density and spin fluctuations. Both effects are found to be important and to lead to an overall quenching of the pairing gap. This result, whose quantitative value is dependent on the effective interaction used to generate the single-particle levels, is a consequence of the balance between the attractive (repulsive) induced interaction arising from the exchange of density (spin) modes, balance which in turn is influenced by the presence of the protons and depends on the single-particle structure of the system.

Neutron matter without and with impurities (Neutron Star)

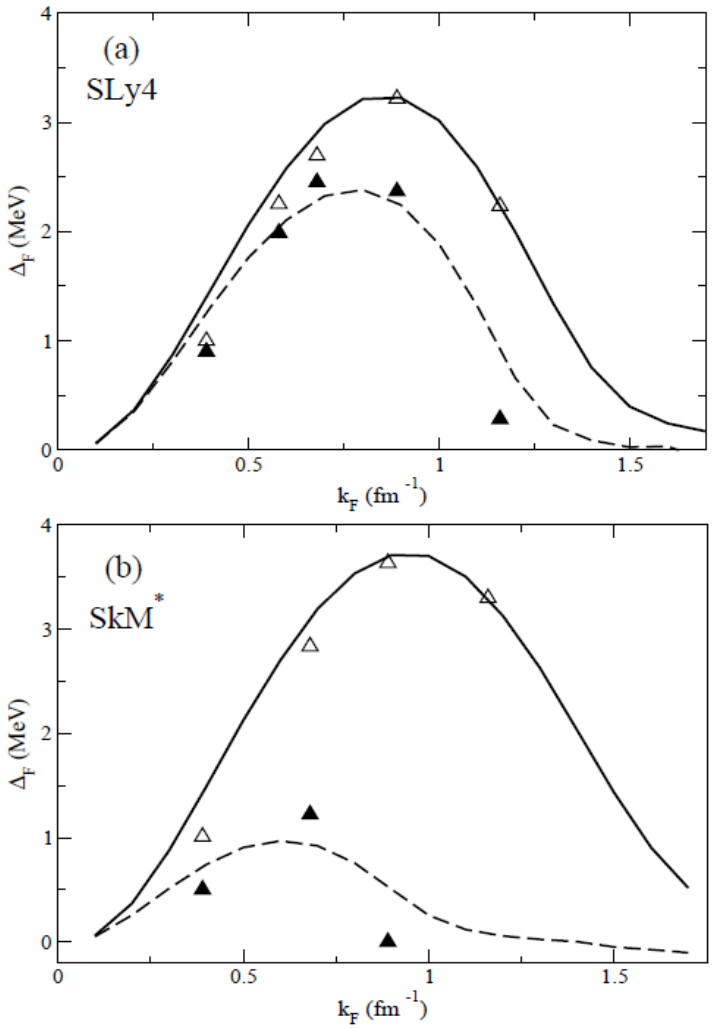

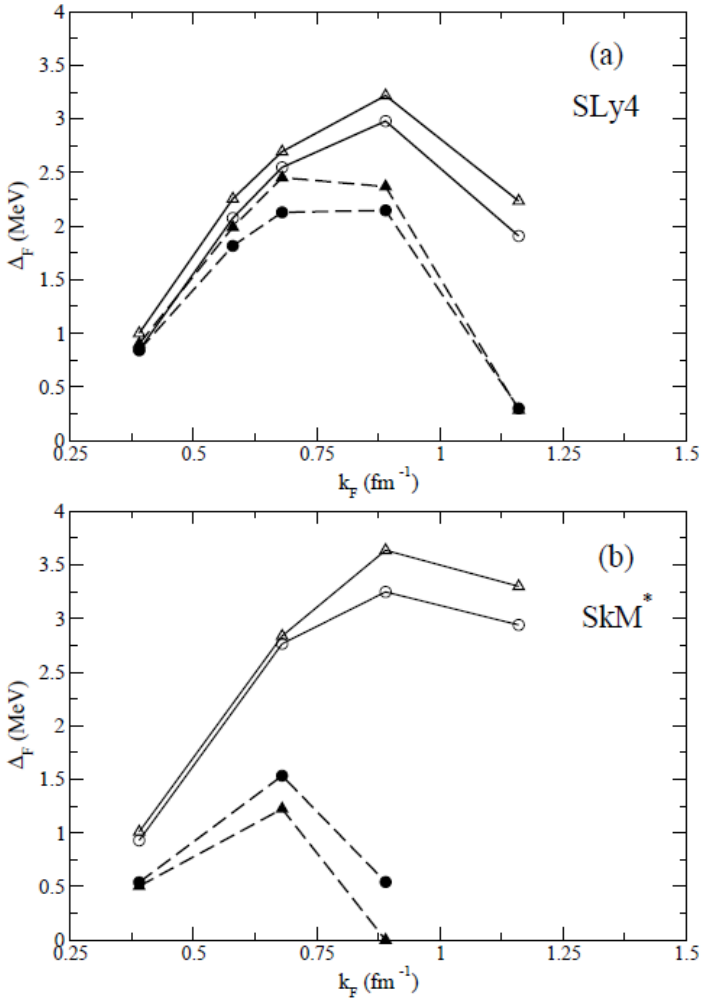

FIG. 8: Pairing gap calculated at the Fermi energy for the

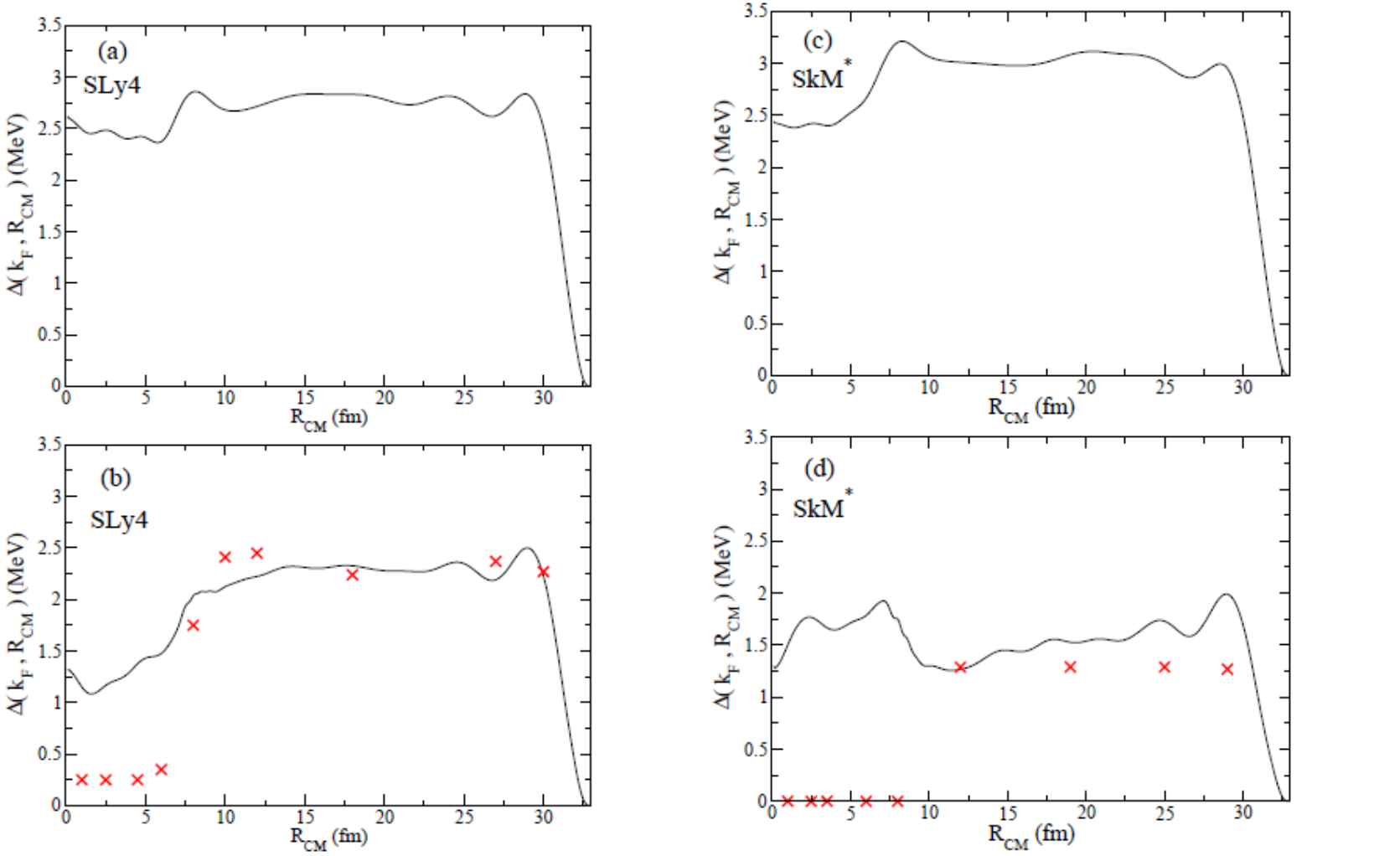

FIG. 9: Pairing field $\Delta(k_F, R_{CM})$ for the cell ^{1364}Sn, calcu-

INCLUDING FRAGMENTATION

Two step calculation:

i)HFB with Vbare in a large space ---> “unperturbed” qp-properties

ii) Using the above HFB/V_bare results, diagonalize the PVC effects using the One Shell Aproximation.

Approximation justified by the large scale sepration between induced and bare interaction.

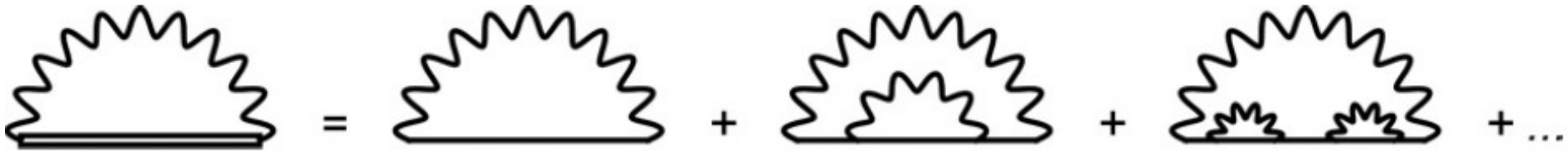

$$\begin{pmatrix} (\epsilon_a - \epsilon_F) + \tilde{\Sigma}^{11}_{a(n)} & \tilde{\Sigma}^{12}_{a(n)} \\ \tilde{\Sigma}^{12}_{a(n)} & -(\epsilon_a - \epsilon_F) + \tilde{\Sigma}^{22}_{a(n)} \end{pmatrix} \begin{pmatrix} \tilde{u}_{a(n)} \\ \tilde{v}_{a(n)} \end{pmatrix} = \tilde{E}_{a(n)} \begin{pmatrix} \tilde{u}_{a(n)} \\ \tilde{v}_{a(n)} \end{pmatrix}$$

$$\Sigma^{11\mathrm{pho}}_{a(n)} = \sum_{b,m,\lambda,\nu} \frac{(f+g)^2\,[ab(m)\lambda\nu]\,S^2}{\tilde{E}_{a(n)} - \tilde{E}_{b(m)} - \hbar\omega_{\lambda\nu}} + \sum_{b,m,\lambda,\nu} \frac{(f-g)^2\,[ab(m)\lambda\nu]\,P^2}{\tilde{E}_{a(n)} + \tilde{E}_{b(m)} + \hbar\omega_{\lambda\nu}}$$

$$\Sigma^{12\mathrm{pho}}_{a(n)} = -\sum_{b,m,\lambda,\nu} (f^2-g^2)[ab(m)\lambda\nu]\; G \times \left[\frac{1}{\tilde{E}_{a(n)} - \tilde{E}_{b(m)} - \hbar\omega_{\lambda\nu}} - \frac{1}{\tilde{E}_{a(n)} + \tilde{E}_{b(m)} + \hbar\omega_{\lambda\nu}} \right].$$

$S = u_a u'_b - v_a v'_b$

$P = u_a v'_b + v_a u'_b$

$G = S^* P$

Terasaki et al.

$$\tilde{\Sigma}^{12}_{a(n)} = \Delta^{\mathrm{BCS}}_a + \tilde{\Sigma}^{12,\mathrm{pho}}_{a(n)}$$

T=1(time reversal)BCS with Self energy effects

$$(2j_a+1)\tilde{\Delta}_{a(n)} = -Z_{a(n)} \sum_{b,m} V_{\text{eff}}[a(n)b(m)] N_{b(m)} \frac{\tilde{\Delta}_{b(m)}}{2\tilde{E}_{b(m)}}$$

$$V_{\text{eff}}[a(n)b(m)] = V_{\text{bare}}[ab] + V_{\text{ind}}[a(n)b(m)]$$

$V_{\text{ind}}[a(n)b(m)] = \Sigma_{jz,j'z}$ <a(n);jz-jz|V_{ind}|b(m);j'z-j'z>

A.Idini, et al
PRC85,14331

<a(n);j_z-j_z|V_{ind}|b(m);j'$_z$-j'$_z$> = Σ_{LJM} $(f+g)_{LJM}$ $(f-g)_{LJM}$ x

$$\left[\frac{1}{\tilde{E}_{a(n)} - \tilde{E}_{b(m)} - \hbar\omega_{\lambda\nu}} - \frac{1}{\tilde{E}_{a(n)} + \tilde{E}_{b(m)} + \hbar\omega_{\lambda\nu}} \right].$$

$$Z_{a(n)} = \left(1 - \frac{\Sigma^{11}_{a(n)} - \Sigma^{11}_{a(-n)}}{2\tilde{E}_{a(n)}} \right)^{-1} \qquad N_{a(n)} = x^2_{a(n)} + y^2_{a(n)}$$

$$\tilde{E}_{a(n)} = \sqrt{(\tilde{\epsilon}_{a(n)} - \epsilon_F)^2 + \tilde{\Delta}^2_{a(n)}} \qquad \tilde{\epsilon}_{a(n)} - \epsilon_F = Z_{a(n)} \left[(\epsilon_a - \epsilon_F) + \Sigma^{\text{even}}_{a(n)} \right]$$

COMPARISON WITH DATA

Open-shell nuclei around 50Sn70

Which mean field?

Observables:

- Low-energy quasiparticle spectrum
- Multiplet splitting
- Electromagnetic transition strength
- One-neutron transfer reactions
- Two-nucleon transfer cross sections
- Pairing gaps

PHYSICAL REVIEW C **92**, 031304(R) (2015)

Pairing gaps

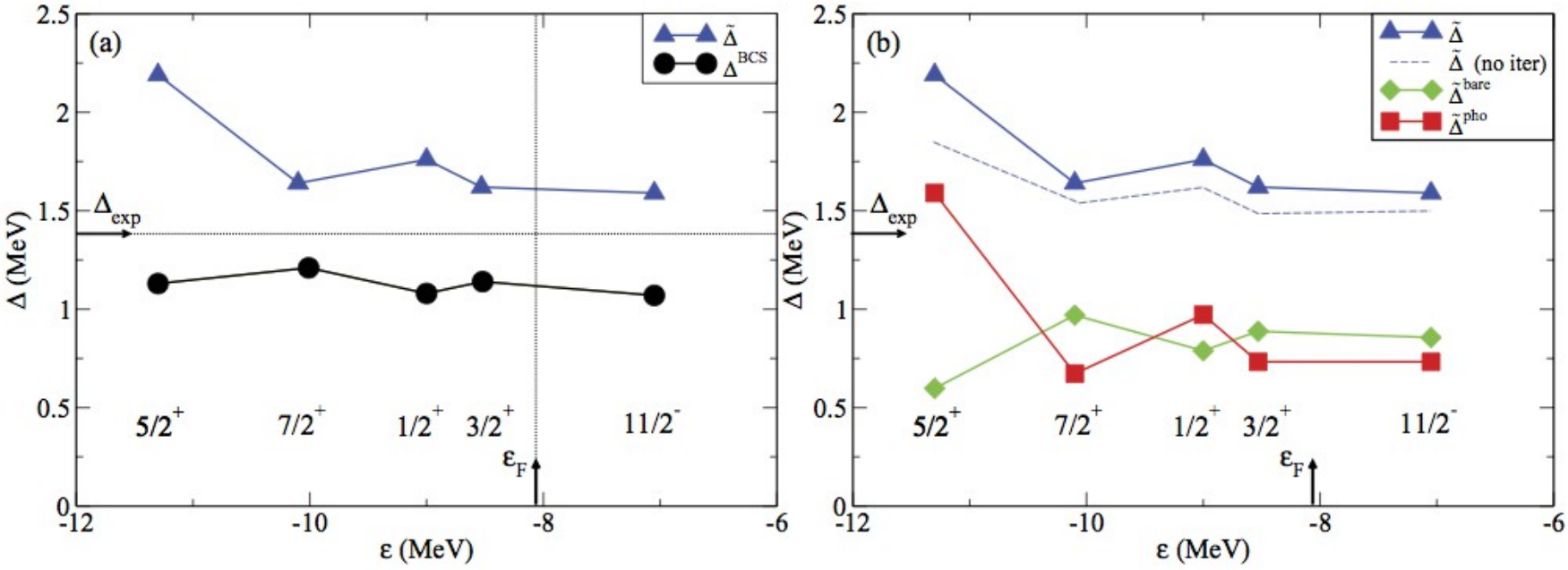

120Sn

excitation spectrum
odd neighbors

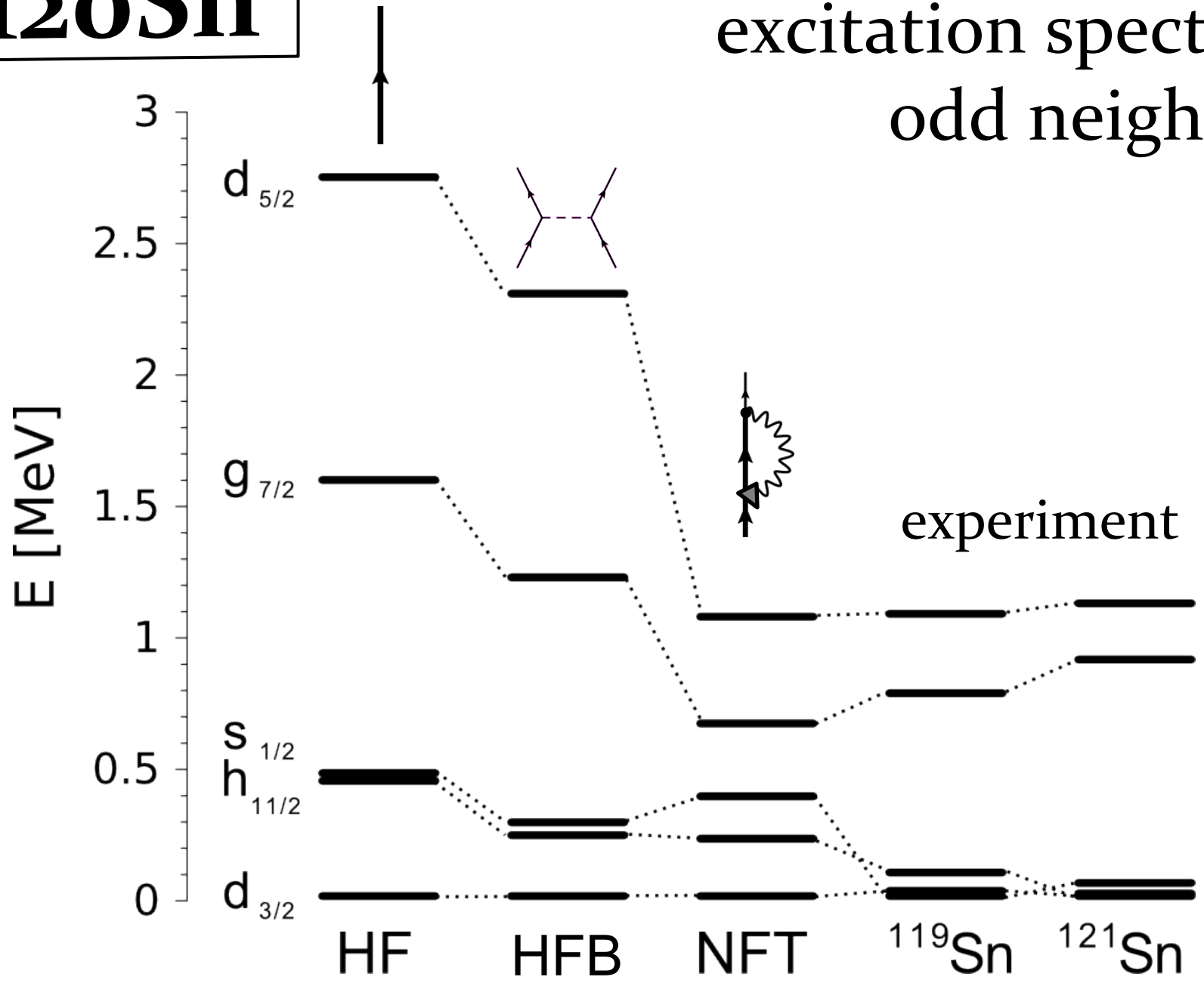

experiment

Transfer reactions: 120Sn(d,p)121Sn

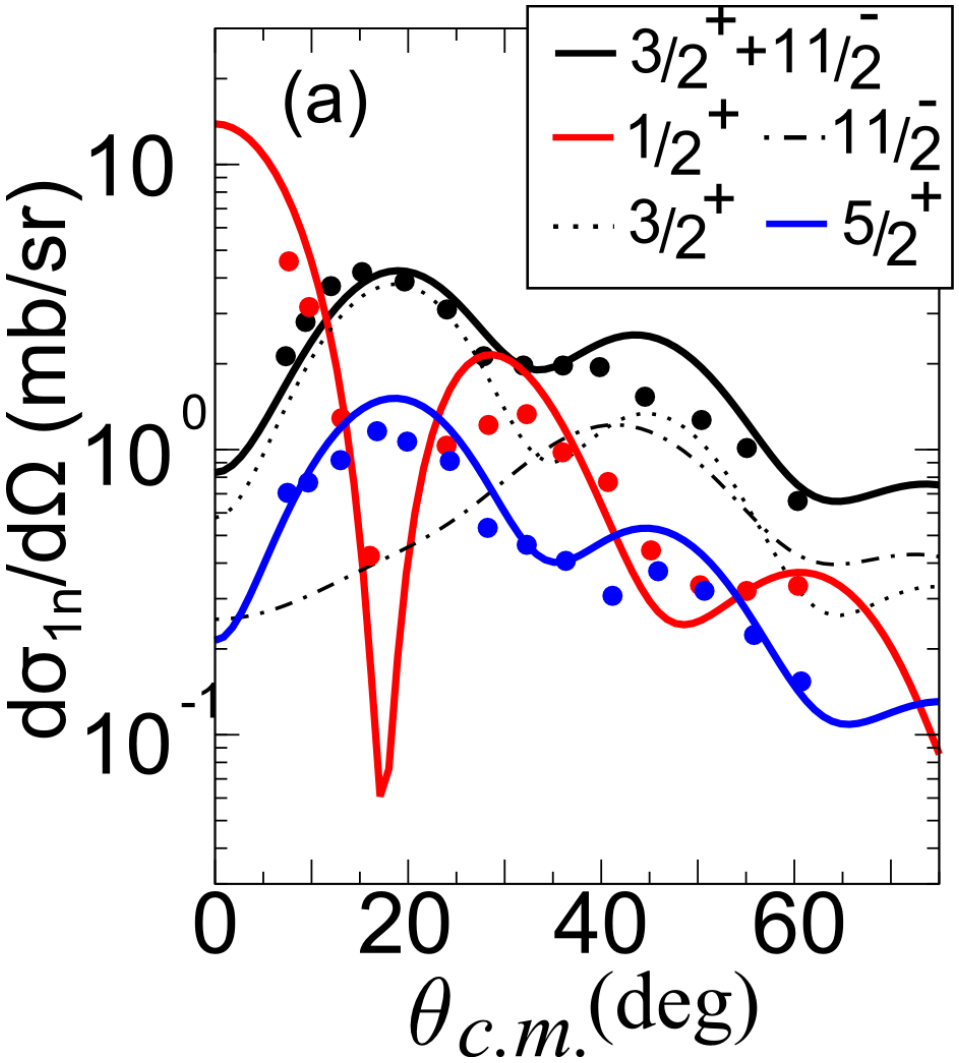

Transfer reactions: 120Sn(p,d)119Sn (5/2+)

ϵ_i	Expt.		SLy4			SLy4 ($d_{5/2}$ shift)		
	σ	$d\sigma/d\Omega$	ϵ_i	σ	$d\sigma/d\Omega$	ϵ_i	σ	$d\sigma/d\Omega$
921	0.63	0.75						
1090	5.35	7.0	1150	1.80	2.3	1050	4.40	5.60
1354	1.66	2.3	1290	1.20	1.7	1250	0.45	0.58
1562	0.13	0.16	1710	0.25	0.32	1540	0.07	0.09
1730	0.16	0.18	1910	2.90	4.0	1710	1.45	1.90
	7.93 ± 2	10.39		6.15	8.32		6.37	8.17

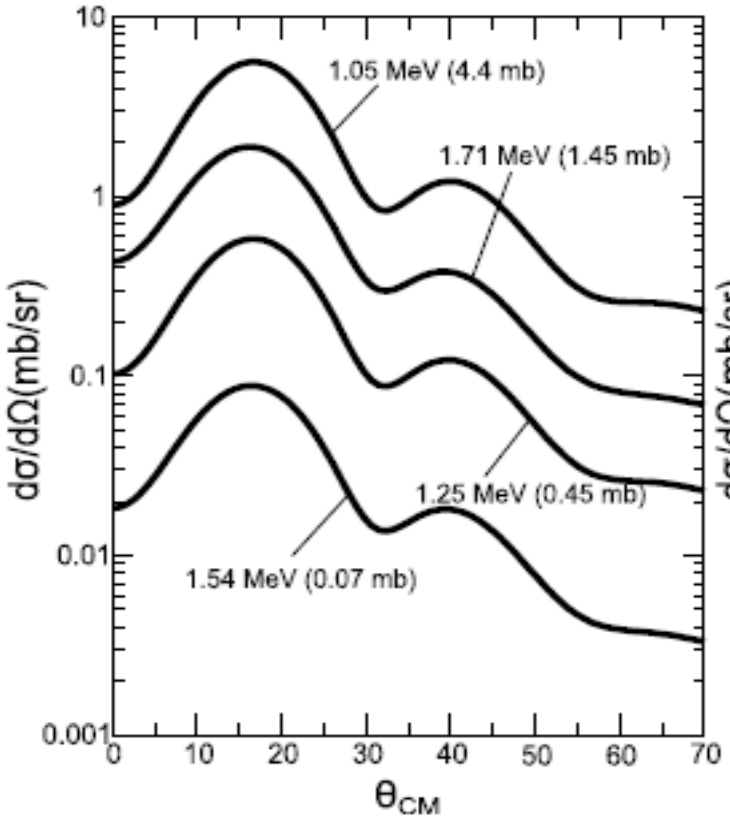

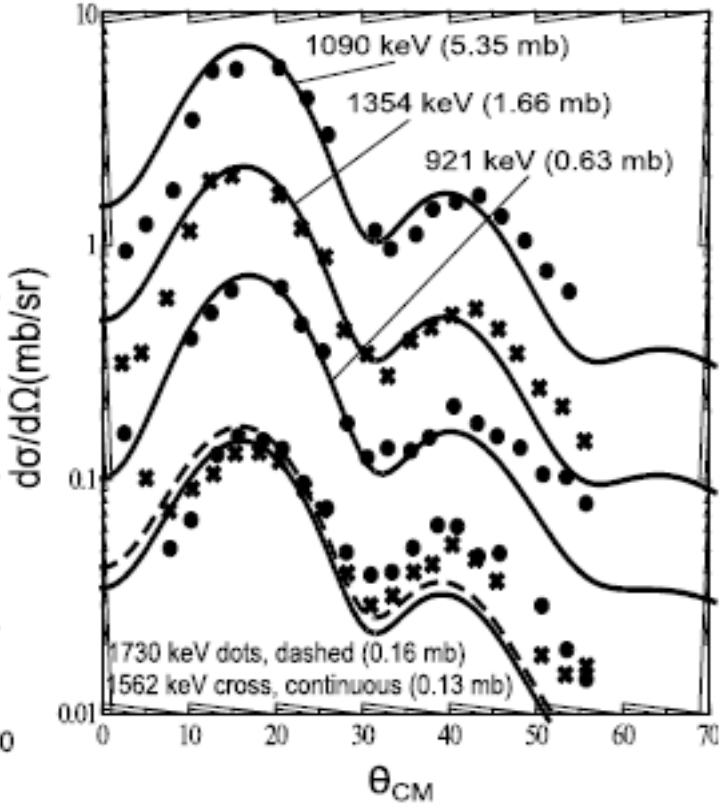

Two particle transfer

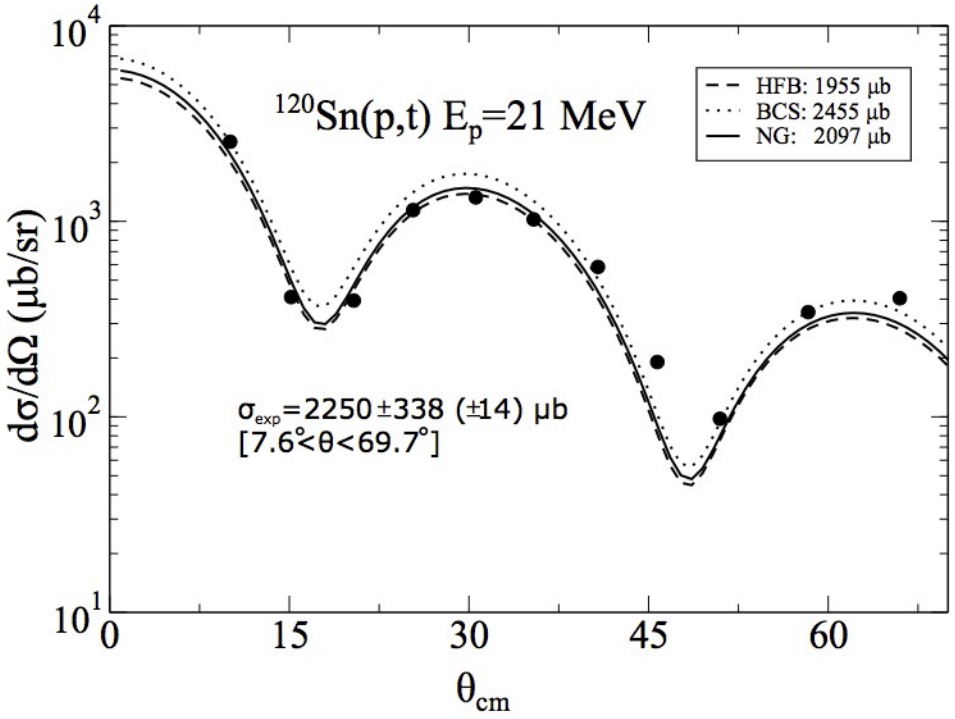

Potel et al. PRC96(2017)034606

Multiplet Splitting

$(qp. \otimes \lambda^{\pi})_{j^{\pi'}}$

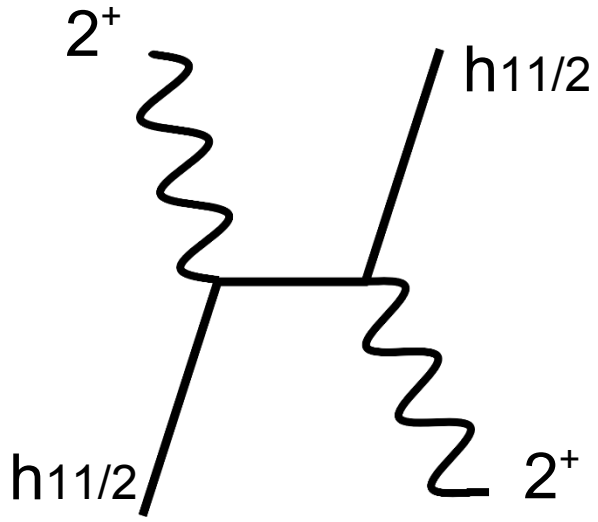

$(h_{11/2} \otimes 2^+)_{j^-}$

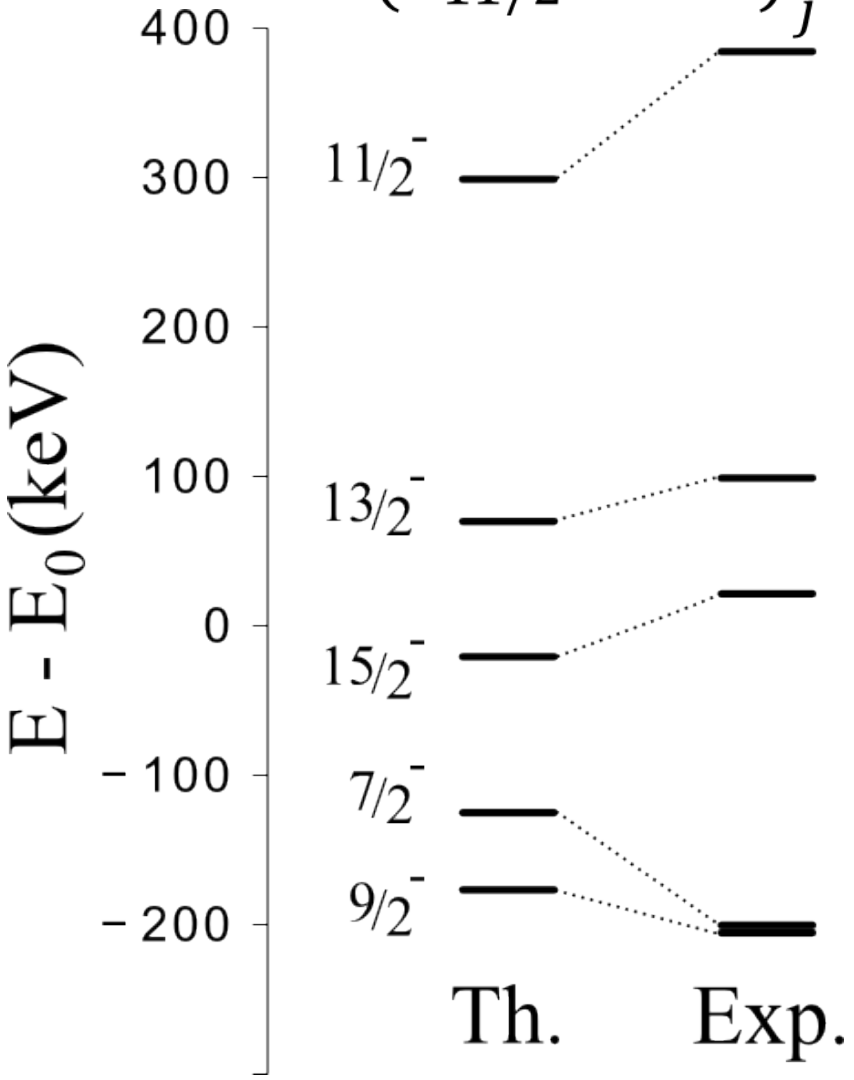

The splitting would be zero without PVC, and is highly independent of the used mean field: ESSENTIALLY IT IS A MEASURE OF THE PVC VERTEX

Electromagnetic E2 Transitions

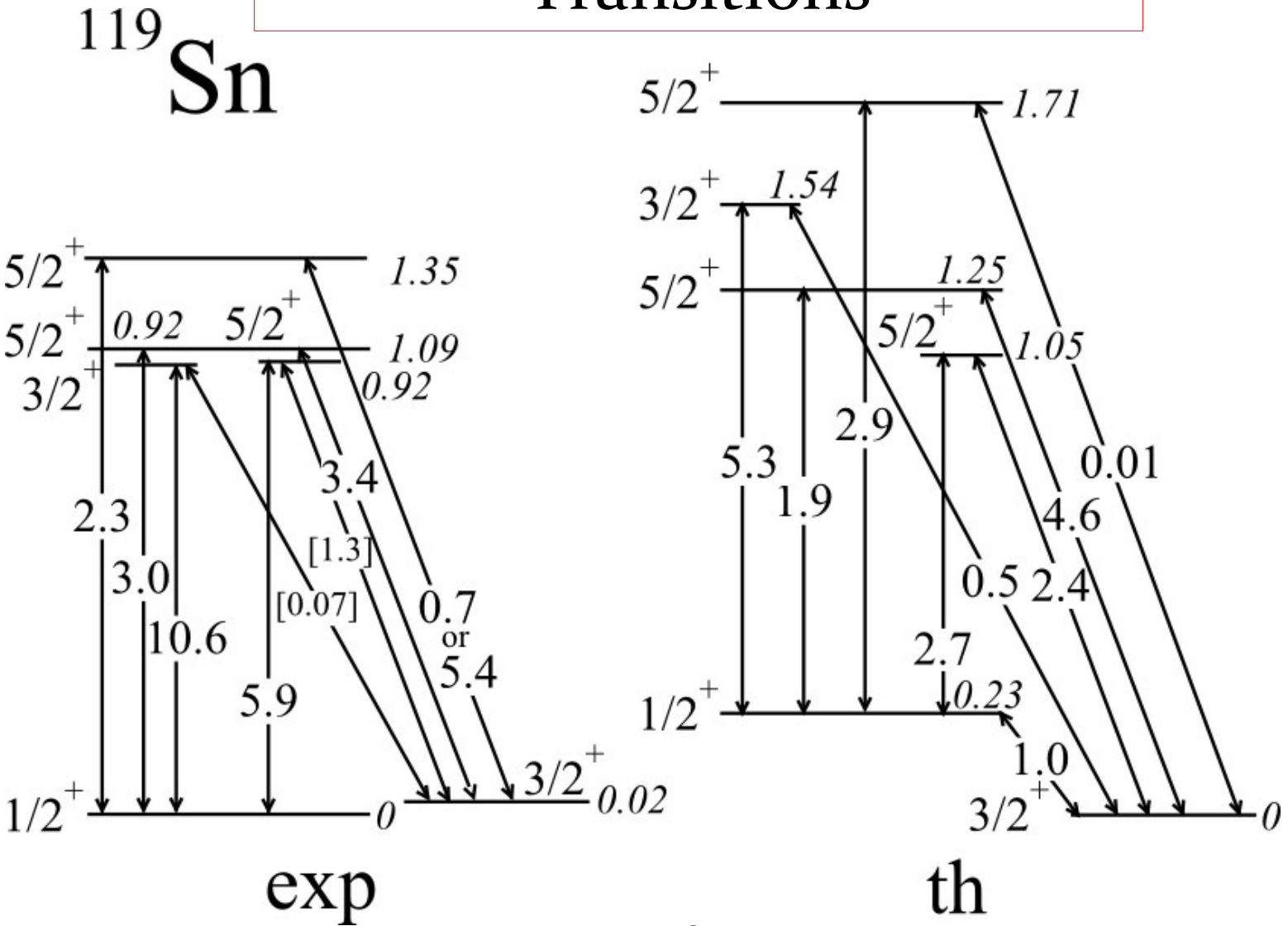

All of them would be zero without PVC!

$(\beta_2)_0$= 0.12 Go = 0.22 MeV mk=0.7

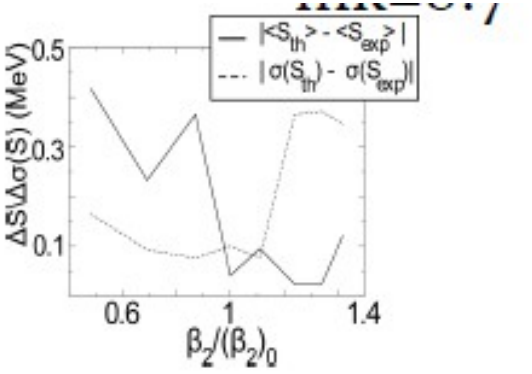

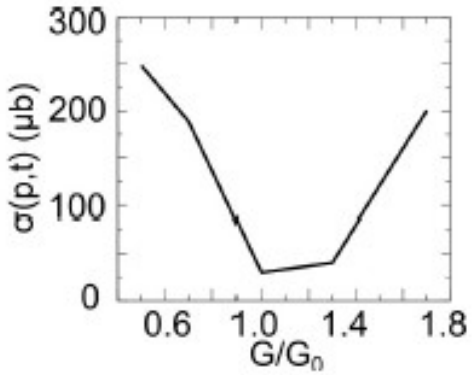

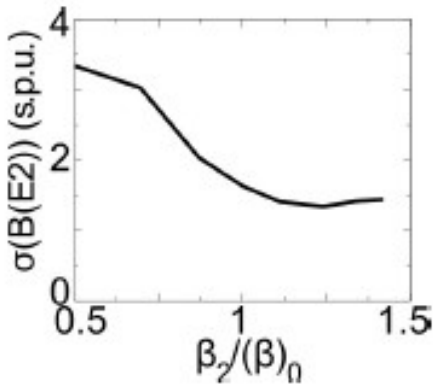

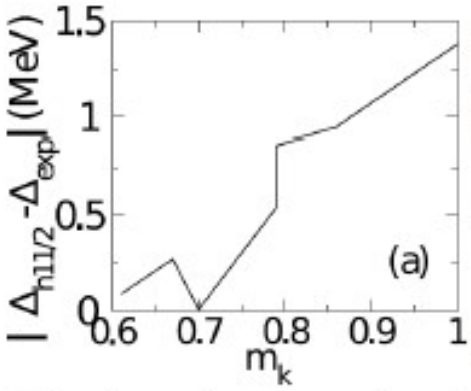

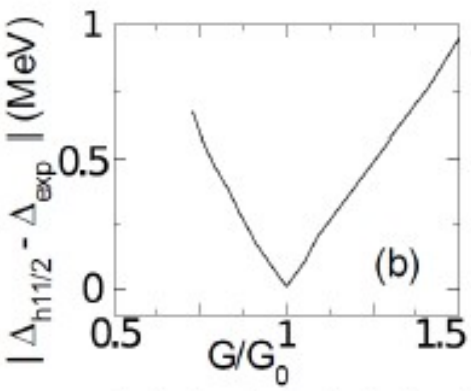

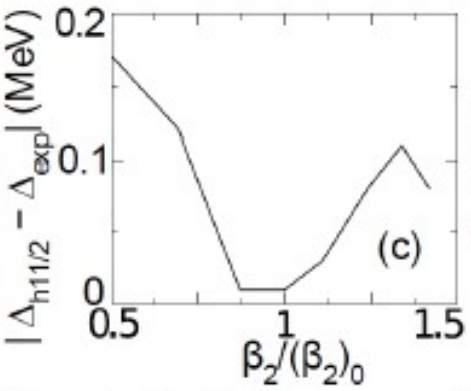

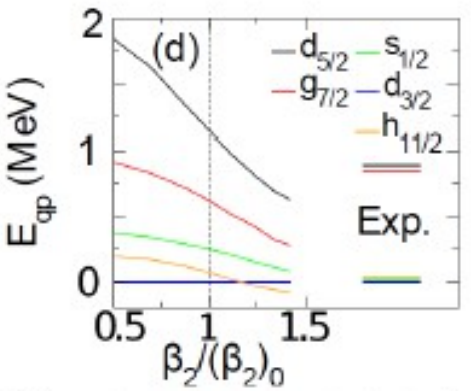

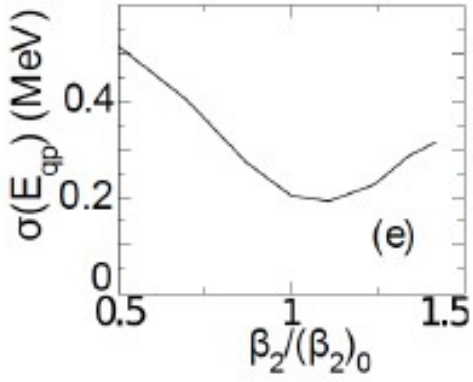

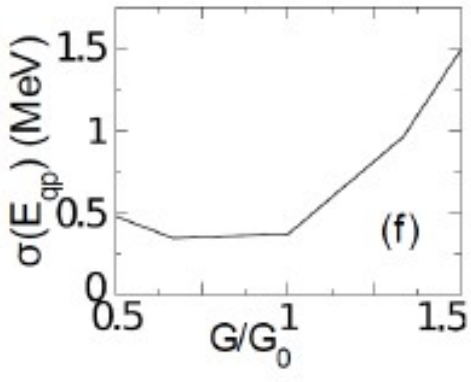

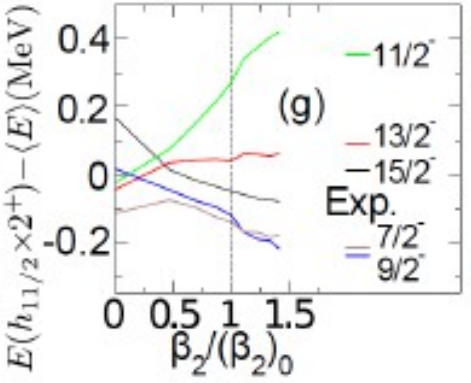

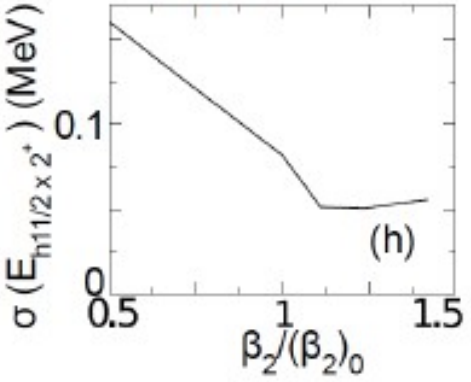

About the necessity of V_ind in Nuclear Struture Studies,

note that it appears when BMF calculations are performed

INEVITABILY.....

meaning that if you are not aware of V_ind, and you use empirical pairing interactions in your BMF calculations, as a matter of fact your results (whatever) are associated to a too large pairing gap.

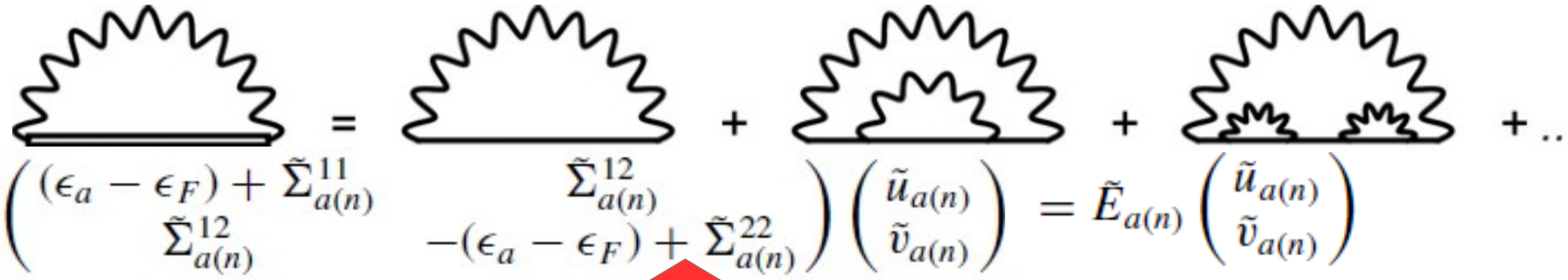

$$\begin{pmatrix} (\epsilon_a - \epsilon_F) + \tilde{\Sigma}^{11}_{a(n)} & \tilde{\Sigma}^{12}_{a(n)} \\ \tilde{\Sigma}^{12}_{a(n)} & -(\epsilon_a - \epsilon_F) + \tilde{\Sigma}^{22}_{a(n)} \end{pmatrix} \begin{pmatrix} \tilde{u}_{a(n)} \\ \tilde{v}_{a(n)} \end{pmatrix} = \tilde{E}_{a(n)} \begin{pmatrix} \tilde{u}_{a(n)} \\ \tilde{v}_{a(n)} \end{pmatrix}$$

$$\langle a(n);j_z\text{-}j_z|V_{ind}|b(m);j'_z\text{-}j'_z\rangle = \sum_{LJM} (f+g)_{LJM}\,(f-g)_{LJM} \times \left[\frac{1}{\tilde{E}_{a(n)} - \tilde{E}_{b(m)} - \hbar\omega_{\lambda\nu}} - \frac{1}{\tilde{E}_{a(n)} + \tilde{E}_{b(m)} + \hbar\omega_{\lambda\nu}}\right]$$

Future developments

- V_ind in larger spaces: coupling to continuum.

  Some experience in pair addition/removal cases
  In light halo nuclei 11Li.

- T=0 pairing in finite nuclei.

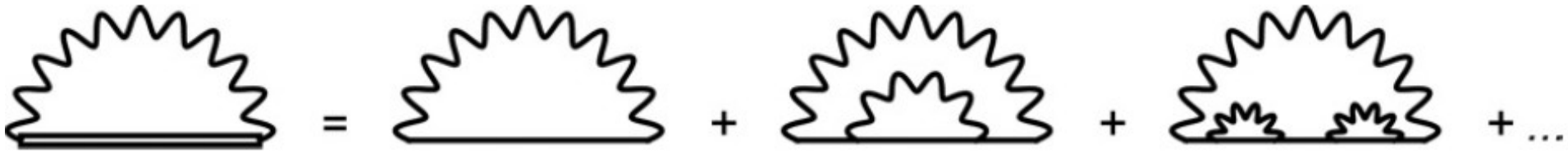

$$\begin{pmatrix} (\epsilon_a - \epsilon_F) + \tilde{\Sigma}^{11}_{a(n)} & \tilde{\Sigma}^{12}_{a(n)} \\ \tilde{\Sigma}^{12}_{a(n)} & -(\epsilon_a - \epsilon_F) + \tilde{\Sigma}^{22}_{a(n)} \end{pmatrix} \begin{pmatrix} \tilde{u}_{a(n)} \\ \tilde{v}_{a(n)} \end{pmatrix} = \tilde{E}_{a(n)} \begin{pmatrix} \tilde{u}_{a(n)} \\ \tilde{v}_{a(n)} \end{pmatrix}$$

$$\Sigma^{11\mathrm{pho}}_{a(n)} = \sum_{b,m,\lambda,\nu} \frac{(f+g)^2\,[ab(m)\lambda\nu]\,S^2}{\tilde{E}_{a(n)} - \tilde{E}_{b(m)} - \hbar\omega_{\lambda\nu}} + \sum_{b,m,\lambda,\nu} \frac{(f-g)^2\,[ab(m)\lambda\nu]\,P^2}{\tilde{E}_{a(n)} + \tilde{E}_{b(m)} + \hbar\omega_{\lambda\nu}}$$

$$\Sigma^{12\mathrm{pho}}_{a(n)} = -\sum_{b,m,\lambda,\nu} (f^2-g^2)[ab(m)\lambda\nu]\; G \times \left[\frac{1}{\tilde{E}_{a(n)} - \tilde{E}_{b(m)} - \hbar\omega_{\lambda\nu}} - \frac{1}{\tilde{E}_{a(n)} + \tilde{E}_{b(m)} + \hbar\omega_{\lambda\nu}} \right].$$

$S = u_a u'_b - v_a v'_b$

$P = u_a v'_b + v_a u'_b$

$G = S^* P$

Terasaki et al.

$$\tilde{\Sigma}^{12}_{a(n)} = \Delta^{\mathrm{BCS}}_a + \tilde{\Sigma}^{12,\mathrm{pho}}_{a(n)}$$

T=1(time reversal)BCS with Self energy effects

$$(2j_a+1)\tilde{\Delta}_{a(n)} = -Z_{a(n)} \sum_{b,m} V_{\text{eff}}[a(n)b(m)] N_{b(m)} \frac{\tilde{\Delta}_{b(m)}}{2\tilde{E}_{b(m)}}$$

$$V_{\text{eff}}[a(n)b(m)] = V_{\text{bare}}[ab] + V_{\text{ind}}[a(n)b(m)]$$

$V_{\text{ind}}[a(n)b(m)] = \Sigma_{jz,j'z}$ <a(n);jz-jz|V_{ind}|b(m);j'z-j'z>

A.Idini, et al
PRC85,14331

<a(n);j_z-j_z|V_{ind}|b(m);j'$_z$-j'$_z$> = Σ_{LJM} $(f+g)_{LJM}$ $(f-g)_{LJM}$ x

$$\left[\frac{1}{\tilde{E}_{a(n)} - \tilde{E}_{b(m)} - \hbar\omega_{\lambda\nu}} - \frac{1}{\tilde{E}_{a(n)} + \tilde{E}_{b(m)} + \hbar\omega_{\lambda\nu}} \right].$$

$$Z_{a(n)} = \left(1 - \frac{\Sigma^{11}_{a(n)} - \Sigma^{11}_{a(-n)}}{2\tilde{E}_{a(n)}} \right)^{-1} \qquad N_{a(n)} = x^2_{a(n)} + y^2_{a(n)}$$

$$\tilde{E}_{a(n)} = \sqrt{(\tilde{\epsilon}_{a(n)} - \epsilon_F)^2 + \tilde{\Delta}^2_{a(n)}} \qquad \tilde{\epsilon}_{a(n)} - \epsilon_F = Z_{a(n)} \left[(\epsilon_a - \epsilon_F) + \Sigma^{\text{even}}_{a(n)} \right]$$

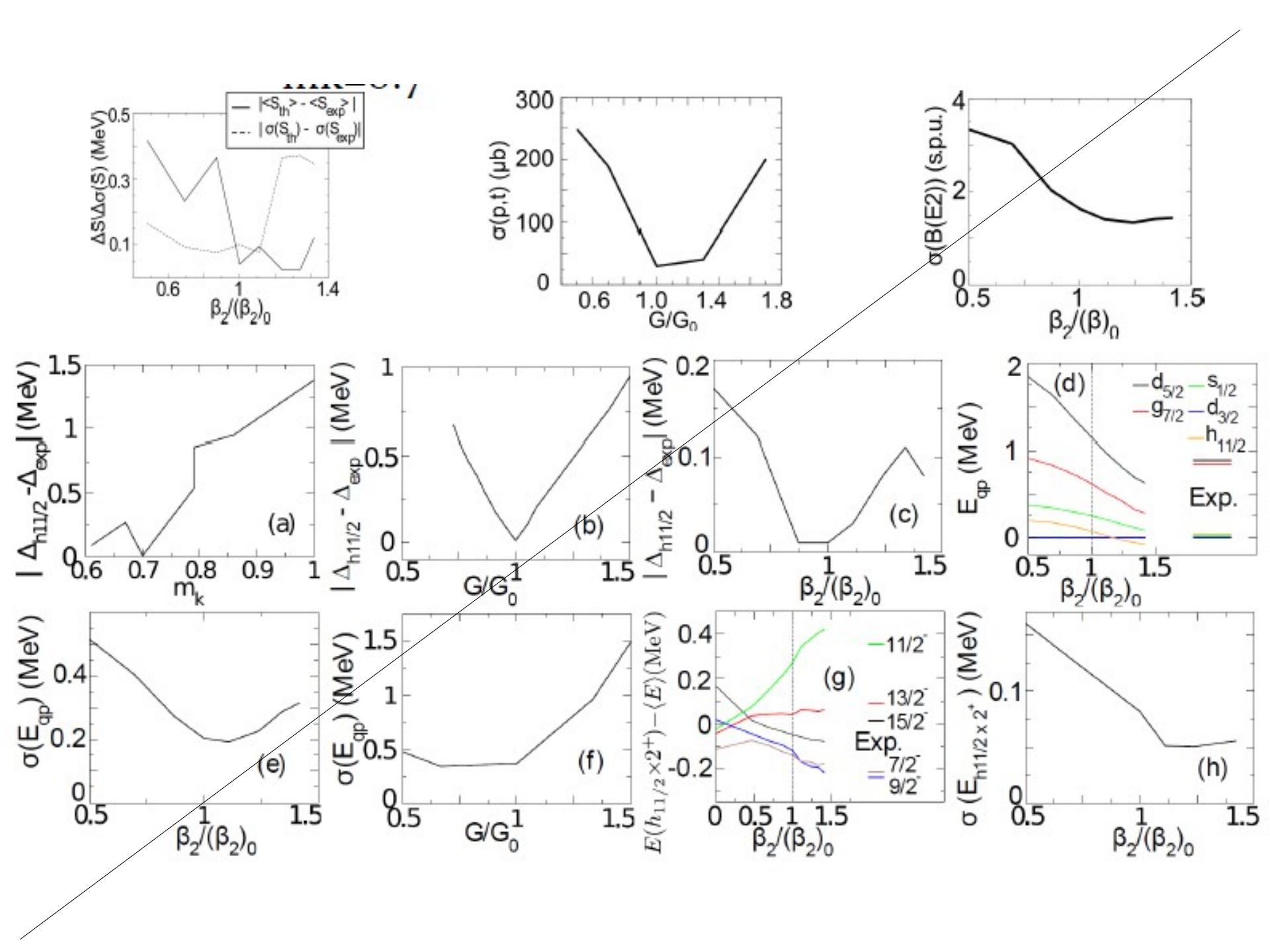
$\Delta S \backslash \Delta\sigma(S)$ (MeV)
$|\langle S_{th}\rangle - \langle S_{exp}\rangle|$
$|\sigma(S_{th}) - \sigma(S_{exp})|$
$\beta_2/(\beta_2)_0$
$\sigma(p,t)$ (μb)
G/G_0
$\sigma(B(E2))$ (s.p.u.)
$\beta_2/(\beta)_0$
$|\Delta_{h11/2} - \Delta_{exp}|$ (MeV)
m_k
(a)
G/G_0
(b)
(c)
E_{qp} (MeV)
(d)
$d_{5/2}$ $s_{1/2}$ $g_{7/2}$ $d_{3/2}$ $h_{11/2}$
Exp.
$\sigma(E_{qp})$ (MeV)
(e)
(f)
$E(h_{11/2}\times 2^+) - \langle E\rangle$ (MeV)
(g)
$11/2^-$
$13/2^-$
$15/2^-$
Exp.
$7/2^-$
$9/2^-$
$\sigma(E_{h11/2\times 2^+})$ (MeV)
(h)

Collegamento con neutron matter – role of spin fluctuations – Dickhoff+Polls - T=0 pairing

Le slides seguenti avevano materiale su questi argomenti, bisogna scegliere le migliori

T=0 pairing problem

Alm et al. Z.Phys.A337,355 (1990)
Vonderfecht et al. PLB253,1 (1991)
Baldo et al. PLB283, 8 (1992)

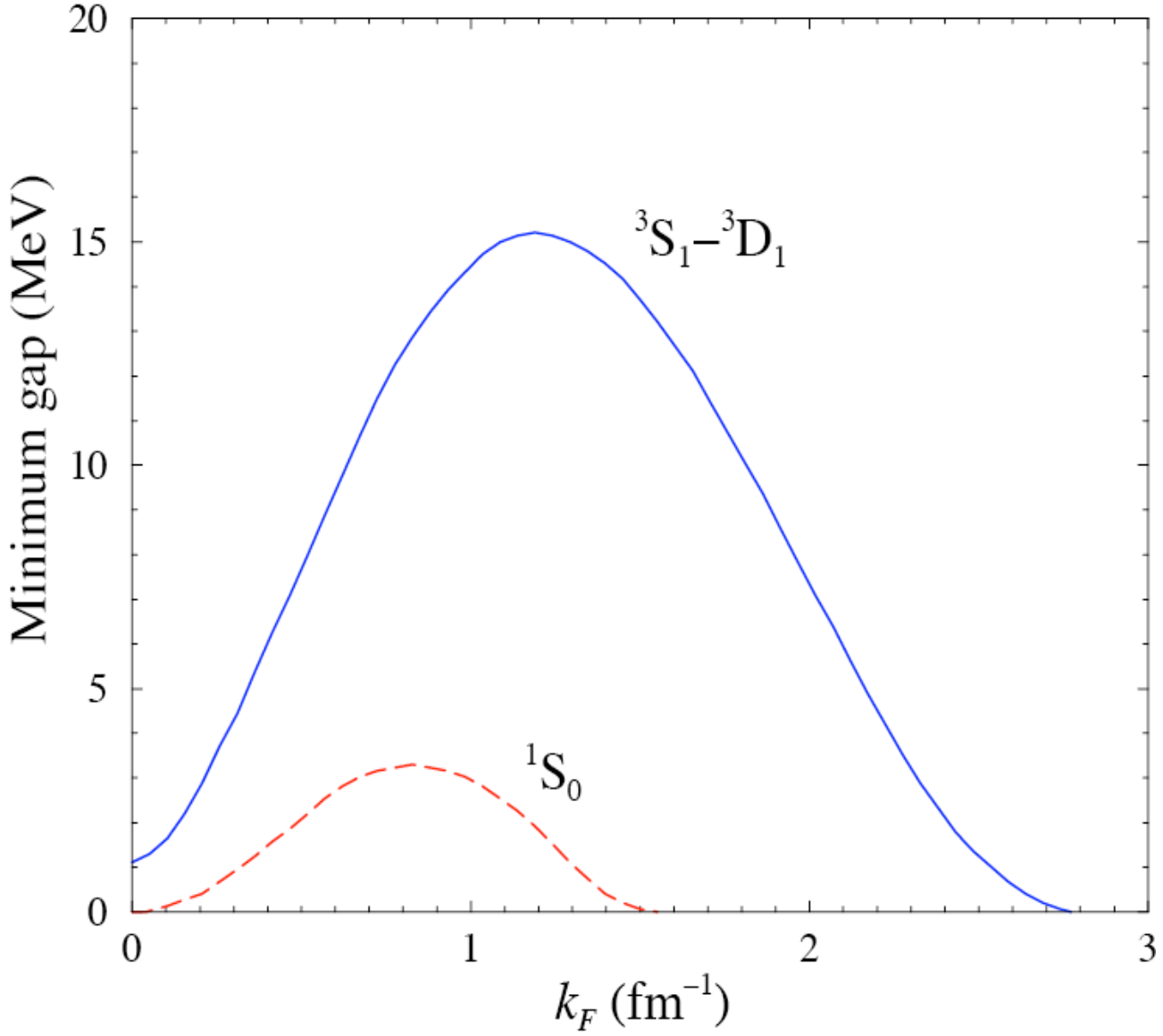

Proton-neutron pairing in symmetric nuclear matter

$^3S_1$-$^3D_1$

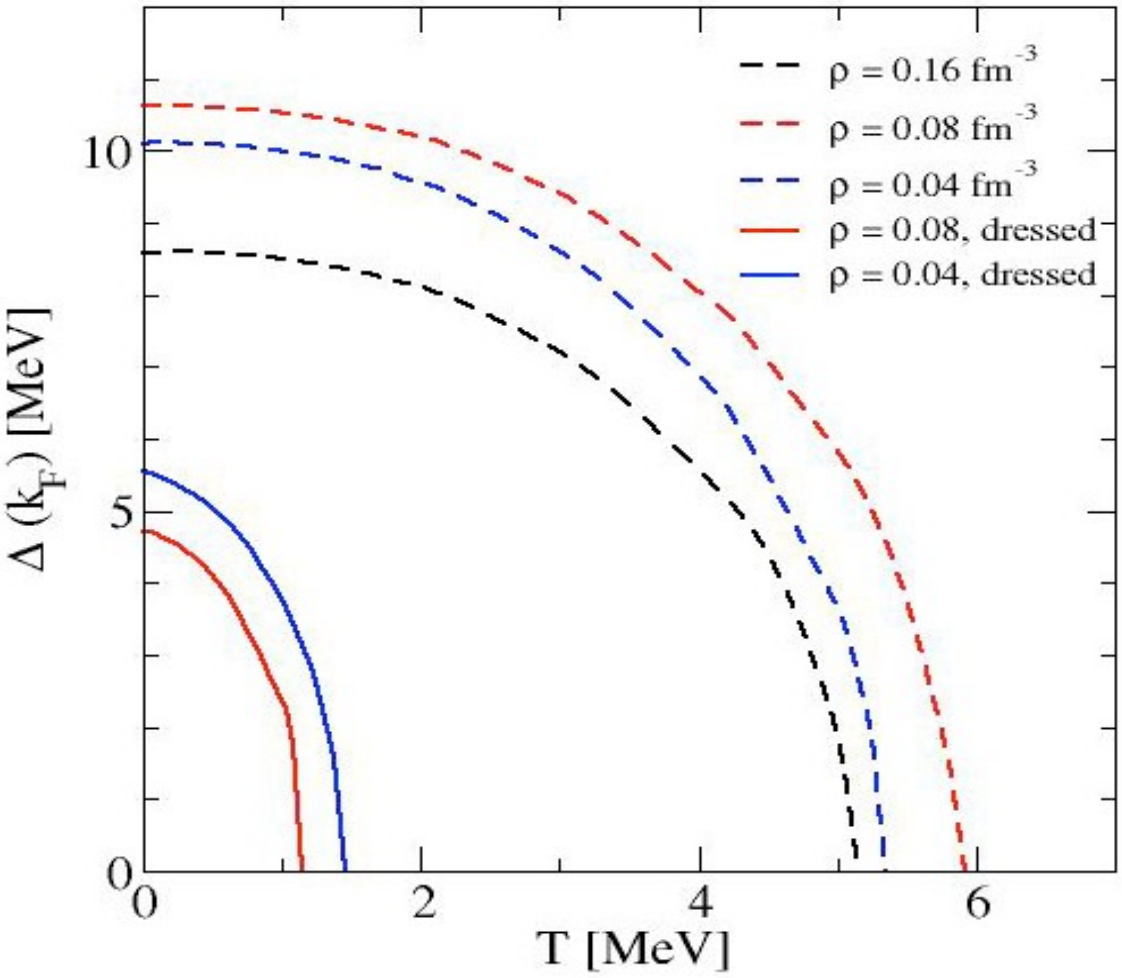

Using CDBonn

Dashed lines:
quasiparticle poles

Solid lines:
dressed nucleons

No pairing at saturation density!!!!

Dickhoff talk

A similar scheme could be adopted to calculate the T=0 pairing gap in finite nuclei

Microscopic calculation of the matrix elements of the induced interaction in spherical open-shell nuclei including spin modes

Vibrations are calculated with QRPA and SKM* interaction

Particle-hole interaction:

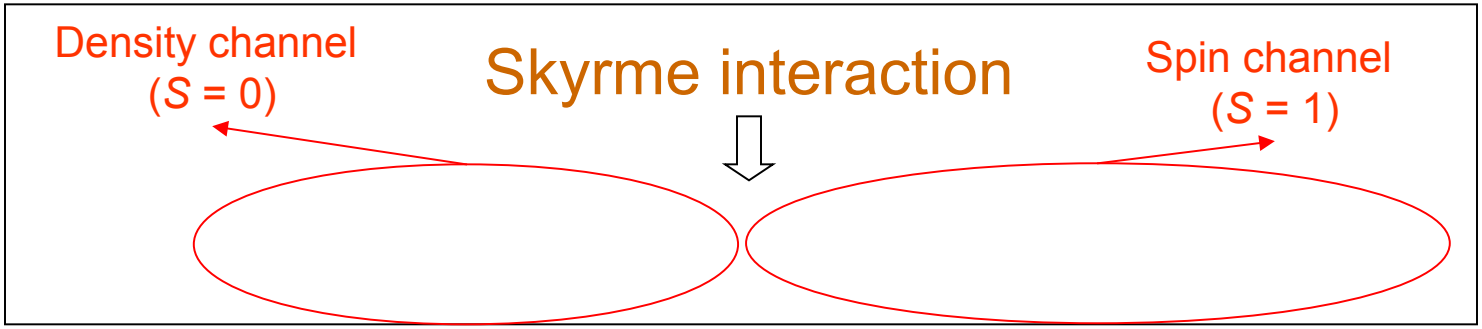

G. Gori et al., Phys. Rev. C72(2005)11302

Finirei qua..

PAIRING GAP IN FINITE NUCLEI

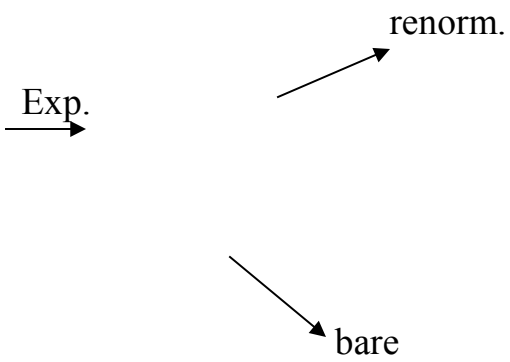

Medium effects **increase** the gap in ^{120}Sn and bring it in agreement with experiment

F. Barranco et al., Eur. J. Phys. A21(2004) 57

PAIRING GAP IN NEUTRON MATTER

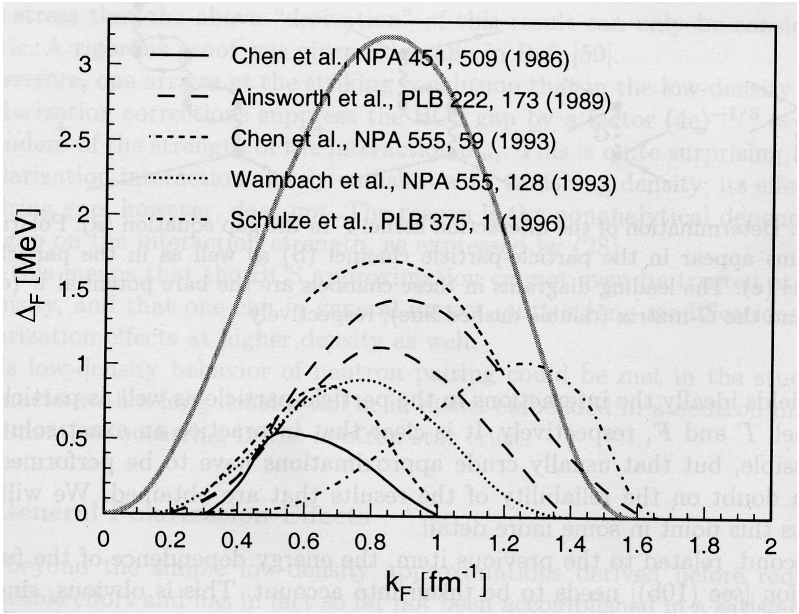

Medium effects **decrease** the gap

C. Shen et al., PRC 67(2003) 061302

Pairing interaction in neutron and nuclear matter and exchange of p.h. excitations

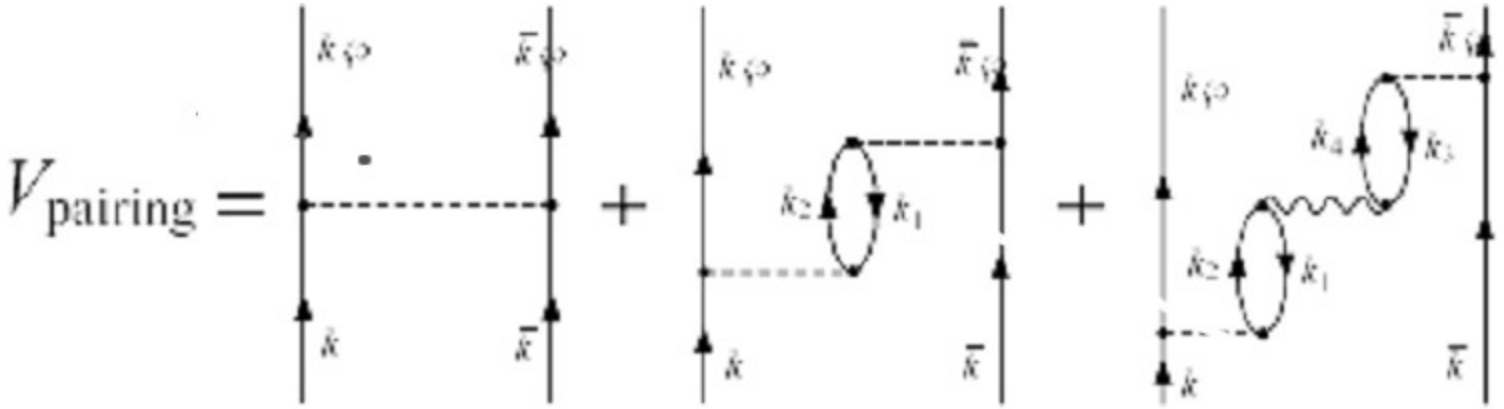

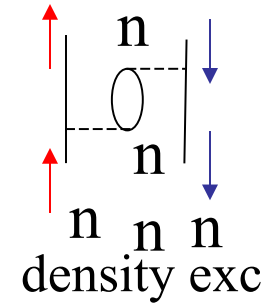

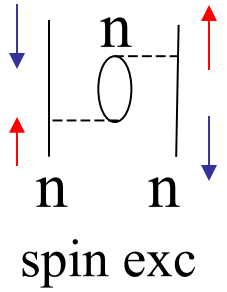

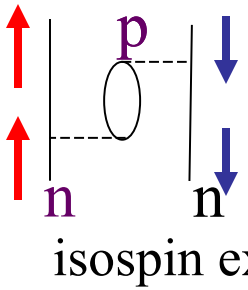

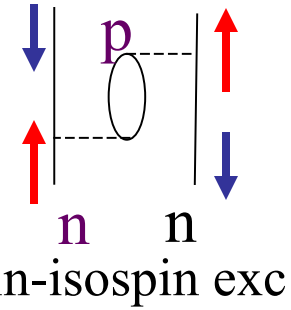

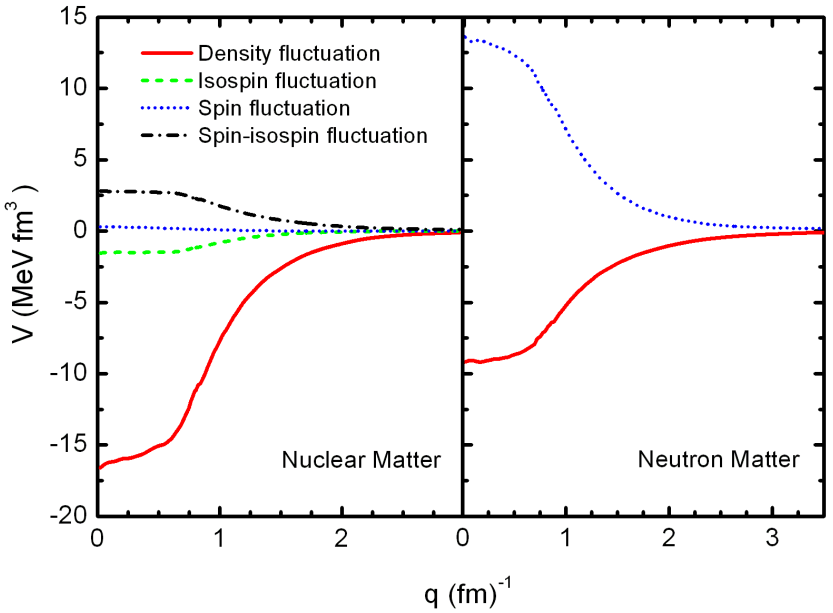

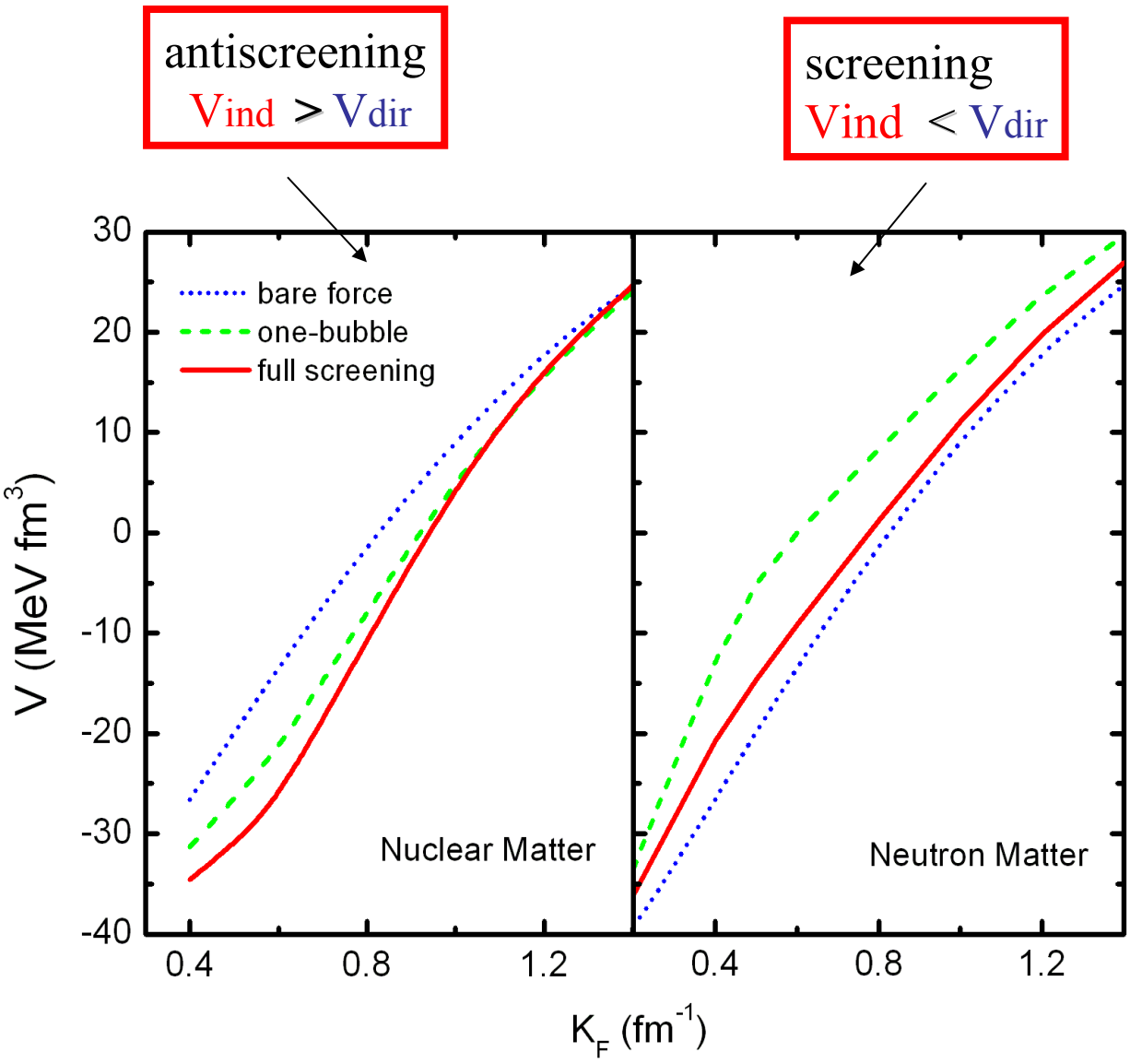

L.G. Cao, U. Lombardo, P. Schuck, PRC 74(2006)64301

Microscopic calculation of the matrix elements of the induced interaction in spherical open-shell nuclei including spin modes

Vibrations are calculated with QRPA and SKM* interaction

Particle-hole interaction:

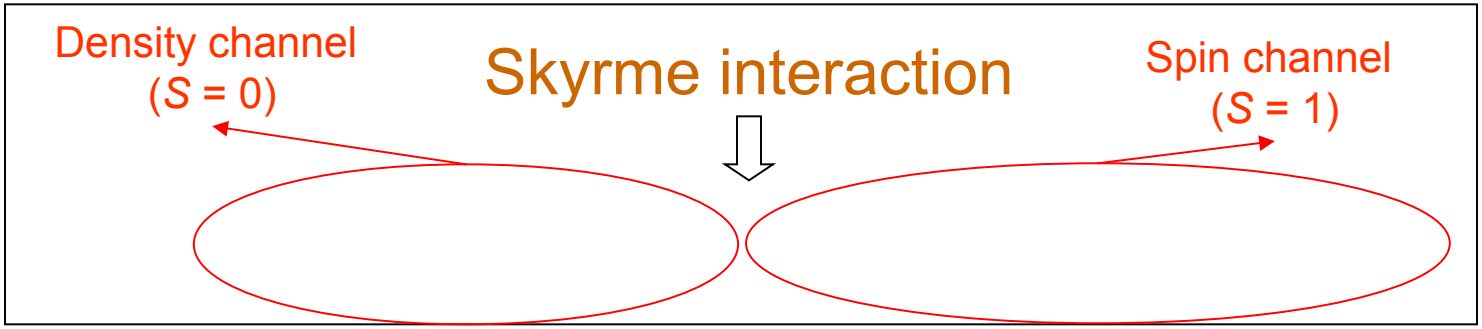

G. Gori et al., Phys. Rev. C72(2005)11302

Microscopic calculation of the matrix elements of the induced interaction

S=0 (attractive)

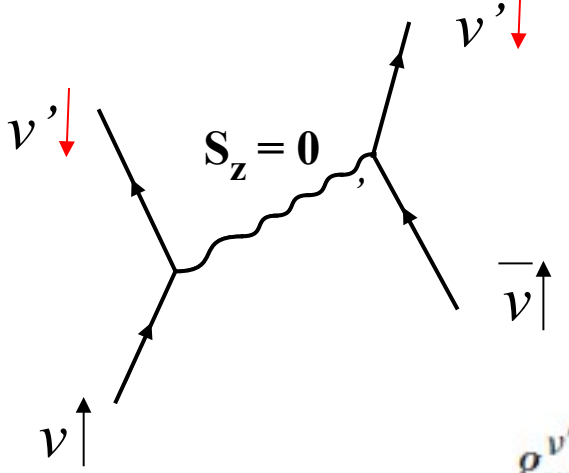

$$f^{\nu'm'}_{\nu m;J^\pi Mi} = i^{l-l'}\langle j'm'|(i)^J Y_{JM}|jm\rangle \times \int dr\varphi_{\nu'}\left[(F_0+F_0')\delta\rho^i_{J^\pi n}+(F_0-F_0')\delta\rho^i_{J^\pi p}\right]\varphi_\nu$$

S=1 (repulsive)

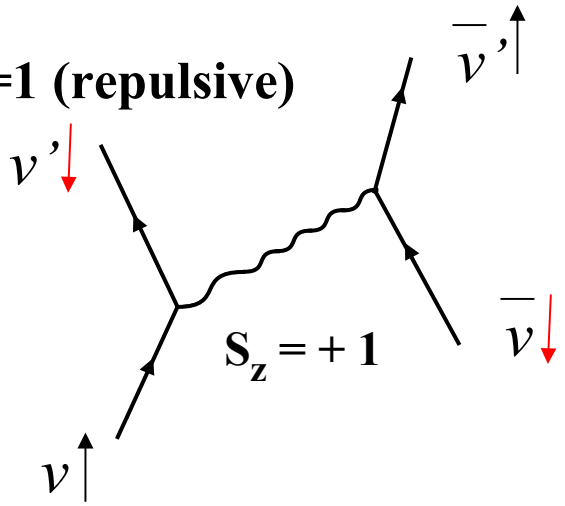

$$g^{\nu'm'}_{\nu m J^\pi Mi} = \sum_{L=J-1}^{J+1} i^{l-l'}\langle j'm'|(i)^L[Y_L\times\sigma]_{JM}|jm\rangle \times \int dr\varphi_{\nu'}\left[(G_0+G_0')\delta\rho^i_{J^\pi Ln} + (G_0-G_0')\delta\rho^i_{J^\pi Lp}\right]\varphi_\nu$$

FINITE NUCLEI (^{120}Sn):

The induced interaction arising from the coupling to surface and spin modes is attractive and leads to a pairing gap of about 0.7 MeV (50 % of the experimental value). Excluding the coupling to spin modes, the gap increases to about 1.1 MeV.

One must then add the bare interaction.

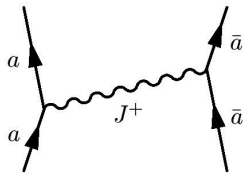

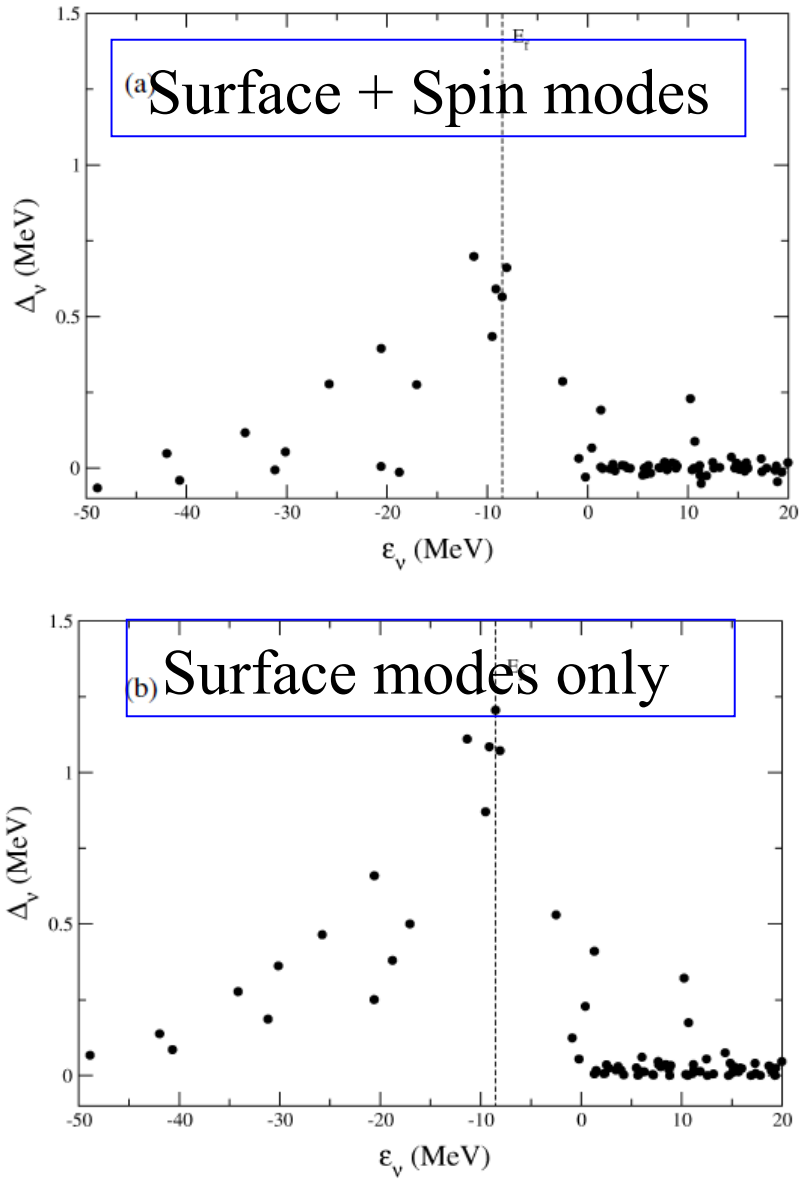

FIG. 4. (a) The state-dependent pairing gap as a function of the single-particle energies obtained by solving the BCS equations associated with the total induced interaction matrix elements; (b) same as (a) but for the matrix elements associated with the spin-independent part of the particle-hole interaction.

Why such a difference with neutron matter?

Crucial: the surface nature of density modes. This assures an important overlap between the transition density and the single-particle wave-function at the Fermi energy.

Volume nature of Spin-modes

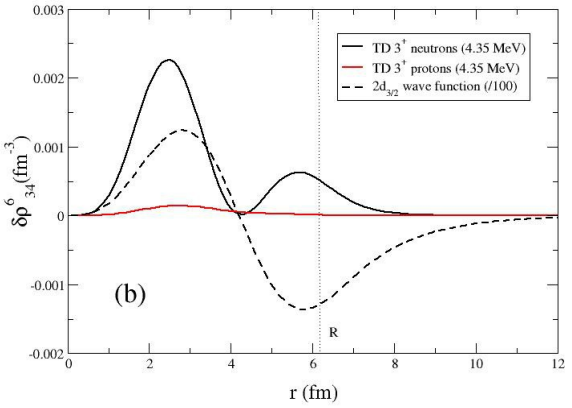

$$= (-)^{M+J} \langle j'm' | (i)^J Y_{J-M} | jm \rangle \int \mathrm{d}r \varphi_{j'}(r) \varphi_j(r) \zeta_{JL}(r),$$

$$= (-)^{J+M+1} \sum_{L=J-1}^{J+1} \langle j'm' | (i)^L [Y_L \times \sigma]_{J-M} | jm \rangle \int \mathrm{d}r \varphi_{j'}(r) \varphi_j(r) \xi_{JL}(r),$$

G-matrix

Gogny force

SkM* force

Density dependence of Landau parameters (at k=0)

Why such a difference with neutron matter?

The proton-neutron interaction in the particle vibration coupling plays an essential role. If we cancel it, a net repulsive effect is obtained for the induced interaction.

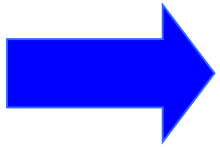

Strong difference between induced interaction in neutron and nuclear matter

Landau parameters of SkM* force in ^{120}Sn

PHYSICAL REVIEW C **72**, 011302(R) (2005)

Attractive and repulsive contributions of medium fluctuations to nuclear superfluidity

G. Gori,[1,2] F. Ramponi,[1,2] F. Barranco,[3] P. F. Bortignon,[1,2] R. A. Broglia,[1,2,4] G. Colò,[1,2] and E. Vigezzi[2]

[1]*Dipartimento di Fisica, Università degli Studi di Milano, via Celoria 16, I-20133 Milano, Italy*

[2]*INFN, Sezione di Milano, via Celoria 16, I-20133 Milano, Italy*

[3]*Departamento de Fisica Aplicada III, Escuela Superior de Ingenieros, Camino de los Descubrimientos s/n, E-41092 Sevilla, Spain*

[4]*The Niels Bohr Institute, University of Copenhagen, Blegdamsvej 17, DK-2100 Copenhagen Ø, Denmark*

(Received 10 December 2003; published 18 July 2005)

Oscillations of mainly surface character ($S = 0$ modes) give rise, in atomic nuclei, to an attractive (induced) pairing interaction, while spin ($S = 1$) modes of mainly volume character generate a repulsive interaction, the net effect being an attraction which accounts for a sizeable fraction of the experimental pairing gap. Suppressing the particle-vibration coupling mediated by the proton degrees of freedom, i.e., mimicking neutron matter, the total surface plus spin-induced pairing interaction becomes repulsive.

DOI: 10.1103/PhysRevC.72.011302 PACS number(s): 21.30.Fe, 21.60.Jz, 21.65.+f, 27.60.+j

$$v_{\rm ph}(\vec{r},\vec{r}') = \delta(\vec{r}-\vec{r}')\{[F_0 + F_0'\vec{\tau}\cdot\vec{\tau}'] + [(G_0 + G_0'\vec{\tau}\cdot\vec{\tau}')\,\vec{\sigma}\cdot\vec{\sigma}']\}$$

$$\langle \nu' m' \nu' \bar{m}' | v_{\rm ind} | \nu m \nu \bar{m}\rangle = \sum_{J^\pi M i} \frac{2(f+g)^{\nu' m'}_{\nu m; J^\pi M i}(f-g)^{\nu' m'}_{\nu m; J^\pi M i}}{E_0 - E_{\rm int}}$$

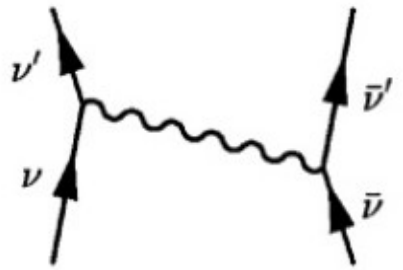

(a)

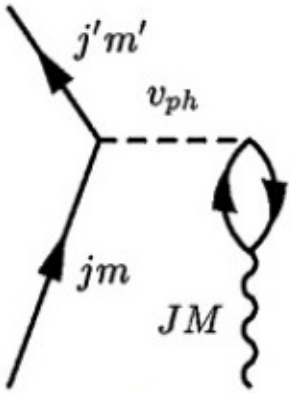

(b)

$$f^{\nu' m'}_{\nu m; J^\pi M i} = i^{l-l'}\langle j' m' | (i)^J Y_{JM} | j m\rangle \times \int dr \varphi_{\nu'}\left[(F_0 + F_0')\delta\rho^i_{J^\pi n} + (F_0 - F_0')\delta\rho^i_{J^\pi p}\right]\varphi_\nu$$

$$g^{\nu' m'}_{\nu m J^\pi M i} = \sum_{L=J-1}^{J+1} i^{l-l'}\langle j' m' | (i)^L [Y_L \times \sigma]_{JM} | j m\rangle \times \int dr \varphi_{\nu'}\left[(G_0 + G_0')\delta\rho^i_{J^\pi L n} + (G_0 - G_0')\delta\rho^i_{J^\pi L p}\right]\varphi_\nu$$

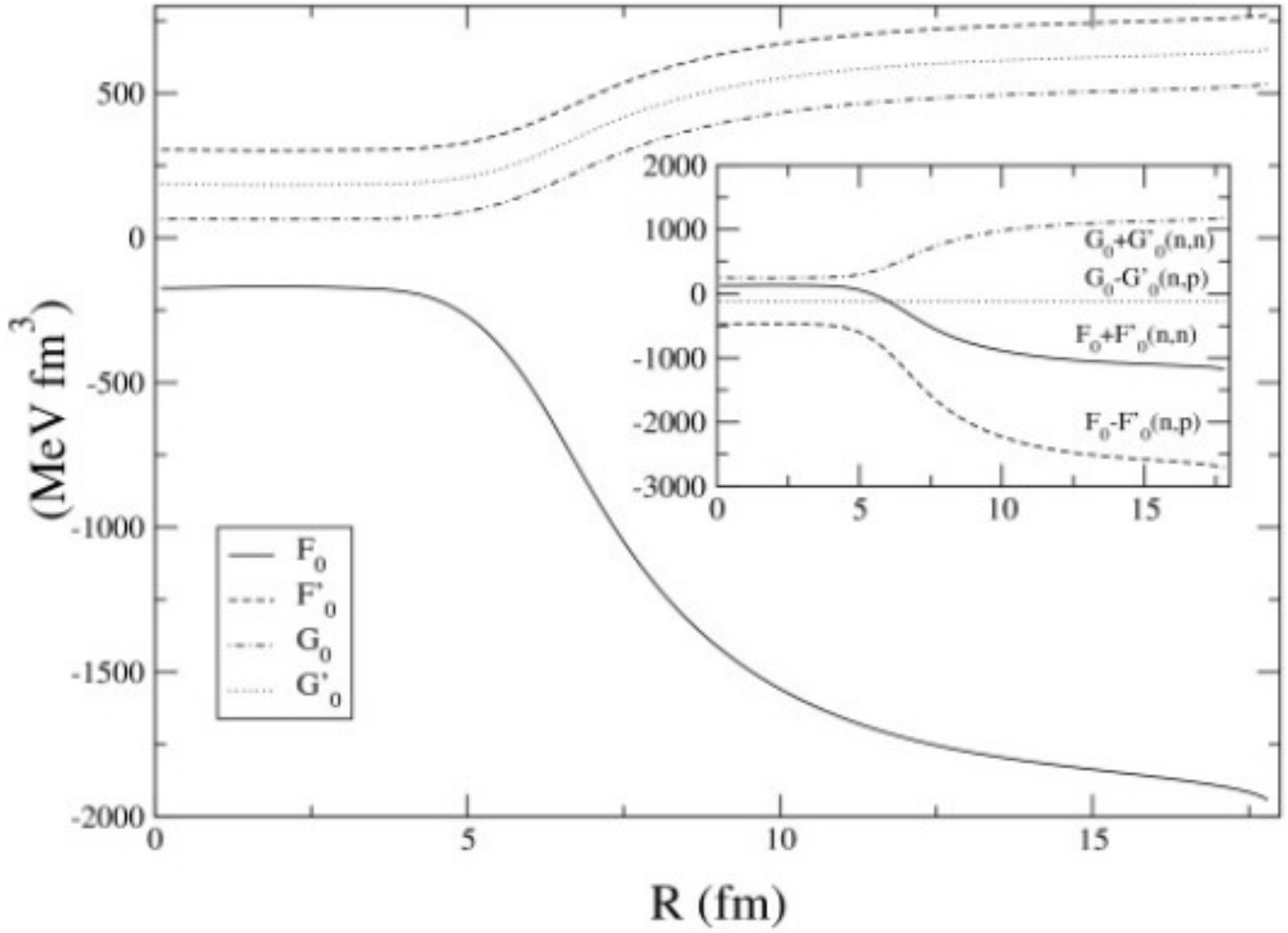

FIG. 1. Generalized Landau parameters associated with the interaction SkM* defining the strength of the particle-hole interaction in the isoscalar (F_0), isovector (F_0'), spin isoscalar (G_0), and spin isovector (G_0') channels. In the inset, the functions $F_0 + F_0'$ (n-n interaction), $F_0 - F_0'$ (n-p), $G_0 + G_0'$ (n-n), and $G_0 - G_0'$ (n-p) are also shown.

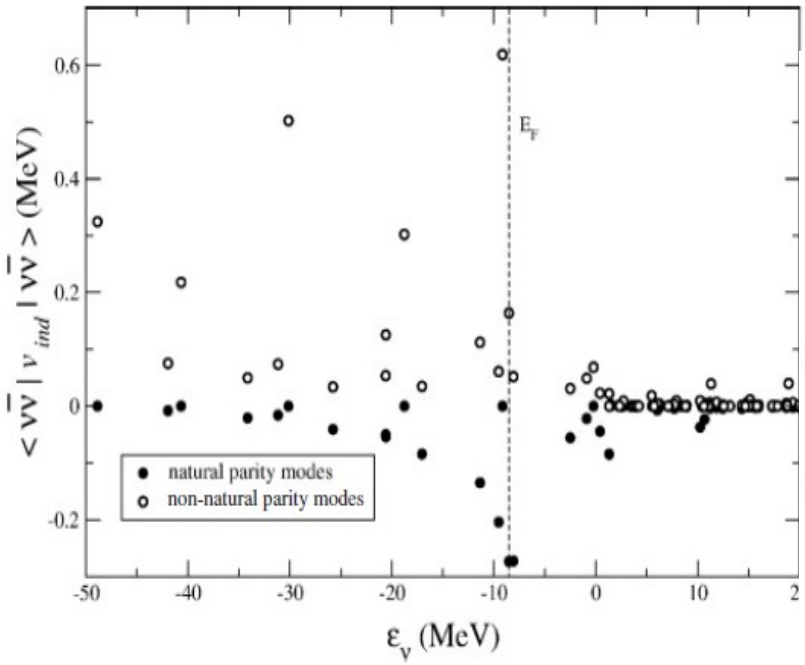

FIG. 3. Diagonal induced pairing matrix elements resulting fror the exchange of phonons with natural parity (filled circles) and thos resulting from the exchange of phonons with non-natural parit vibrations (empty circles), displayed as a function of the energy c the single-particle state ϵ_ν.

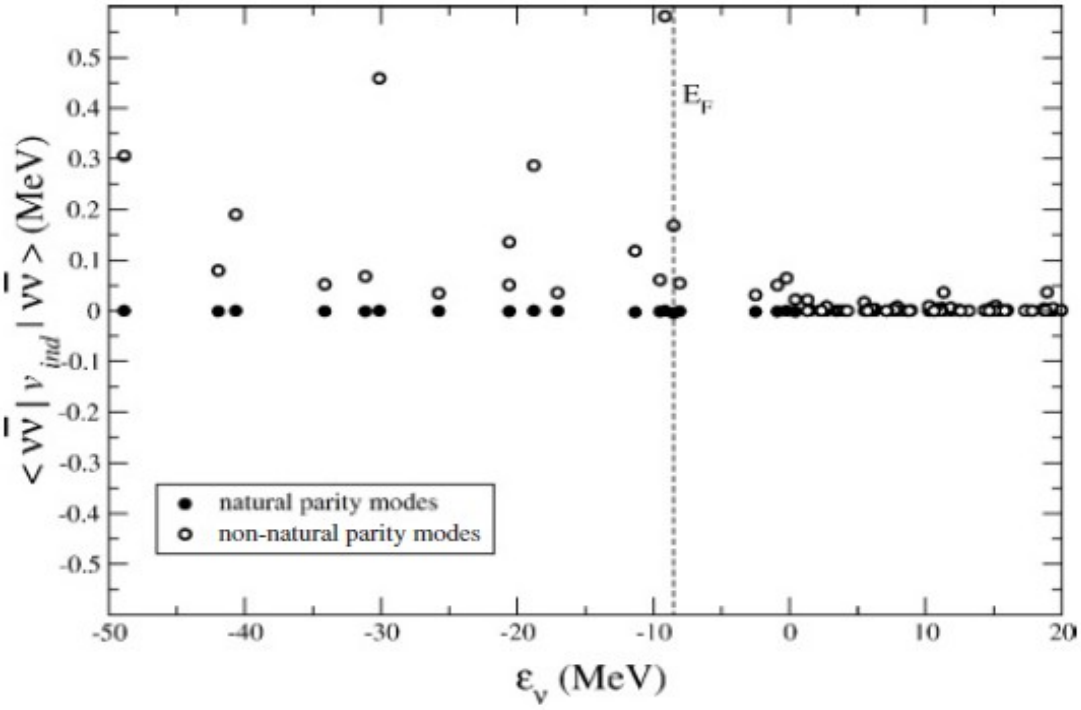

FIG. 6. The diagonal matrix elements associated with the exchange of phonons of natural (filled circles) and non-natural (open circles) parity as a function of the energy of the single-particle states. The proton part of the phonon wave functions was not included in the calculation.

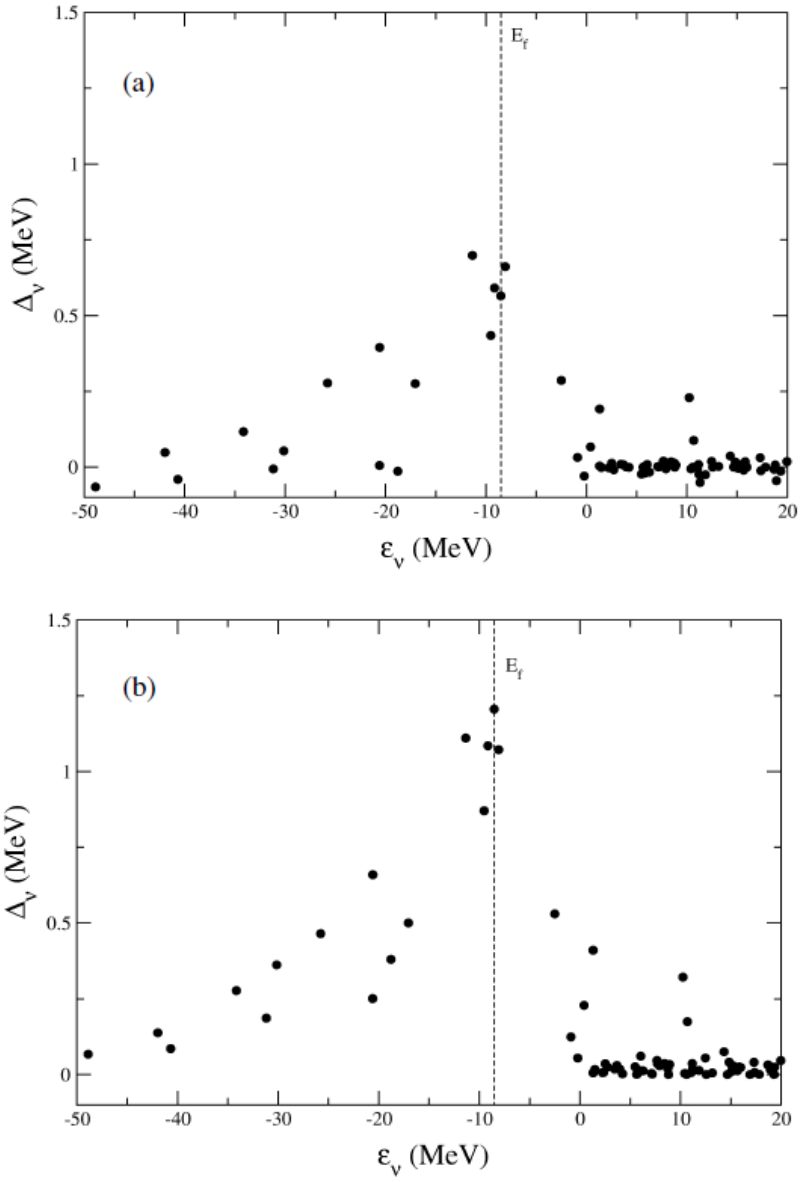

FIG. 4. (a) The state-dependent pairing gap as a function of the single-particle energies obtained by solving the BCS equations associated with the total induced interaction matrix elements; (b) same as (a) but for the matrix elements associated with the spin-independent part of the particle-hole interaction.

T=0 pairing problem

Alm et al. Z.Phys.A337,355 (1990)
Vonderfecht et al. PLB253,1 (1991)
Baldo et al. PLB283, 8 (1992)

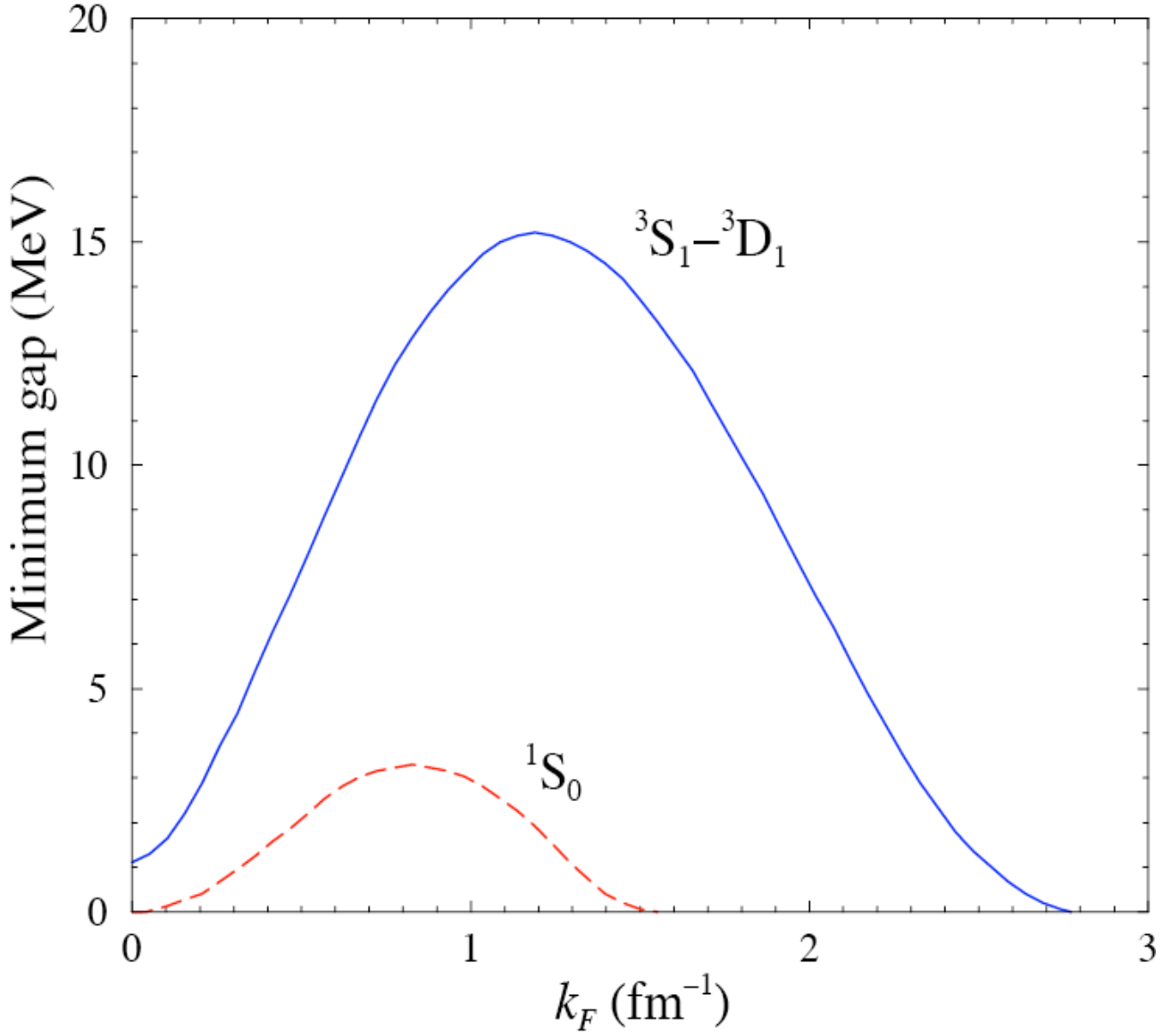

Proton-neutron pairing in symmetric nuclear matter

$^3S_1$-$^3D_1$

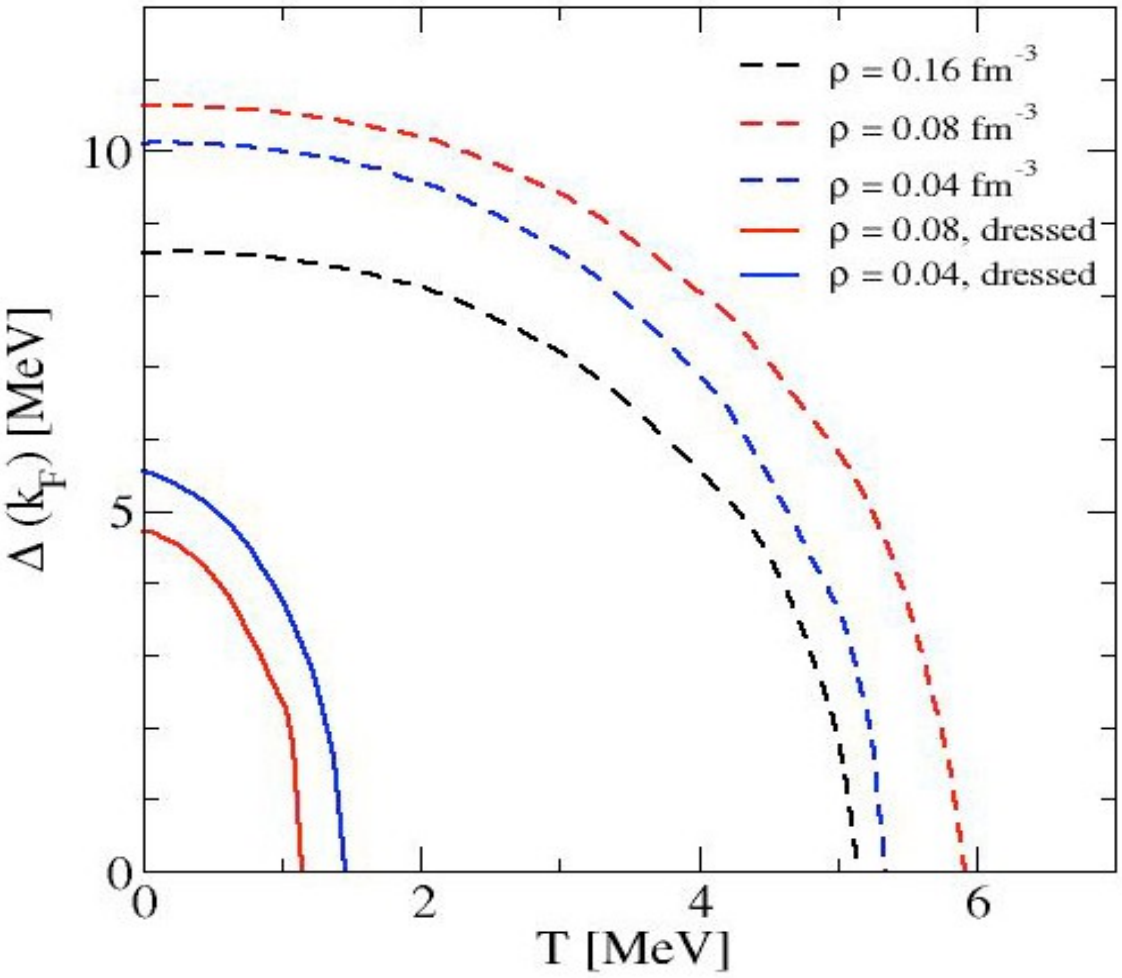

Using CDBonn

Dashed lines:
quasiparticle poles

Solid lines:
dressed nucleons

No pairing at saturation density!!!!

Dickhoff et al.

Slides che non mostrerei

PHYSICAL REVIEW C **85**, 014331 (2012)

Quasiparticle renormalization and pairing correlations in spherical superfluid nuclei

A. Idini,[1,2] F. Barranco,[3] and E. Vigezzi[2]

[1]*Dipartimento di Fisica, Università degli Studi di Milano, Via Celoria 16, IT-20133 Milano, Italy*

[2]*INFN, Sezione di Milano, Via Celoria 16, IT-20133 Milano, Italy*

[3]*Departamento de Fisica Aplicada III, Escuela Superior de Ingenieros, Universidad de Sevilla, Camino de los Descubrimientos s/n, ES-41092 Sevilla, Spain*

(Received 25 May 2011; revised manuscript received 15 November 2011; published 31 January 2012)

Within the framework of nuclear field theory (NFT), the spectrum of atomic nuclei is described in terms of collective and quasiparticle degrees of freedom, that is, of elementary modes of excitation that are directly related to experiment and of their coupling, whose strength and form factors are the basic ingredients entering in the calculations of absolute cross sections of inelastic and of one- and two-particle transfer reactions. We present a detailed discussion of the solution of the Dyson equation, also known as the Nambu-Gor'kov equations in the case of a superfluid system, which propagates medium polarization processes calculated making use of NFT to all orders of perturbation, resulting in the dressing of quasiparticles and in the induced pairing interaction. The formalism is applied to the superfluid nucleus ^{120}Sn. Results concerning the low-energy spectrum, that is, the quasiparticle strength distribution of the neighboring odd-A nuclei ^{119}Sn and ^{121}Sn, are presented and compared with the experimental findings.

General (HFB like) beyond time-reversal BCS is needed in coupling to continuum and in non-homogeneus systems

ELSEVIER

Physics Letters B 390 (1997) 13–17

Role of finite nuclei on the pairing gap of the inner crust of neutron stars

F. Barranco [a], R.A. Broglia [b,c], H. Esbensen [d], E. Vigezzi [b]

[a] *Dpto. de Física Aplicada, Escuela Superior de Ingenieros, Universidad de Sevilla, Spain*
[b] *Dipartimento di Fisica, Università di Milano and INFN, Sezione di Milano, Italy*
[c] *The Niels Bohr Institute, University of Copenhagen, Denmark*
[d] *Physics Division, Argonne National Laboratory, Argonne, IL 60439, USA*

Received 20 August 1996; revised manuscript received 8 October 1996
Editor: C. Mahaux

Abstract

The state dependent pairing gap is calculated for a Wigner cell lying in the inner crust of a neutron star, allowing neutrons o interact through the Argonne v_{14} potential. Although the values of the pairing gap will be renormalized by the induced nteraction, the result found, that the pairing gap is sensitive to the presence of the finite atomic nucleus in the sea of free ieutrons, is expected to be quite general.

Pairing interaction: V-14 Argonne $^1S_0$

$$\begin{pmatrix} \epsilon - \epsilon_F & \Delta \\ -\Delta & -(\epsilon - \epsilon_F) \end{pmatrix} \begin{pmatrix} U^i \\ V^i \end{pmatrix} = E_i \begin{pmatrix} U^i \\ V^i \end{pmatrix}, \qquad (1)$$

$$\Delta_{a_1 a_2} = -\tfrac{1}{2} \sum_{b_1 b_2} \sum_i U^i_{b_1} V^i_{b_2} \langle a_1 \tilde{a}_2 | v(12) | b_1 \tilde{b}_2 \rangle. \qquad (2)$$

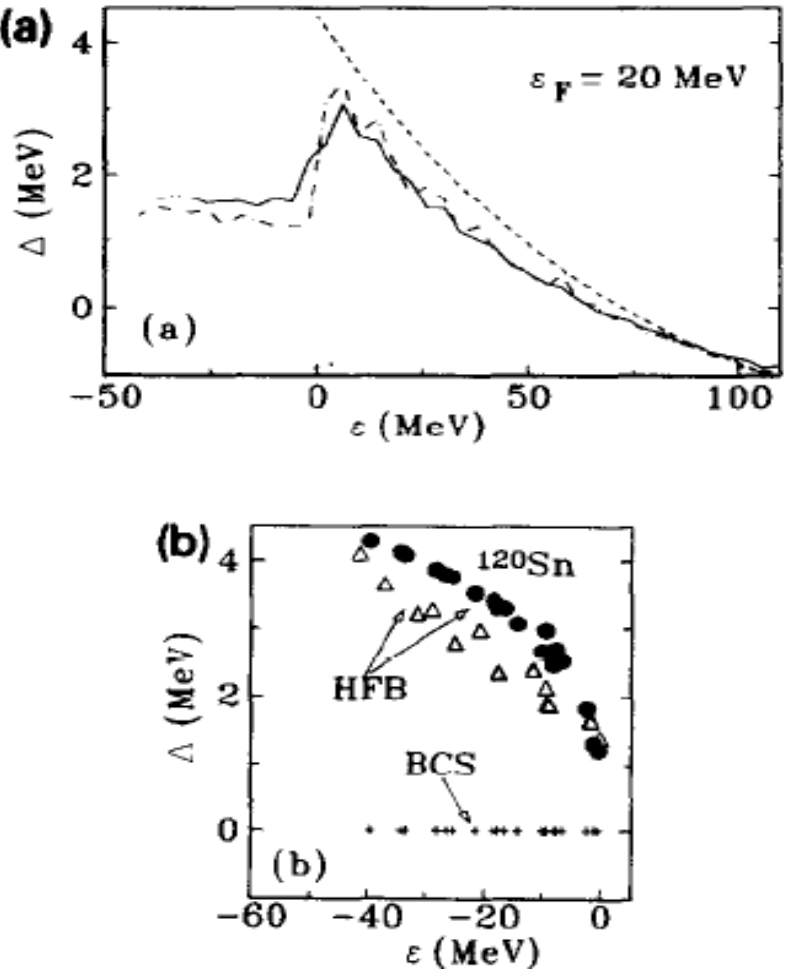

Fig. 1. (a) The pairing gaps obtained in a Wigner-Seitz cell of radius equal to 15 fm, and ϵ_F = 20 MeV, containing the nucleus Sn whose bound states are described in terms of a Woods-Saxon potential with a radius of 6.26 fm and a depth of 45.5 MeV, are shown by a solid and dash-dotted curve, respectively for a diffusivity a = 0.67 fm and a = 0 fm. The gaps obtained for the discrete states have been averaged over 4 MeV. The gaps obtained for uniform neutron matter are shown by the dashed line. (b) The pairing gaps obtained for the bound states in the potential used already in connection with Fig. (a) with the diffusivities a = 0.67 fm and 0 fm are shown by filled circles and by open triangles respectively. The Fermi energy has been set at the values ϵ_F = −7.2 MeV (for a= 0.67 fm) and ϵ_F = −10.5 MeV (for a= 0 fm), appropriate for the nucleus ^{120}Sn. Also shown is the BCS result (small crosses).

$$\Delta_k = -\frac{1}{2\pi^2}\int_0^\infty dk' k'^2 V_{kk'} \frac{\Delta_{k'}}{2E_{k'}} \longrightarrow = U_k V_k$$

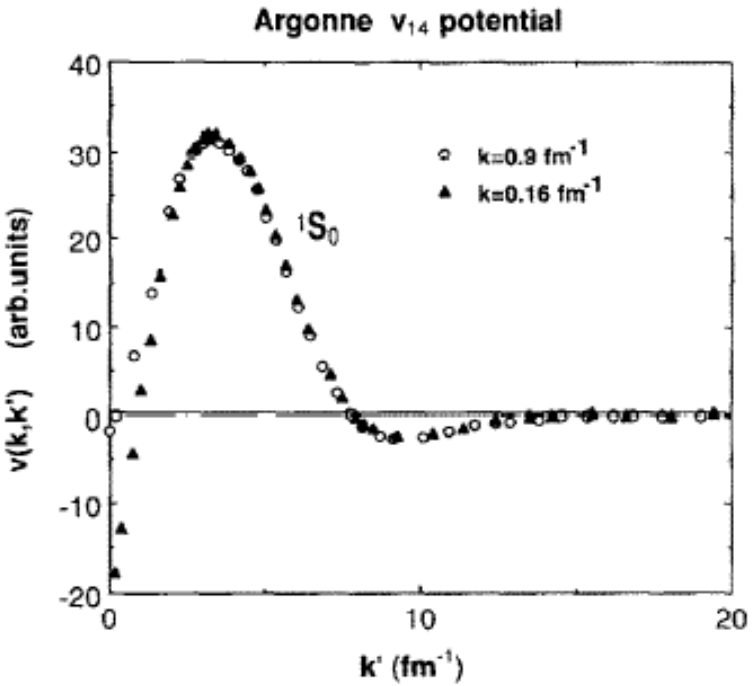

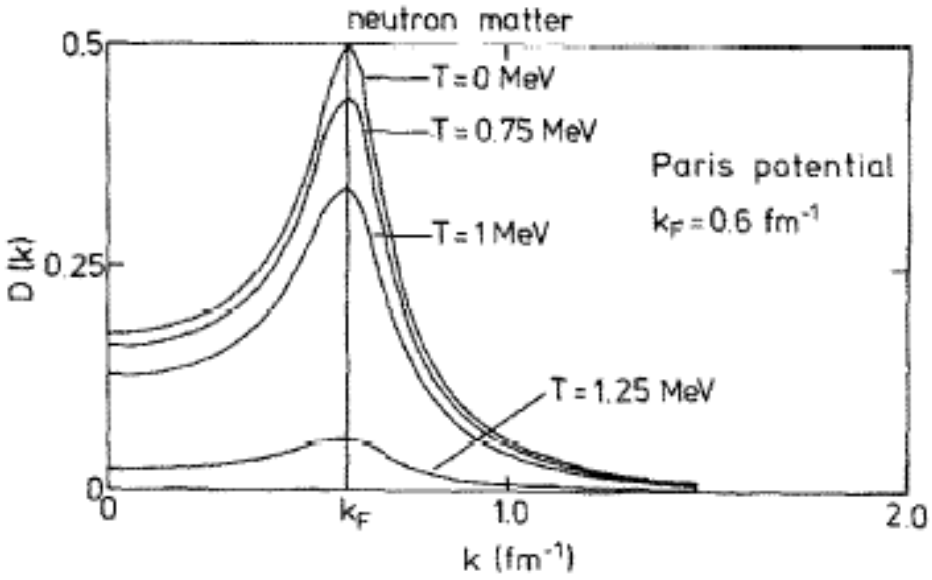

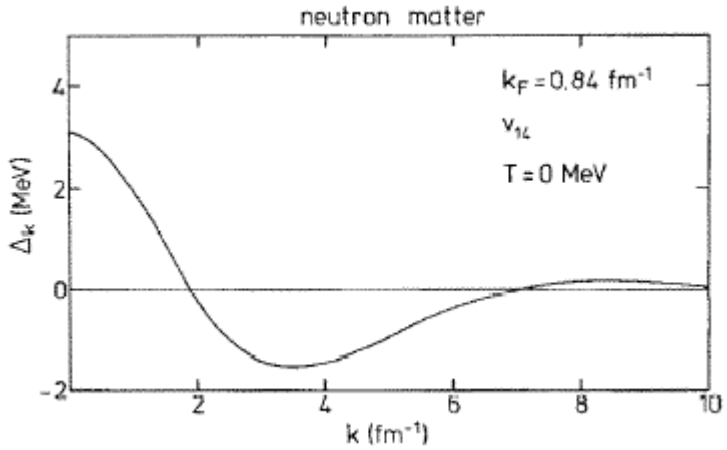

M .Baldo, J. Cugnon,
A. Lejeune, U. Lombardo,
NPA 515(1990) 409

30/01/13

Effective forces: $V_{low\text{-}k}$ vs. Gogny

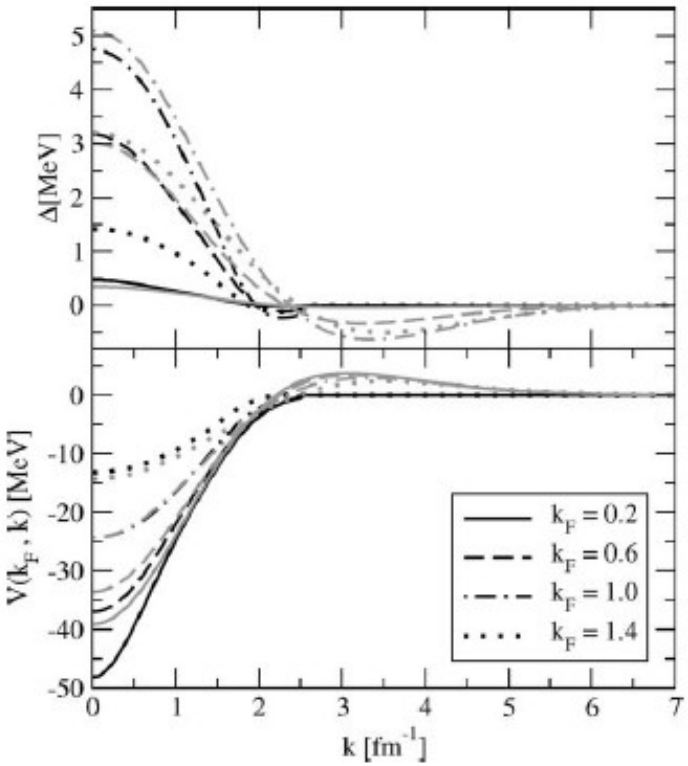

Fig. 1. The pairing gaps in the $^1S_0$ channel and the corresponding pairing potentials $V(k_F, k)$ as functions of the momentum k for several fixed Fermi-momenta k_F. The black and grey lines refer to the $V_{low\text{-}k}$ and the Gogny interaction, respectively. The solid, dashed, dashed-dotted and dotted lines correspond to the values of k_F equal 0.2, 0.6, 1.0 and 1.4 fm^{-1}.

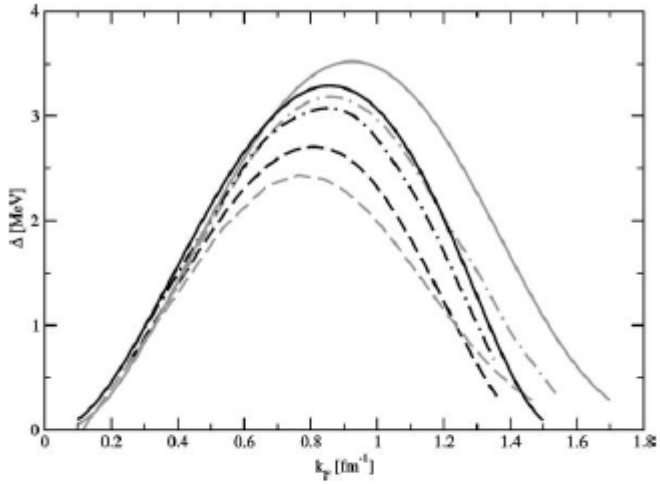

Fig. 2. The pairing gaps in the $^1S_0$ channel as functions of Fermi-momentum (density) of the matter for two effective interactions. The heavy and light lines refer to the $V_{low\text{-}k}$ and the Gogny interaction, respectively. The solid lines correspond to the non-interacting single-particle spectrum, the dashed and dashed-dotted lines—to renormalized single particle spectrum in symmetric nuclear matter and neutron matter, respectively. The single particle spectra are computed in the Hartree–Fock theory for the Gogny interaction and the Brueckner–Hartree–Fock theory for the $V_{low\text{-}k}$ interaction.

A. Sedrakian, T.T.S. Kuo, H. Muther, P. Schuck, Phys. Lett. B576(2003)68

Semiclassical approximation to neutron star superfluidity corrected for proximity effects

F. Barranco,[1] R. A. Broglia,[2,3] H. Esbensen,[4] and E. Vigezzi[2]
[1]*Departamento de Fisica Aplicada, Escuela Superior de Ingenieros, Universidad de Sevilla, Spain*
[2]*Dipartimento di Fisica, Università di Milano and INFN, Sezione di Milano, Italy*
[3]*The Niels Bohr Institute, University of Copenhagen, Denmark*
[4]*Physics Division, Argonne National Laboratory, Argonne, Illinois 60439*
(Received 23 January 1998)

The inner crust of a neutron star is a superfluid and inhomogeneous system, consisting of a lattice of nuclei immersed in a sea of neutrons. We perform a quantum calculation of the associated pairing gap and compare it to the results one obtains in the local density approximation (LDA). It is found that the LDA overestimates the spatial dependence of the gap, and leads to a specific heat of the system which is too large at low temperatures, as compared with the quantal result. This is caused by the neglect of proximity effects and the delocalized character of the single-particle wave functions close to the Fermi energy. It is possible to introduce an alternative, simple semiclassical approximation of the pairing gap which leads to a specific heat that is in good agreement with the quantum calculation. [S0556-2813(98)07308-7]

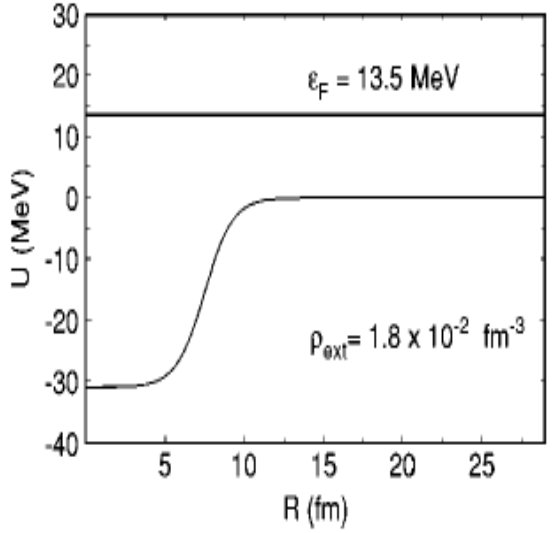

FIG. 1. The Woods-Saxon potential $U(R)$ in the Wigner-Seitz cell of radius $R_b = 29$ fm is shown. We also indicate the Fermi energy ϵ_F and the outer neutron density $\rho_{\rm ext}$.

$$\Phi_{S=0}(\vec{r}_1,\vec{r}_2) = \sum_{nn'lj}\left(\sum_q U^q_{nlj}V^q_{n'lj}\right)\frac{2j+1}{8\pi} \times \phi_{nlj}(r_1)\phi_{n'lj}(r_2)P_l(\cos(\theta_{21})).$$

$$\Delta(\vec{r}_1,\vec{r}_2) = -v(|\vec{r}_1-\vec{r}_2|)\Phi_{S=0}(\vec{r}_1,\vec{r}_2)$$

$$\Delta(\vec{k},\vec{R}) = \int d^3r_{12}\ \Delta(\vec{r}_1,\vec{r}_2)e^{-i\vec{k}\cdot\vec{r}_{12}},$$

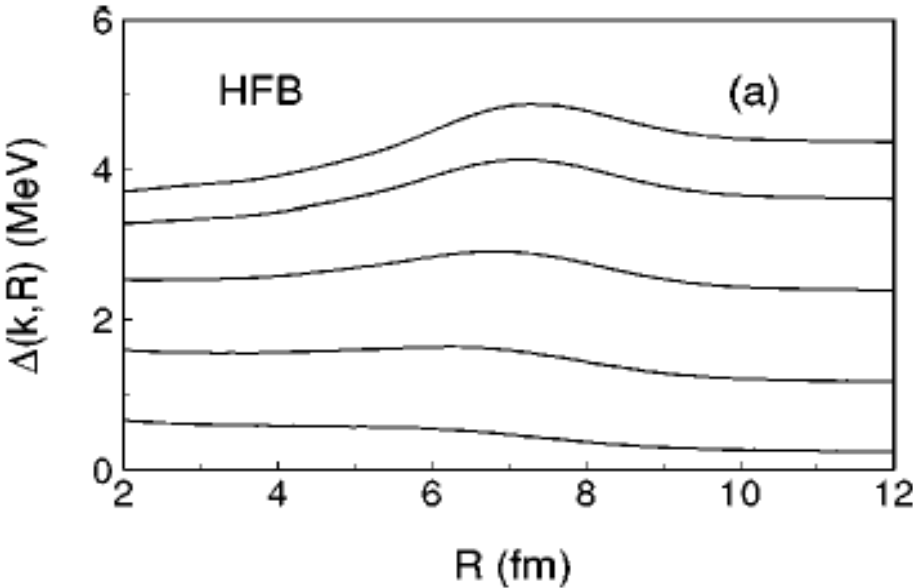

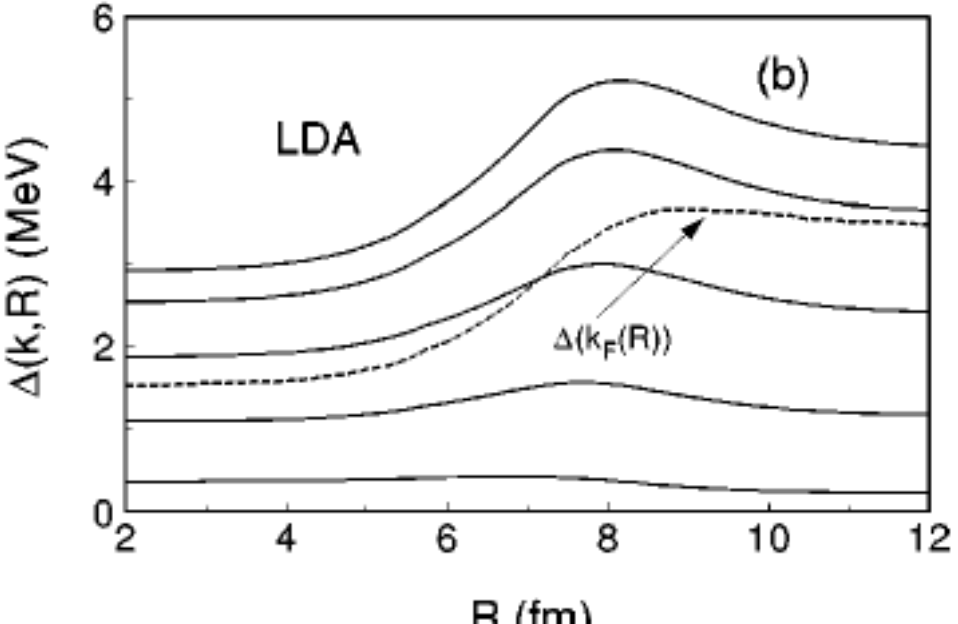

PHYSICAL REVIEW C **75**, 012805(R) (2007)

Quantum calculation of vortices in the inner crust of neutron stars

P. Avogadro,[1,2] F. Barranco,[3] R. A. Broglia,[1,2,4] and E. Vigezzi[2]

[1]*Dipartimento di Fisica, Università degli Studi di Milano, via Celoria 16, I-20133 Milano, Italy*

[2]*INFN, Sezione di Milano, via Celoria 16, 20133 I-Milano, Italy*

[3]*Departamento de Fisica Aplicada III, Escuela Superior de Ingenieros, Camino de los Descubrimientos s/n, E-41092 Sevilla, Spain*

[4]*The Niels Bohr Institute, University of Copenhagen, Blegdamsvej 17, DK-2100 Copenhagen ø, Denmark*

(Received 26 January 2006; revised manuscript received 26 June 2006; published 12 January 2007)

The self-consistent mean-field quantum mechanical solution of a vortex and a nucleus immersed in a sea of free neutrons, a scenario representative of the inner crust of neutron stars, is presented for the first time. Because of quantal size effects the phase space for vortices inside the nucleus is essentially zero, so that the vortex core opens up and surrounds the nucleus. As a consequence, pinned configurations (in which a vortex becomes anchored to the nucleus) are favored at low and high densities in the inner crust. This result is qualitatively different from that obtained in all previous models, which predict pinning at intermediate densities.

$$[K + V(\rho, z) - E_F]U_\alpha + \Delta V_\alpha = E_\alpha U_\alpha,$$
$$-[K + V(\rho, z) - E_F]V_\alpha + \Delta^* U_\alpha = E_\alpha V_\alpha$$

$$U_\alpha(\rho, z, \phi) = e^{il_\alpha\phi}\sum_{n,m} U_\alpha^{n,m}\psi_{n,l_\alpha}(\rho)\chi_m(z),$$
$$V_\alpha(\rho, z, \phi) = e^{i[l_\alpha - \nu]\phi}\sum V_\alpha^{n,m}\psi_{n,l_\alpha-\nu}(\rho)\chi_m(z),$$

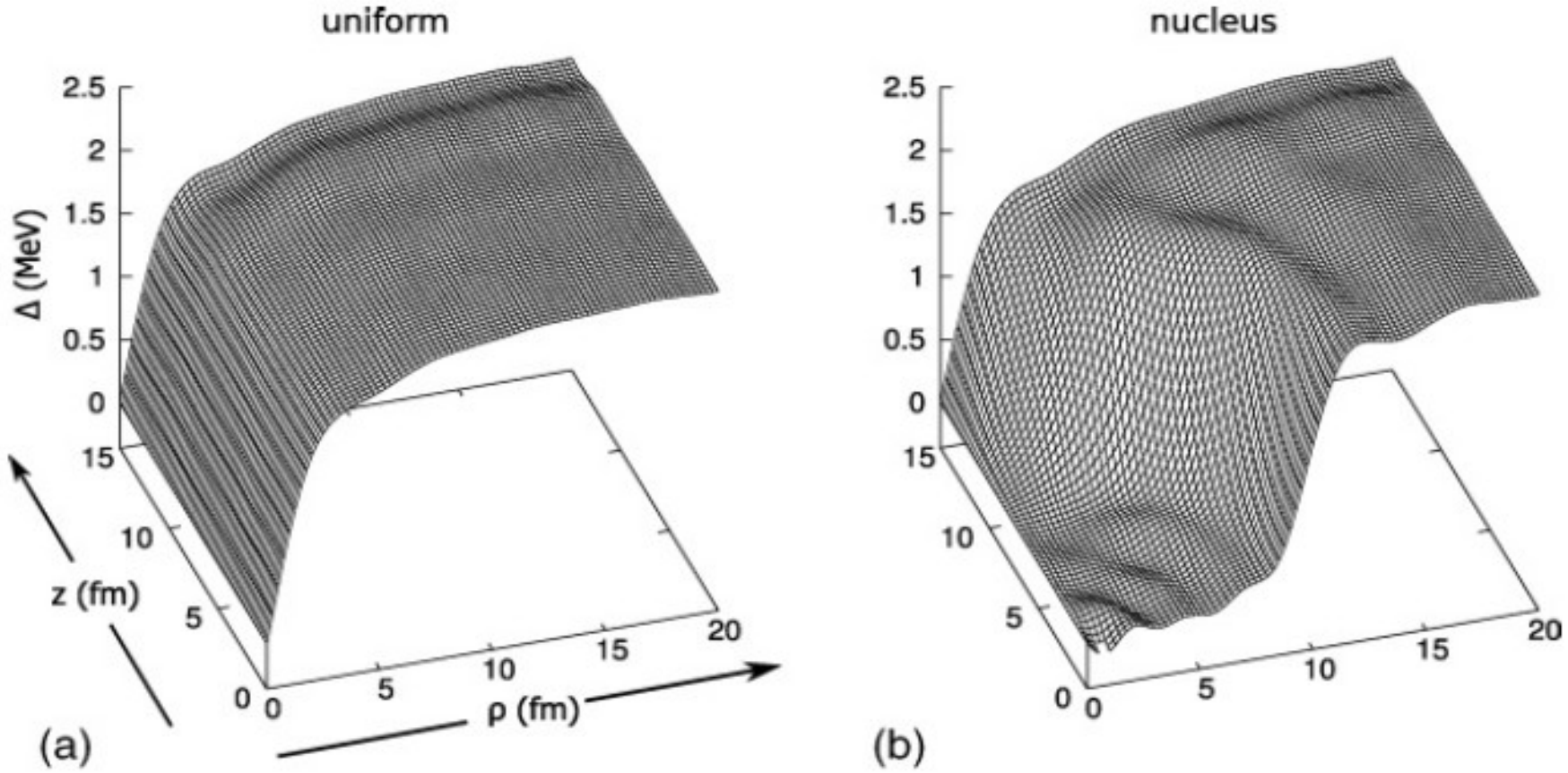

Puting together bare and Induced Interaction

DYNAMICAL SLAB (INFINITE SURFACE)

PHYSICAL REVIEW C, VOLUME 65, 041304(R)

Surface effects in nuclear Cooper pair formation

N. Giovanardi,[1,2,†] F. Barranco,[3] R. A. Broglia,[1,2,4] and E. Vigezzi[2]
[1]*Dipartimento di Fisica, Università di Milano, via Celoria 16, I-20133 Milano, Italy*
[2]*Istituto Nazionale di Fisica Nucleare, via Celoria 16, I-20133 Milano, Italy*
[3]*Departamento de Fisica Aplicada, Escuela Superior de Ingenieros, Universidad de Sevilla, Spain*
[4]*The Niels Bohr Institute, University of Copenhagen, Blegdamsvej 17, DK-2100 Copenhagen, Denmark*
(Received 21 February 2001; published 25 March 2002)

The formation of Cooper pairs resulting from the exchange of vibrations between pairs of fermions moving in time reversal states close to the Fermi surface in a semi-infinite system of nuclear matter (slab model) with parameters adjusted so as to mimic real nuclei, leads to pairing gaps which account for a substantial fraction of the experimental value throughout the mass table. The predictions are in qualitative agreement with detailed calculations carried out for finite nuclei and testify to the central role the surface of nuclei plays in the phenomenon of nuclear superfluidity.

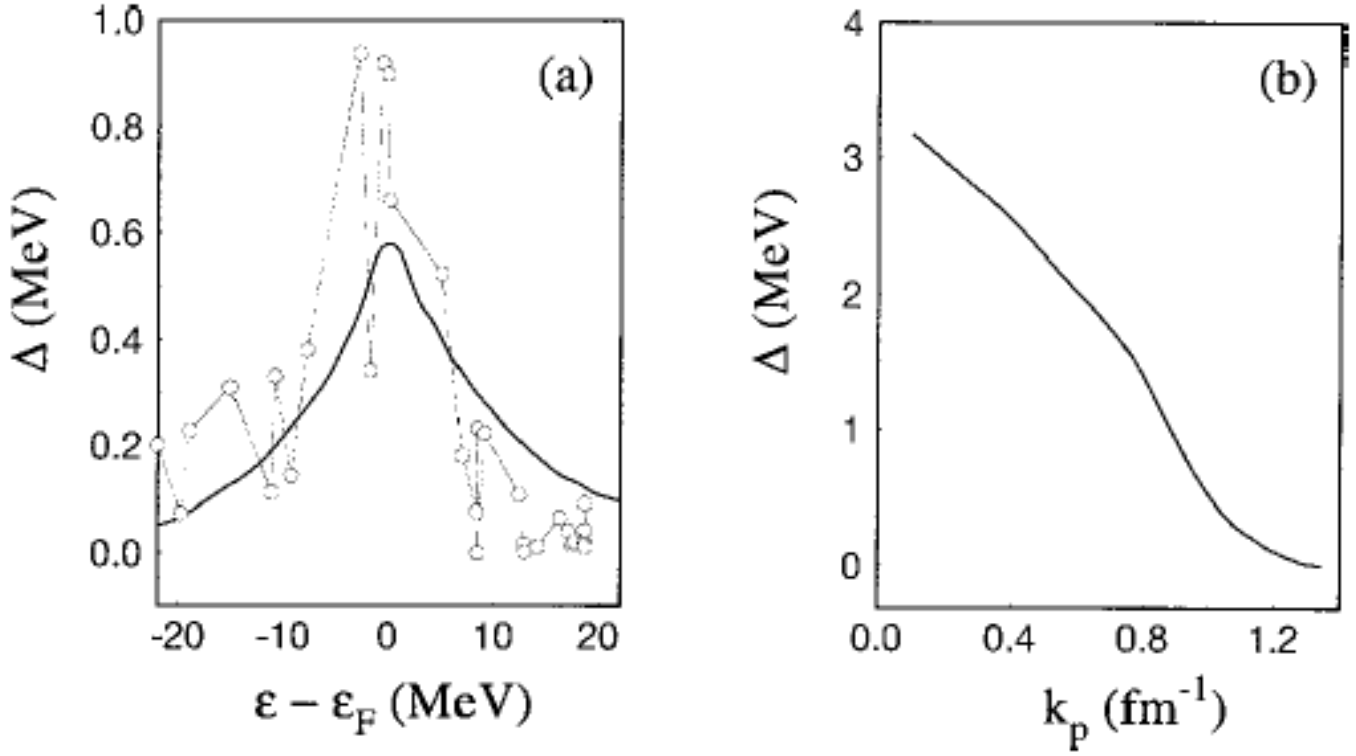

FIG. 1. (a) Pairing gap of particles as a function of the particle energy $\epsilon=(\hbar k_\nu)^2/(2m)$, for $R=6$ fm. For each energy value, the pairing gap Δ has been calculated as an average over the gaps of particles having the same k_ν^2. Detailed results for the nucleus ^{120}Sn are also displayed (open dots, cf. Fig. 1, Ref. [4]). (b) The pairing gap of a particle at the Fermi energy as a function of the momentum component parallel to the surface of the slab. The gap goes to zero when $k_{\nu p}=k_F=1.337$ fm^{-1}, corresponding to the case of particles moving parallel to the surface of the slab ($k_z=0$).

T=0 pairing problem

Alm et al. Z.Phys.A337,355 (1990)
Vonderfecht et al. PLB253,1 (1991)
Baldo et al. PLB283, 8 (1992)

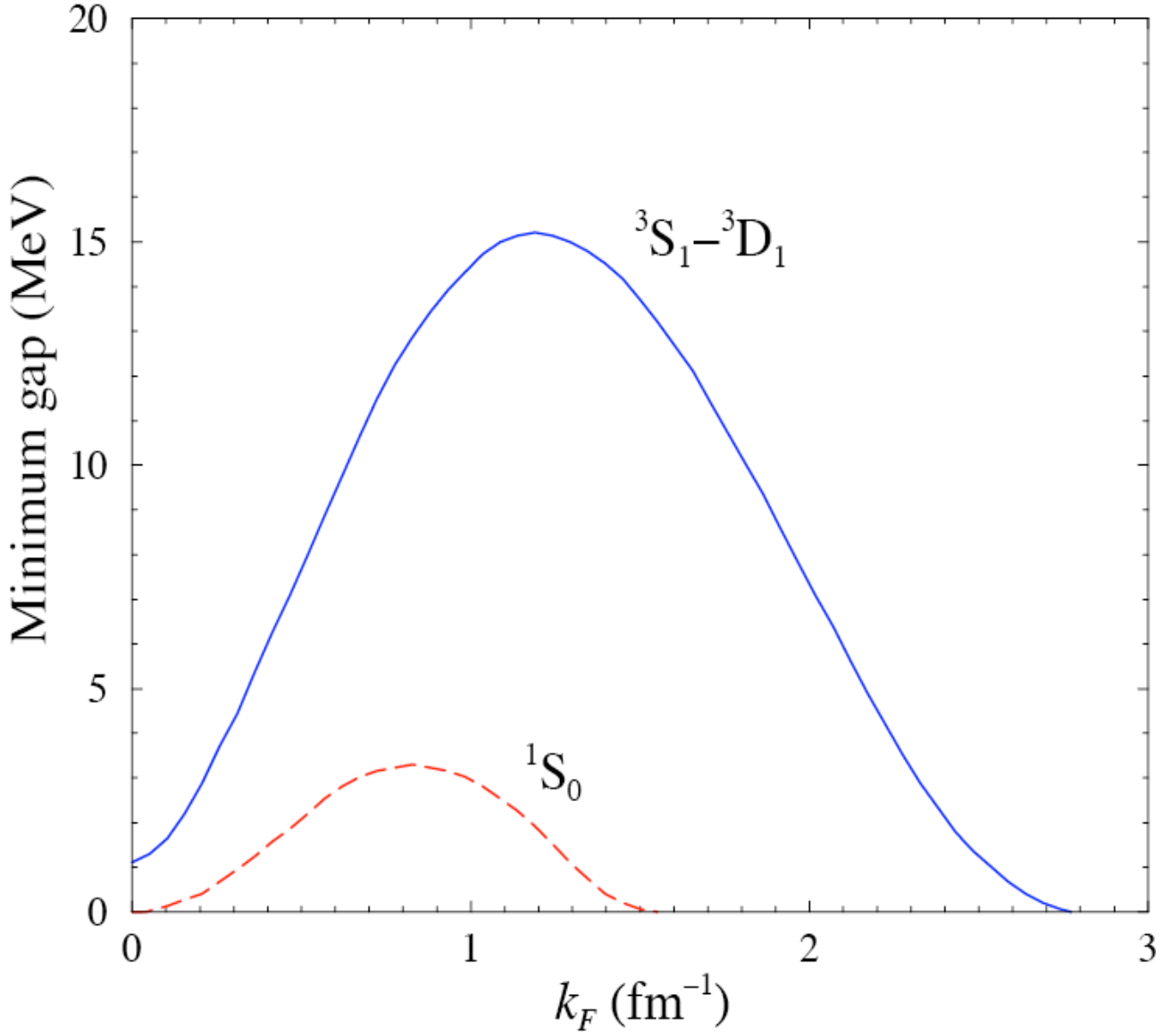

Proton-neutron pairing in symmetric nuclear matter

$^3S_1$-$^3D_1$

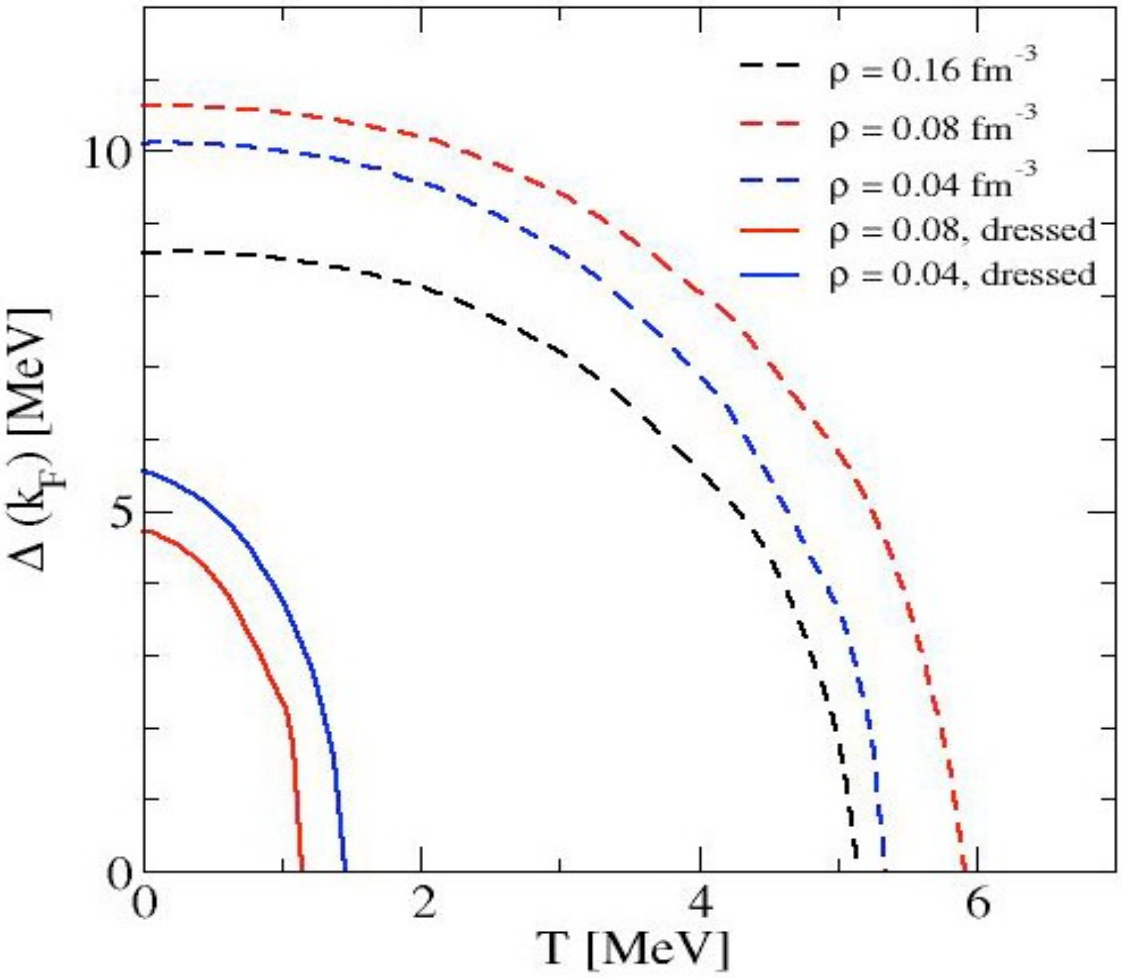

Using CDBonn

Dashed lines:
quasiparticle poles

Solid lines:
dressed nucleons

No pairing at saturation density!!!!

Dickhoff et al.

LOMBARDO'S

COMPARISSON WITH DATA:

Mamotretus and mk problem

PRC 120Sn con tanti osservabili

PRC 120Sn TPT transfer

THIS IS THE END, MY ONLY FRIEND,

THE END.

e-'s Cooper Pair Model; BCS (S=0;L=0); (S=0;L=2,*HiTc?*)

|| *Superconductivity, Superfluidity*

V *mutans muntandi*

n-n pairing in Uniform Neutron Matter (S=0;L=0),(S=1;L=1),(S=0;L=2)

|| *NeutronStars: Cv, Vortices-Glitches*

||

V *add protons (Z=N)*

n-n in Unif. Symm. Nucl. Matt. (S=0;L=0),(S=1;L=1),(S=0;L=2) T=1;Tz=-1

p-p in Unif. Symm. Nucl. Matt. (S=0;L=0),(S=1;L=1),(S=0;L=2) T=1;Tz=+1

AND

n-p in Unif. Symm. Nucl. Matt.(S=0;L=0),(S=1;L=1),(S=0;L=2) T=1:Tz=0

n-p in Unif. Symm. Nucl. Matt.(S=1;L=0),(S=0;L=1),(S=1;L=2) **T=0:Tz=0**

….. OR

Quaternions??

||

V *add less protons (Z<N)*

n-n in U. Asymm. Nucl. M. (S=0;L=0),(S=1;L=1),(S=0;L=2) T=1;Tz=-1

p-p in U. Asymm. Nucl. M. (S=0;L=0),(S=1;L=1),(S=0;L=2) T=1;Tz=+1

Typical forces employed in finite nuclei pairing HFB-like calculations

I) Monopole: $H_p = - G P^+P$ with G = -25/A MeV

being $P^+ = \Sigma_{m>0} a^+_m a^+_{-m}$; restricted to one shell

ii) Contact interactions $V_c(1-\eta*\rho(r)/\rho_0)$ (E_{cut}=60MeV)

Commonly used with Skyrme forces

iii) Gogny force

Continuum is relevant

iv) Argonne int.

Continuum is crucial

Up to 800MeV

v) Nuclear Matter Calculation Based Pairing Interaction

Show some Illustrative results

Contact interaction

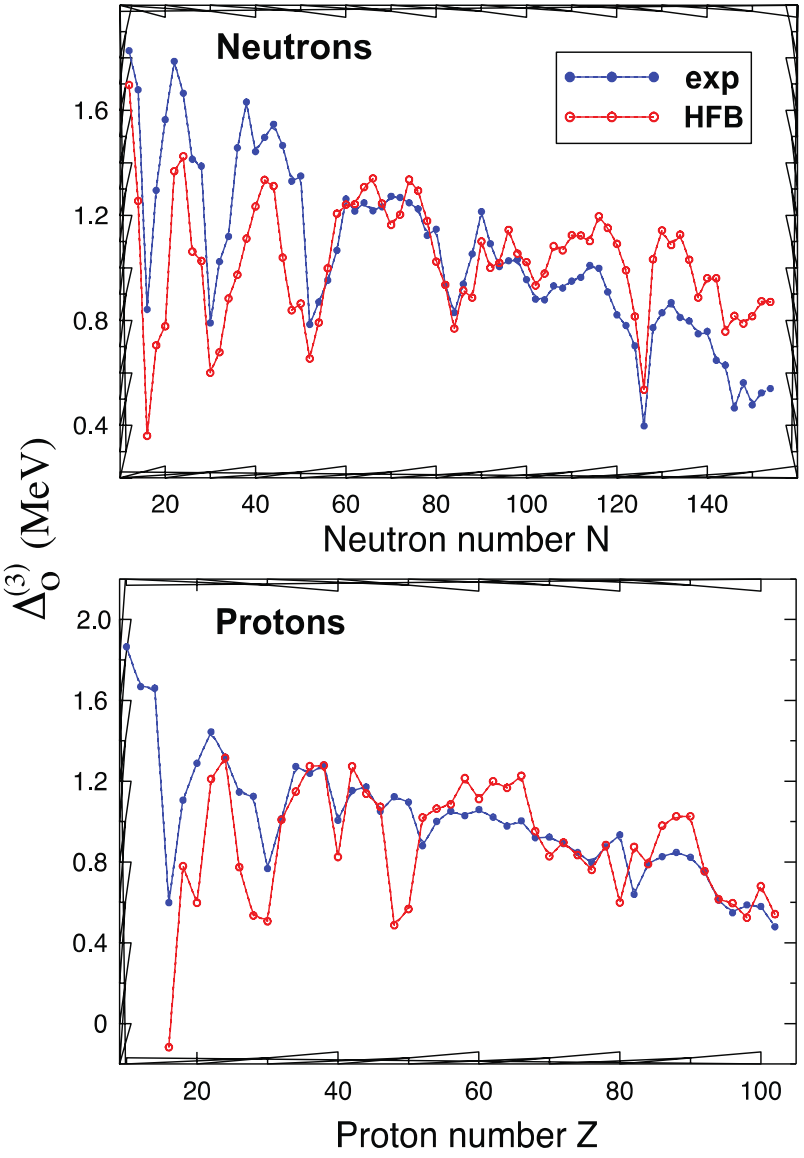

Survey of OES: G.F. Bertsch et al. Phys. Rev. C 79, 034306 (2009)

$$V(r-r') = V_c(1-\eta^*\rho(r)/\rho_0)\ \delta^3(r-r')$$

η=0; 0.5 and 1.0 (vol.; mix.; surf.)

(Ecut=60MeV);

TABLE IV: RMS residuals of $\Delta_o^{(3)}$ obtained in various models. All energies are in MeV. The last column shows the ratio of proton and neutron effective pairing strengths obtained through the optimization procedure. The mass predictions of the HFB-14 model [16] were taken from [51].

Theory	pairing	residual neutrons	residual protons	$V_0^{\rm eff}(p)/V_0^{\rm eff}(n)$
Constant		0.31	0.27	
c/A^α		0.24	0.22	
HF+BCS	volume	0.31	0.38	1.05
HF+BCS	mixed	0.30	0.36	1.08
HF+BCS	surface	0.27	0.35	1.12
HFB	mixed	0.27	0.32	1.11
HFB+LN	mixed	0.23	0.28	1.11
HFB-14		0.46	0.44	1.10

GOGNY GAPS (Robledo,Bernard,Bertsch,PRC86(2012))

PHYSICAL REVIEW C **86**, 064313 (2012)

Pairing gaps in the Hartree-Fock-Bogoliubov theory with the Gogny D1S interaction

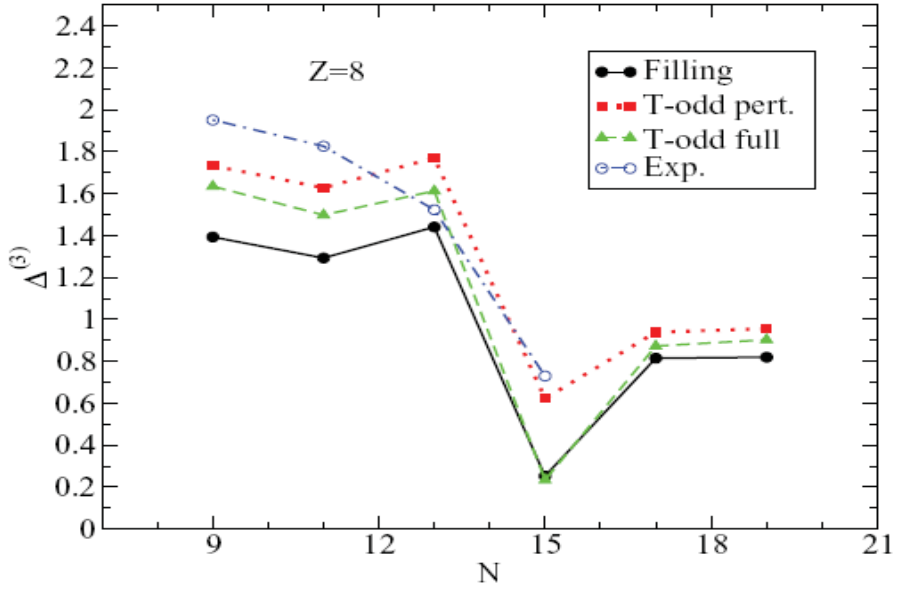

FIG. 1. (Color online) Neutron pairing gaps $\Delta^{(3)}$ in the oxygen isotope chain. Energies were computed in the $N_{sh} = 10$ harmonic oscillator space.

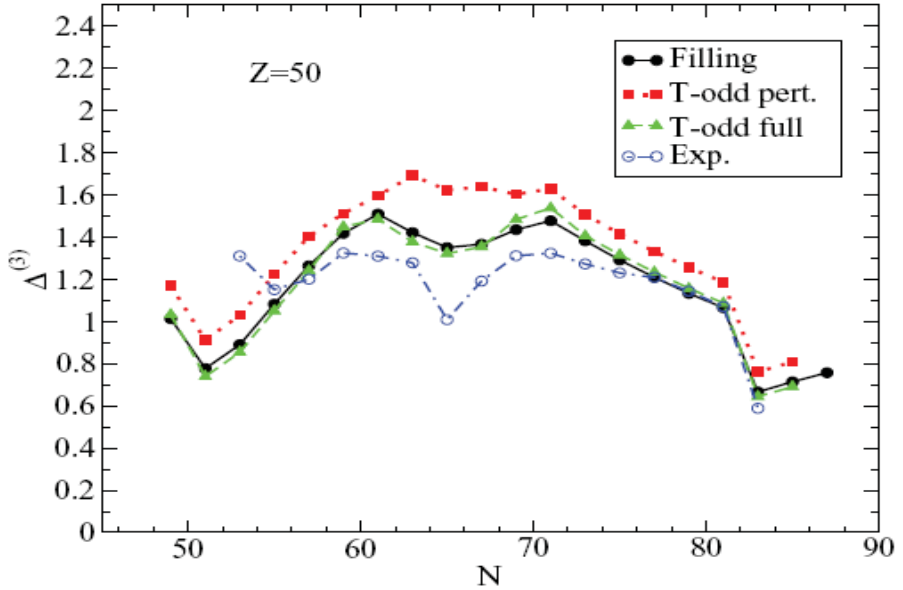

FIG. 2. (Color online) Neutron pairing gaps $\Delta^{(3)}$ in the Sn isotope chain. Energies were computed in the $N_{sh} = 12$ harmonic oscillator space.

GOGNY GAPS (cont.)

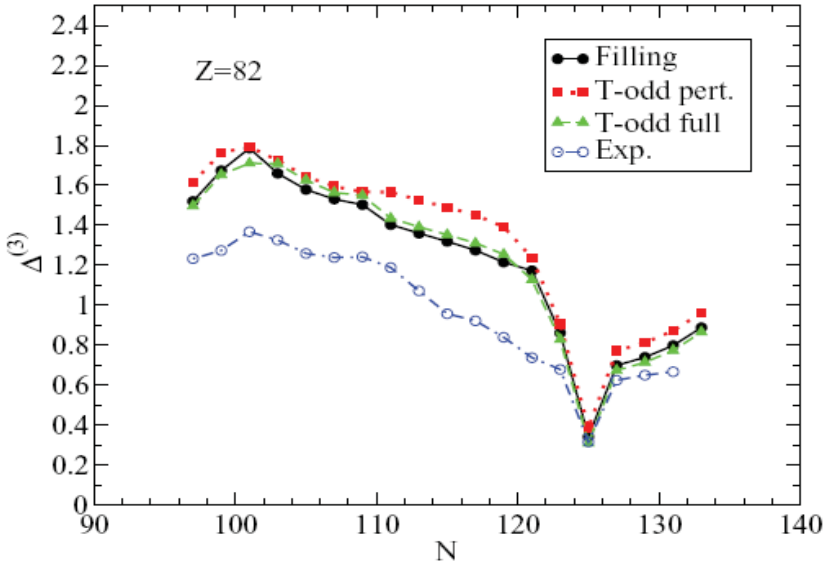

FIG. 3. (Color online) Neutron pairing gaps $\Delta^{(3)}$ in the Pb isotope chain. Energies were computed in the $N_{sh} = 12$ harmonic oscillator space.

Another correlation is associated with the polarization of the nucleus by the valence nucleons. The resulting induced pairing interaction has been calculated to give as strong a contribution as the nucleon-nucleon interaction in the pairing channel [32], Such induced interactions are long-ranged and energy-dependent, and vary from nucleus to nucleus depending on its structure. It would not be surprising that the effects were beyond the scope of the simple energy functionals in current use.

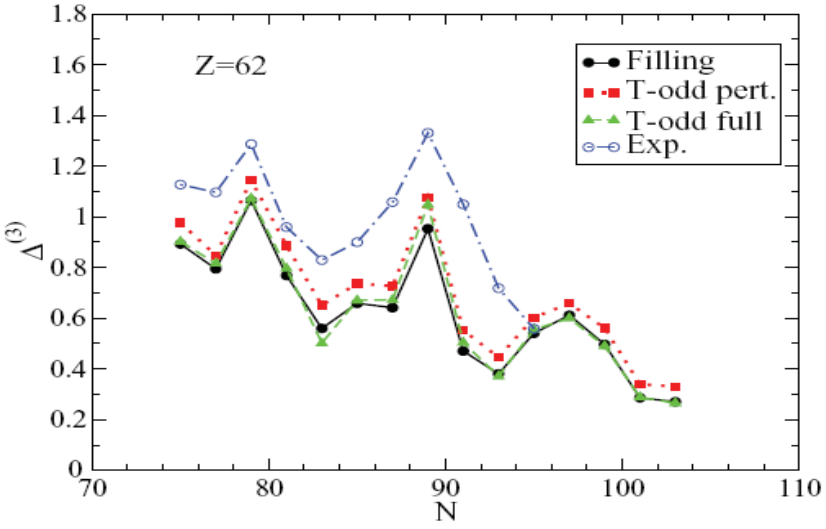

FIG. 4. (Color online) Neutron pairing gaps $\Delta^{(3)}$ in the Sm isotope chain. Energies were computed in the $N_{sh} = 12$ harmonic oscillator space.

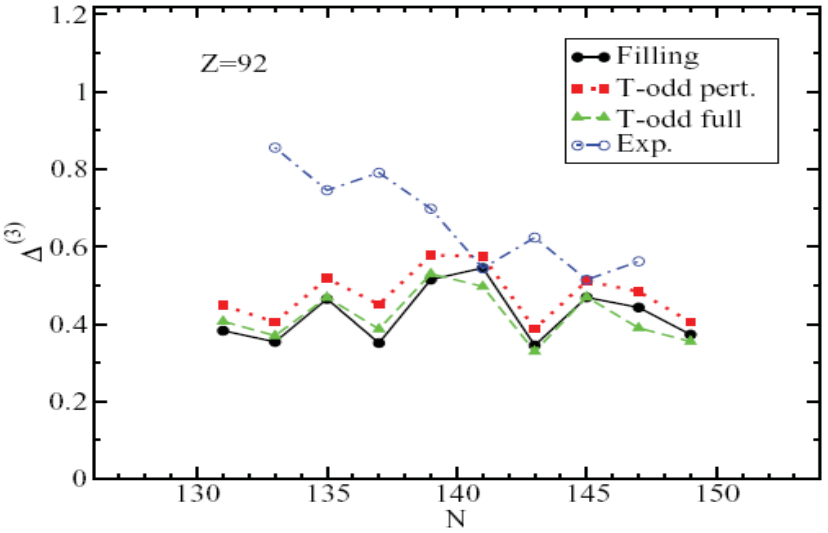

FIG. 5. (Color online) Neutron pairing gaps $\Delta^{(3)}$ in the U isotope chain. Energies were computed in the $N_{sh} = 14$ harmonic oscillator space.

Argonne ($1S_0$)

Barranco, Broglia, Esbensen, Vigezzi, PLB(1997)

Neutron saturated nucleus (Z=50) inmersed in a superfluid neutron sea

We have repeated the calculations, but this time setting the Fermi energy at −7.2 MeV, that is, for the isolated atomic nucleus $^{120}_{50}$Sn. The value of R_{box} has been varied within the range 8–15 fm to check the stability of the results. The values of the pairing gaps become stable once $R_{box} \geqslant 12$ fm. The results of the calculation with R_{box} =15 fm are displayed in Fig. 1(b). The value of the pairing gap at the Fermi energy is $2.2\ ^{+0.4}_{-0.8}$ MeV, the "errors" reflecting the conspicuous state dependence of Δ.[1] This value is about 50% higher than the experimental value of 1.47 MeV deduced from the odd-even mass differences [22]. This also in keeping with the fact that the free nucleon-nucleon interaction seems to provide too strong pairing correlations in finite nuclei (cf. e.g. [23]). In any case, theory provides a sound framework for an eventual quantitative description of pairing in nuclei.

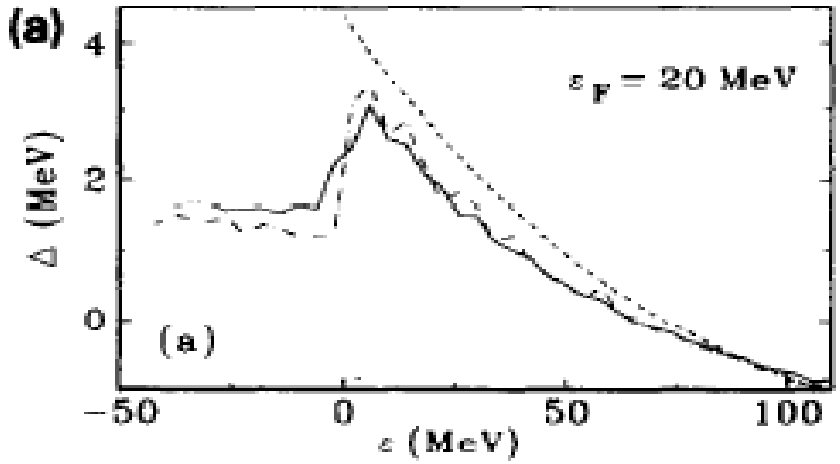

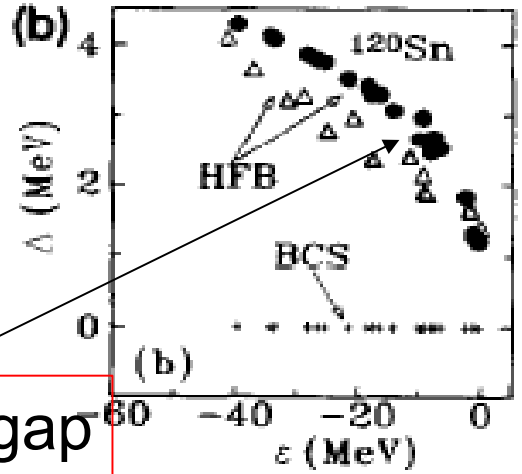

m=1.0 m_0=> Too large gap

Finite size effects on the pairing field (BCS with the bare force)

Potential in the Wigner cell

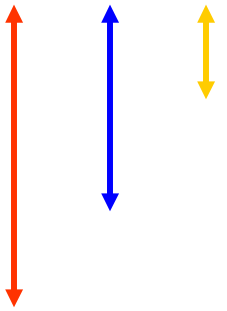

ε_F=13.5MeV

Pairing gap in uniform neutron matter

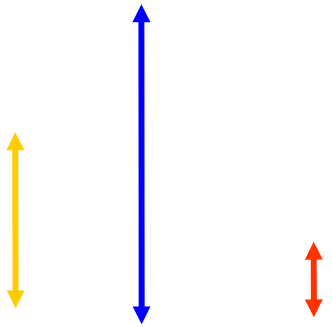

P.M. Pizzochero, F. Barranco, E. Vigezzi, R.A. Broglia,APJ 569(2003)381
N. Sandulescu, Phys. Rev. C70(2004)025801
F. Montani, C. May, H. Muther, PRC 69 (2004) 065801
M. Baldo, U. Lombardo, E.E. Saperstein, S.V. Tolokonnikov, Nucl. Phys. A750 (2005) 409

Spatial dependence of pairing densities and pairing gaps

FINITE NUCLEI, FINITE RANGE FORCE

HFB Equations are expanded on a basis

$$\begin{pmatrix} h_{nn'lj} - \lambda & \Delta_{nn'lj} \\ \Delta_{nn'lj} & -h_{nn'lj} + \lambda \end{pmatrix} \begin{pmatrix} U_{nlj}^{\alpha} \\ V_{nlj}^{\alpha} \end{pmatrix} = E_{lj}^{\alpha} \begin{pmatrix} U_{nlj}^{\alpha} \\ V_{nlj}^{\alpha} \end{pmatrix}$$

$$\kappa(R_{cm}, r_{12}) = \frac{1}{8\pi} \sum_{nn'lj\alpha} (2j+1)\, U_{nlj}^{\alpha *} V_{n'lj}^{\alpha} \varphi_{nlj}^{*}(r_1)\, \varphi_{n'lj}(r_2)\, P_l(\cos(\vartheta_{12}))$$

$$\Delta(R_{cm}, r_{12}) = -V_{eff}(r_{12}) \kappa(R_{cm}, r_{12})$$

$$\Delta(R_{cm}, k) = \int dr_{12} \Delta(R_{cm}, r_{12}) \;\; \exp(ikr_{12})$$

Spatial description of (non-local) pairing gap
Essential for a consistent description of vortex pinning!

The range of the force is small compared to the coherence length, but not compared to the diffusivity of the nuclear potential

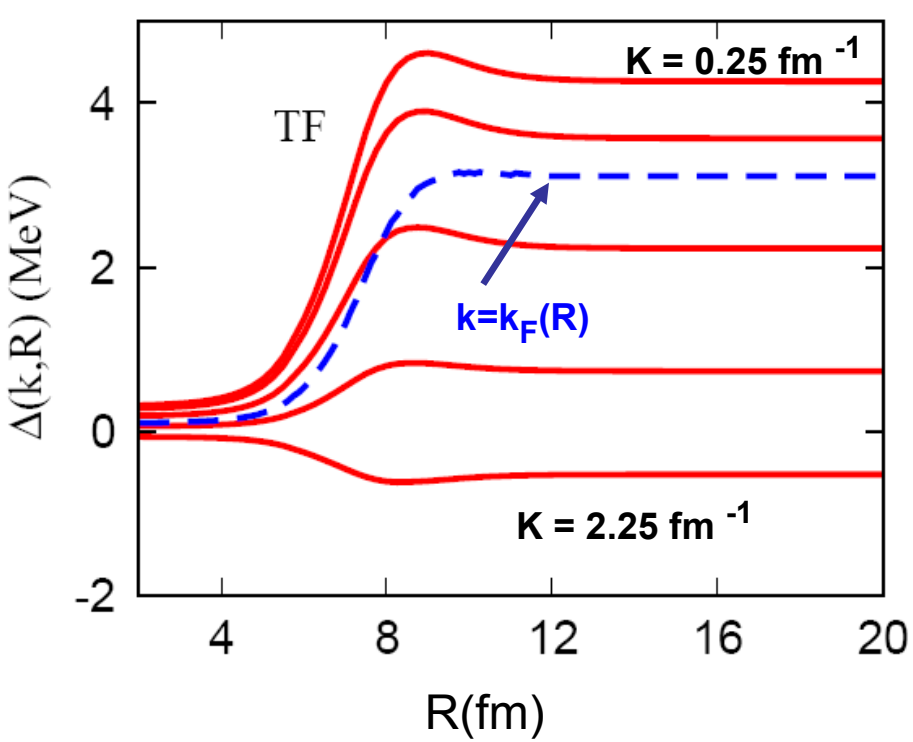

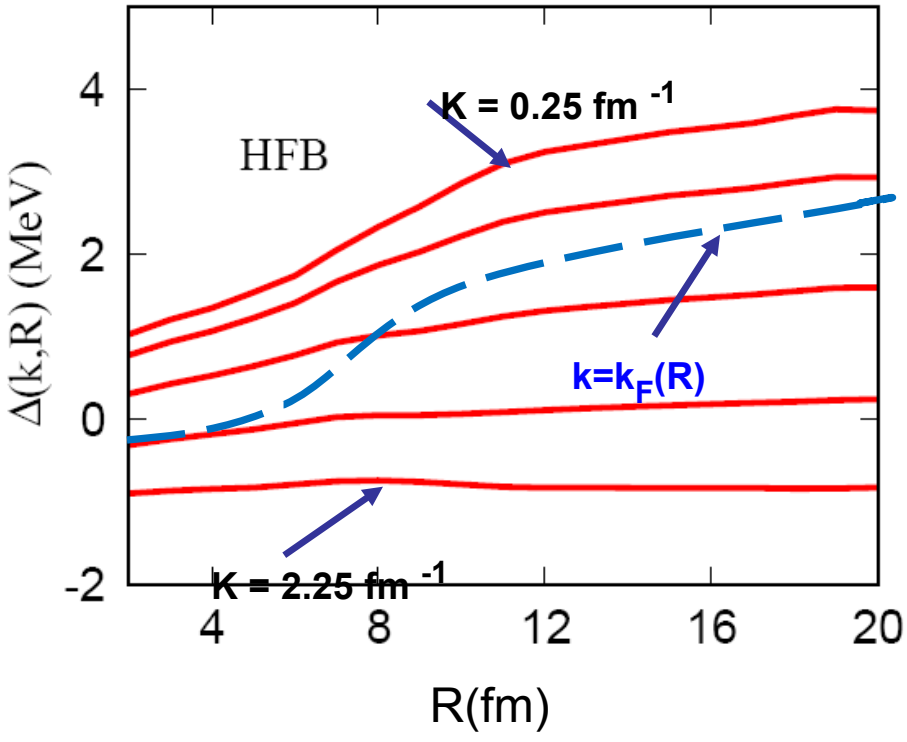

The local-density approximation overstimates the decrease of the pairing gap in the interior of the nucleus. (PROXIMITY EFFECTS)

V_low-k pairing gaps in Sly4 HF field

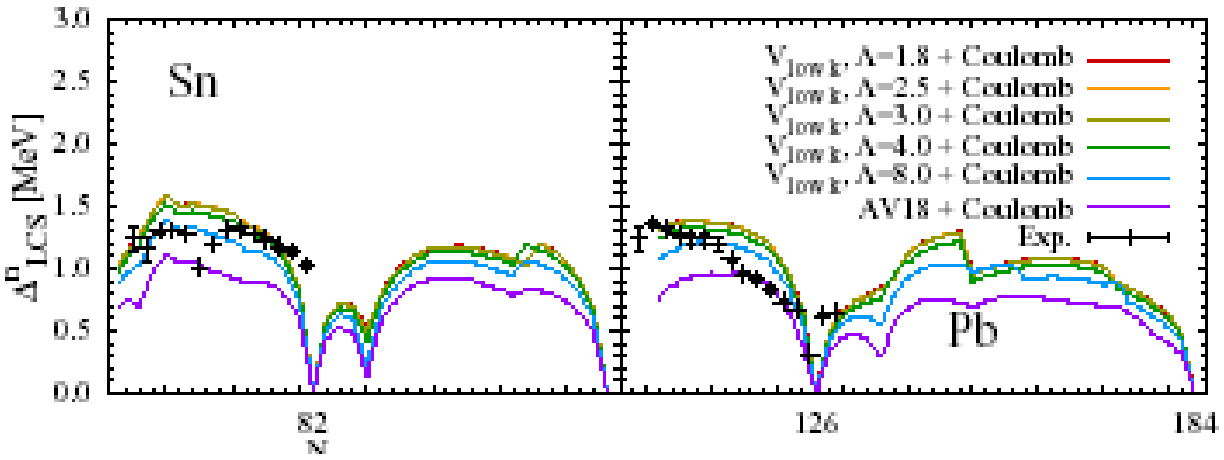

Dependence on the effective mass at high momenta? (Vlow-k vs V18)

Mean field calculation with Vlow-k pairing force: 3-body force reduces the pairing gaps

T. Lesinski,K.Hebeler, T. Duguet, A.Schwenk J.Phys.G39(12)

120Sn with
V_18 and Gogny HF-field: 1.1MeV

Results depend on the Central Potential parameters, including nucleon effective mass.

Any way some solid conclusions can be extracted

1. Bare Argonne is tractable at hfB level

2. With “reasonable” potentials as Sly4 a close to experiment pairing gap is obtained: 1.1MeV vs 1.3MeV.

3. Using V_low-K (and NNN forces)
similar results are obtained

Resonable potential are related to a m*=0.7m_o

which also leave room to ***self-energy corrections (mexp=1.0m0)***

Beyond mean field needed?

a). Neutron matter shows important screening

b). Single-particles are importantly affected, why not quasi-particle properties like the pairing gap?

c). In B&M-II book an estimate was made...

d). If simple DF are used:

(Robledo,Bernard,Bertsch,PRC86(2012))

> Another correlation is associated with the polarization of the nucleus by the valence nucleons. The resulting induced pairing interaction has been calculated to give as strong a contribution as the nucleon-nucleon interaction in the pairing channel [32], Such induced interactions are long-ranged and energy-dependent, and vary from nucleus to nucleus
>
> depending on its structure. It would not be surprising that the effects were beyond the scope of the simple energy functionals in current use.(*)

(*)Alternative sophisticated DF: I. Stetcu (LANL, 2013 talk)

Bohr&Mottelson,
Vol.II, 1975

6-5f Polarization Contributions to Effective Two-Particle Interactions

In second order, the particle-vibration coupling gives rise to an interaction between two particles, which can be evaluated in a manner similar to the particle-phonon interaction considered in Sec. 6-5d. To illustrate the magnitude of the polarization force, we consider the limiting case in which the frequency of the exchanged phonon is large compared to the energy differences between the particle states. In this case, one can view the interaction as resulting from the static deformation (6-217) produced by the first particle acting on the second. Thus, for a mode of multipolarity λ, one obtains (see Eq. (6-68))

$$V_\lambda(1,2) = -\frac{2\lambda+1}{4\pi C_\lambda} k_\lambda(r_1) k_\lambda(r_2) P_\lambda(\cos\vartheta_{12}) \qquad (6\text{-}228)$$

The order of magnitude of the polarization interaction (6-228) is given by $f_\lambda^2 \hbar\omega_\lambda$ (as for the particle self-energy). For the high-frequency modes, we have $f_\lambda^2 \hbar\omega_\lambda \sim \varepsilon_F A^{-1}$, which is comparable to the average interaction between nucleons in the nucleus ($\sim V_0 A^{-1}$). The magnitude of the polarization interaction can be seen directly from the fact that the deformation of the closed shells produced by a single particle implies polarization moments comparable with the bare moments of the particles (see p. 510); hence, the corresponding contribution to the polarization interaction (6-228) is similar in magnitude to the direct force.

The polarization interaction resulting from the coupling to the low-frequency modes may be considerably larger than the bare force; since the frequencies of these modes may be comparable with the particle frequencies, it may be necessary to go beyond the static approximation (6-228), as in the evaluation of the particle-phonon interaction.

B. Particle Vibration Coupling

and

Single-particle Self-energy

PVC directly related observables

Effective charges

One-particle transfer leading to Vibrational states

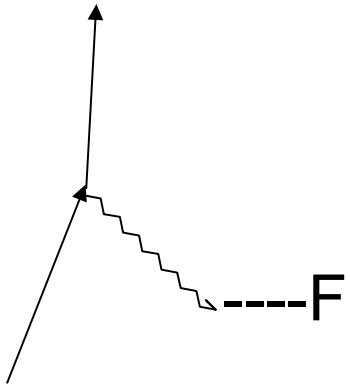

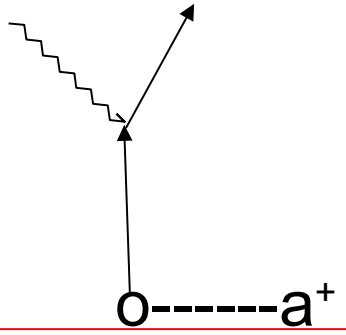

The vertex: Basic Ingredient

hj,j'λ =

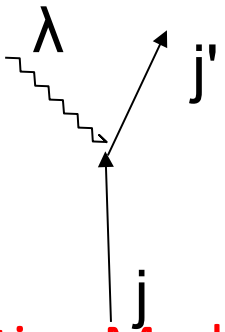

Simple Collective Model value

$$hj,j'\lambda = \beta\lambda(2\lambda+1)^{-1/2}\langle j||Ro\ dU/dr\ Y\lambda||j'\rangle\ (2j+1)^{-1/2}$$

The paradigmatic case; 208Pb(3-) + 1p(h9/2)

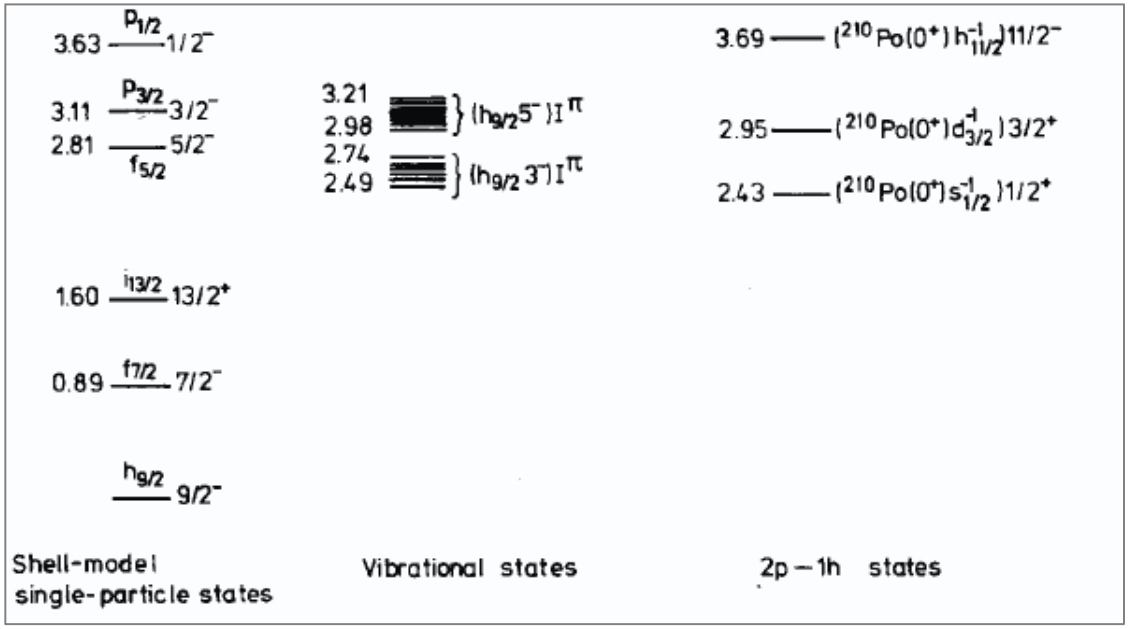

Fig. 11. Observed low-lying energy levels of ^{209}Bi. The coupling of different excitation modes are discussed in the text.

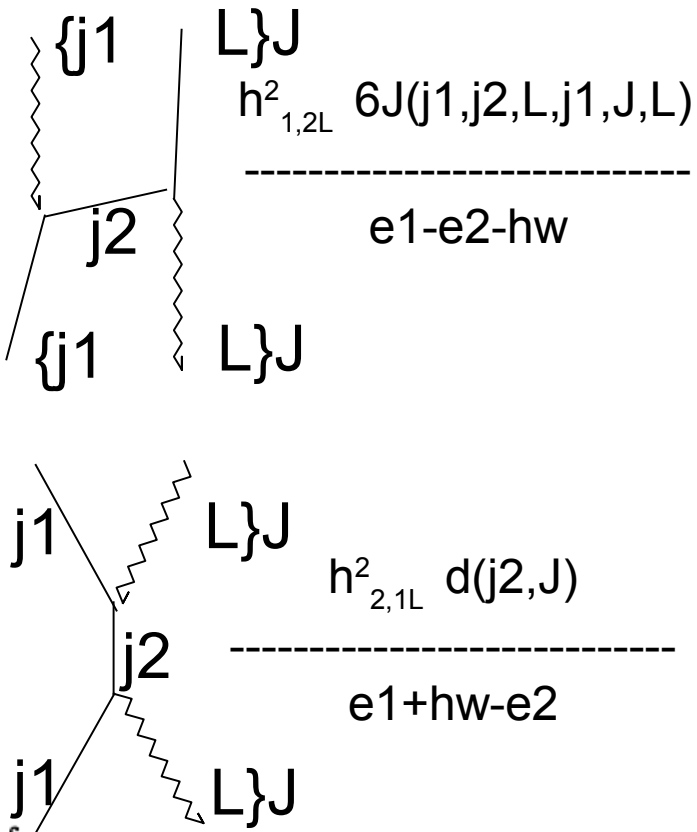

Table 6
Energy shifts of the septuplet members $(h_{9/2}\,3^-)I^\pi$ in ^{209}Bi from the unperturbed vibrational frequency 2.614 MeV. Experimental values are taken from ref. [29]

I	δE_{exp} (keV)	δE_{calc} (keV)
3/2	−120	+36 → −190
5/2	+4	+7
7/2	−29	−6
9/2	−49	−89
11/2	−14	−31
13/2	−14	−63
15/2	+130	+156

I.Hamamoto,1973
Phys.Rep.

SELF ENERGY RENORMALIZATION OF SINGLE-PARTICLE STATES: CLOSED SHELL

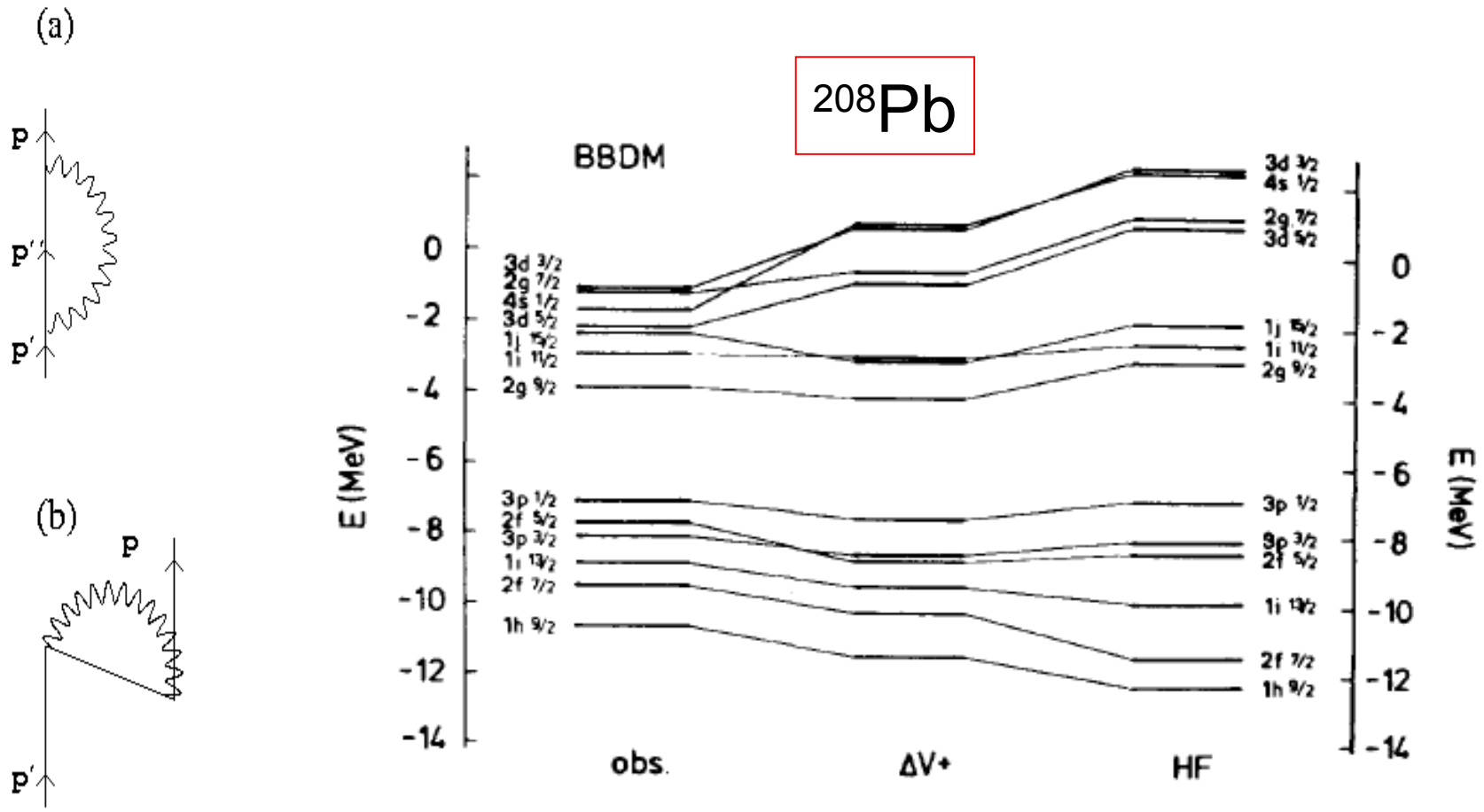

C. Mahaux, P.F. Bortignon, R.A. Broglia, C.H. Dasso and Mahaux, Phys. Rep.(1985)1

Relativistic Mean Field Calculations

Litvinova et al, PRC84, 014305 (2011)

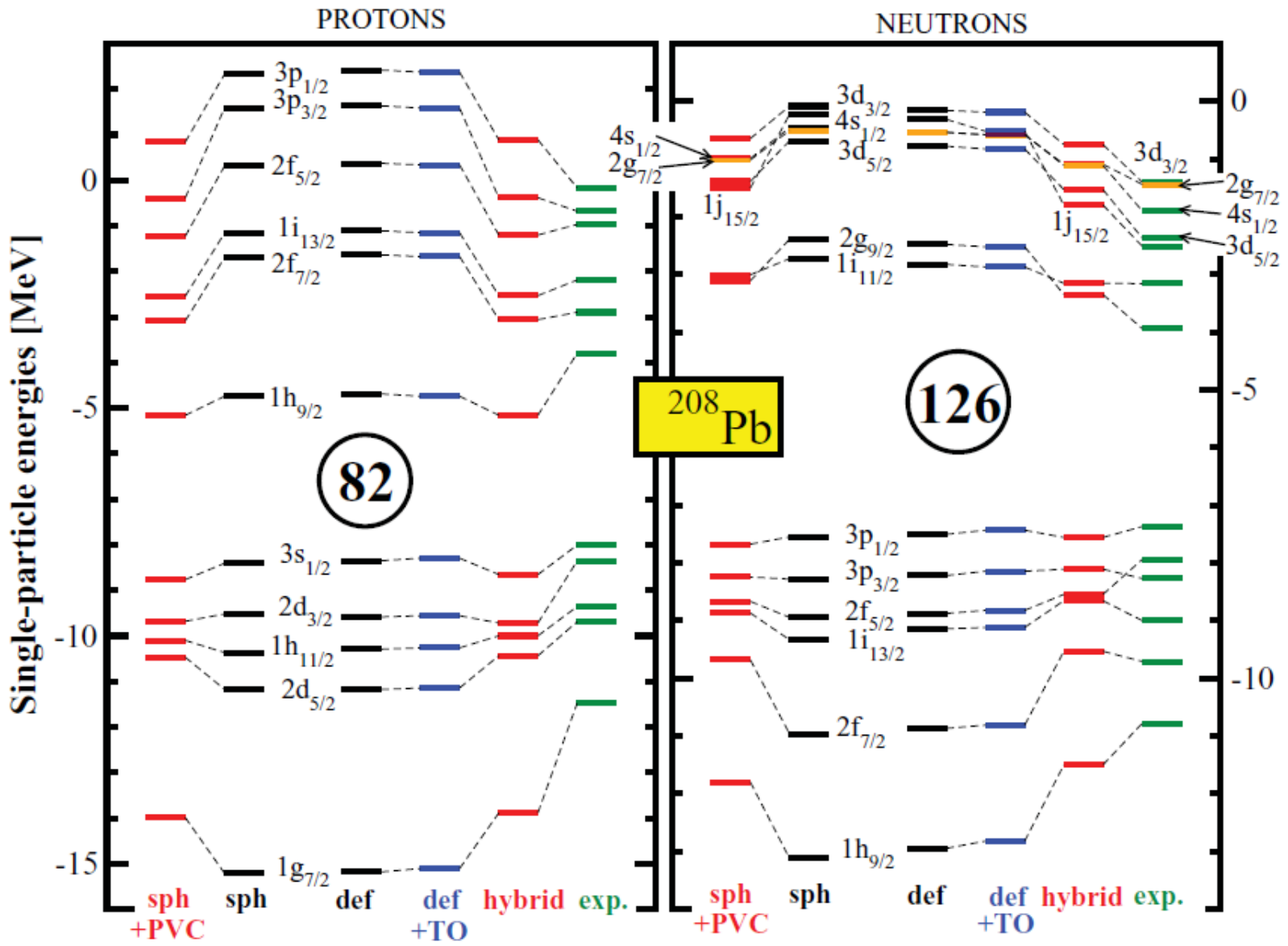

Full Skyrme (Sly5), including momentum dependent terms

Colo' et al, PRC82, 064307

The vertex is deduced from the Transition Densities obtained in RPA calculation

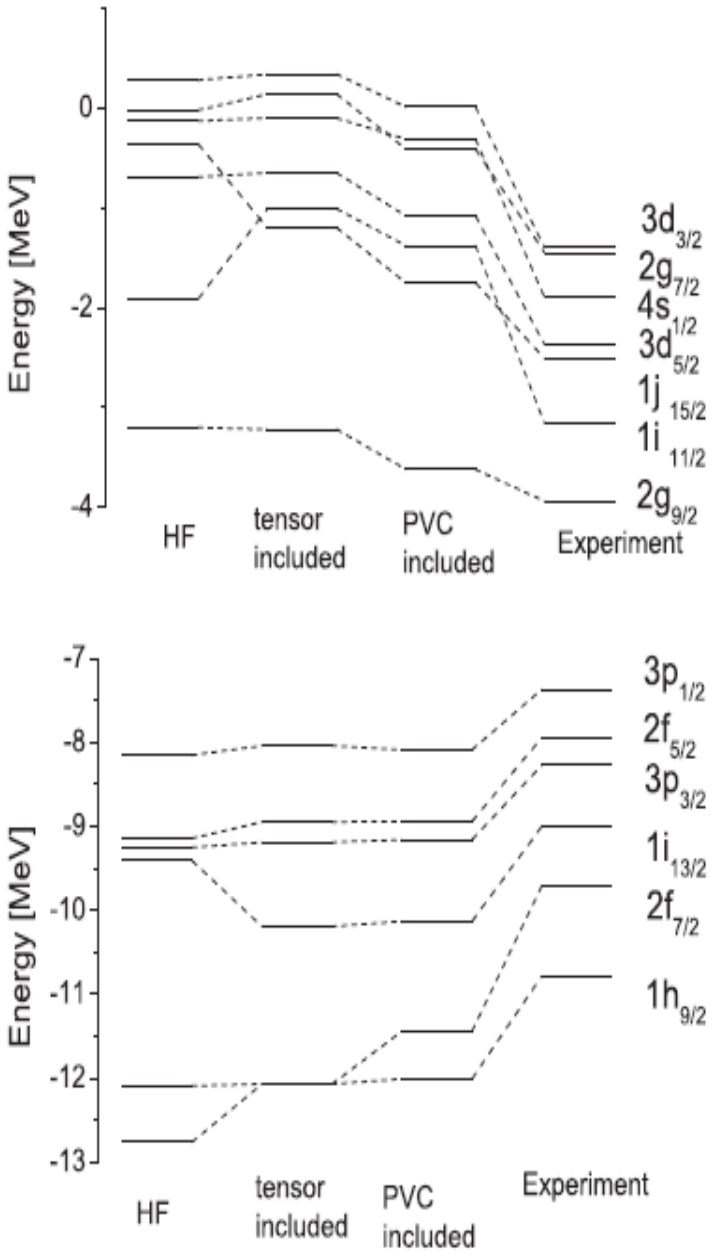

FIG. 6. The same as Fig. 5 for the neutron states in ^{208}Pb.

Similar difficulties in:

Propagation of uncertainties in the Skyrme energy-density-functional model

Y. Gao,[1] J. Dobaczewski,[1,2] M. Kortelainen,[1] J. Toivanen,[1] and D. Tarpanov[2,3]

[1] *Department of Physics, P.O. Box 35 (YFL), FI-40014 University of Jyväskylä, Finland*
[2] *Institute of Theoretical Physics, Faculty of Physics, University of Warsaw, ul. Hoża 69, PL-00-681 Warsaw, Poland*
[3] *Institute for Nuclear Research and Nuclear Energy, 1784 Sofia, Bulgaria*

(Dated: January 28, 2013)

TABLE I: The ^{208}Pb proton (top) and neutron (bottom) s.p. energies $e_{\rm HF}$ (b) and their standard errors (c), as compared to the empirical values (d) [25], residuals, $\Delta(e_{\rm HF}) = e_{\rm HF} - e_{\rm exp}$ (e), PVCs $\delta e_{\rm PVC}$ (f), and residuals of the PVC-corrected s.p. energies $\Delta(e_{\rm PVC}) = e_{\rm HF} + \delta e_{\rm PVC} - e_{\rm exp}$ (g). Where applicable, we also give the root-mean-square (rms) values of entries shown in a given column. All energies are in MeV.

orbital (a)	$e_{\rm HF}$ (b)	$\sigma(e_{\rm HF})$ (c)	$e_{\rm exp}$ (d)	$\Delta(e_{\rm HF})$ (e)	$\delta e_{\rm PVC}$ (f)	$\Delta(e_{\rm PVC})$ (g)
$\pi 3p_{1/2}$	0.219	0.181	−0.16	0.38	−0.440	−0.06
$\pi 3p_{3/2}$	−1.045	0.139	−0.68	−0.37	−0.662	−1.03
$\pi 2f_{5/2}$	−1.284	0.229	−0.97	−0.31	−0.480	−0.79
$\pi 1i_{13/2}$	−2.794	0.238	−2.10	−0.69	−0.221	−0.92
$\pi 1h_{9/2}$	−3.501	0.282	−3.80	0.30	−0.280	0.02
$\pi 2f_{7/2}$	−3.725	0.115	−2.90	−0.83	−0.284	−1.11
$\pi 3s_{1/2}$	−8.036	0.140	−8.01	−0.03	−0.108	−0.13
$\pi 2d_{3/2}$	−8.378	0.199	−8.36	−0.02	0.220	0.20
$\pi 1h_{11/2}$	−9.153	0.207	−9.36	0.21	−0.141	0.07
$\pi 2d_{5/2}$	−10.117	0.117	−9.82	−0.30	0.116	−0.18
$\pi 1g_{7/2}$	−10.908	0.229	−12.00	1.09	0.131	1.22
rms	n.a.	0.196	n.a.	0.52	0.328	0.70
$\nu 3d_{3/2}$	−1.856	0.250	−1.40	−0.46	−0.104	−0.56
$\nu 4s_{1/2}$	−2.051	0.235	−1.90	−0.15	−0.668	−0.82
$\nu 2g_{7/2}$	−2.141	0.258	−1.44	−0.70	−0.280	−0.98
$\nu 1f_{15/2}$	−2.231	0.167	−2.51	0.28	−0.226	0.05
$\nu 3d_{5/2}$	−2.549	0.166	−2.37	−0.18	−0.384	−0.56
$\nu 1i_{11/2}$	−2.680	0.223	−3.16	0.48	−0.271	0.21
$\nu 2g_{9/2}$	−4.336	0.071	−3.94	−0.40	−0.183	−0.58
$\nu 3p_{1/2}$	−7.855	0.109	−7.37	−0.49	0.152	−0.33
$\nu 3p_{3/2}$	−8.503	0.065	−8.26	−0.24	−0.119	−0.36
$\nu 2f_{5/2}$	−8.519	0.143	−7.94	−0.58	0.156	−0.42
$\nu 1i_{13/2}$	−8.603	0.162	−9.24	0.64	−0.130	0.51
$\nu 1h_{9/2}$	−9.922	0.190	−11.40	1.48	0.120	1.60
$\nu 2f_{7/2}$	−10.407	0.103	−9.81	−0.60	0.179	−0.42
rms	n.a.	0.176	n.a.	0.61	0.273	0.68

We will show mainly results obtained using the simple B&MII vertex, based on Experimental beta's

C. Phonon exchange Induced Pairing Interaction (old theory)

Barranco,Broglia,Gori,Vigezzi,Bortignon,Terasaki, PRL11(1999)

$$M^{n}_{\nu,\lambda\nu'} = \frac{\langle \nu' \| R_o \frac{\partial U}{\partial r} Y_\lambda \| \nu \rangle}{\sqrt{2j_\nu + 1}} \frac{\beta_\lambda(n)}{\sqrt{(2\lambda + 1)}} \qquad (1)$$

can be calculated. The quantities entering in the reduced matrix element appearing in Eq. (1) are the nuclear radius R_o, the derivative of the Saxon-Woods potential, and a spherical harmonic of multipolarity λ. Once these matrix elements are known, one can calculate the induced pairing interaction matrix elements (cf. inset of Fig. 1)

$$\upsilon_{\nu\nu'} = \langle (j_{\nu'} m_{\nu'})(j_{\nu'} \tilde{m}_{\nu'}) | v | (j_\nu m_\nu)(j_\nu \tilde{m}_\nu) \rangle_{\text{a.s.}}$$

$$= \sum_{\lambda n} \frac{2}{(2j_{\nu'} + 1)} \frac{2(M^{n}_{\nu,\lambda\nu'})^2}{E_o - [e_\nu + e_{\nu'} + \hbar\omega_\lambda(n)]}, \qquad (2)$$

and thus determine the state dependent BCS pairing gap [2]

$$\Delta_\nu = -\sum_{\nu'} \frac{(2j_{\nu'} + 1)}{2} \frac{\Delta_{\nu'}}{2E_{\nu'}} \upsilon_{\nu\nu'} . \qquad (3)$$

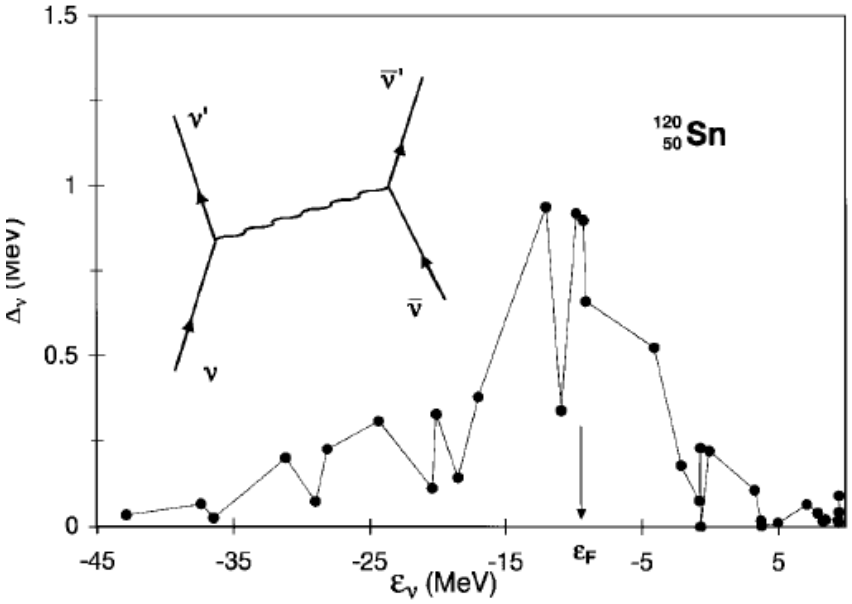

FIG. 1. State dependent pairing gap Δ_ν [cf. Eq. (3)] for the nucleus ^{120}Sn, calculated making use of the induced interaction defined in Eq. (2) (cf. inset, where particles are represented by arrowed lines and phonons by a wavy line).

Comparison between Gogny and Induced Interaction matrix elements

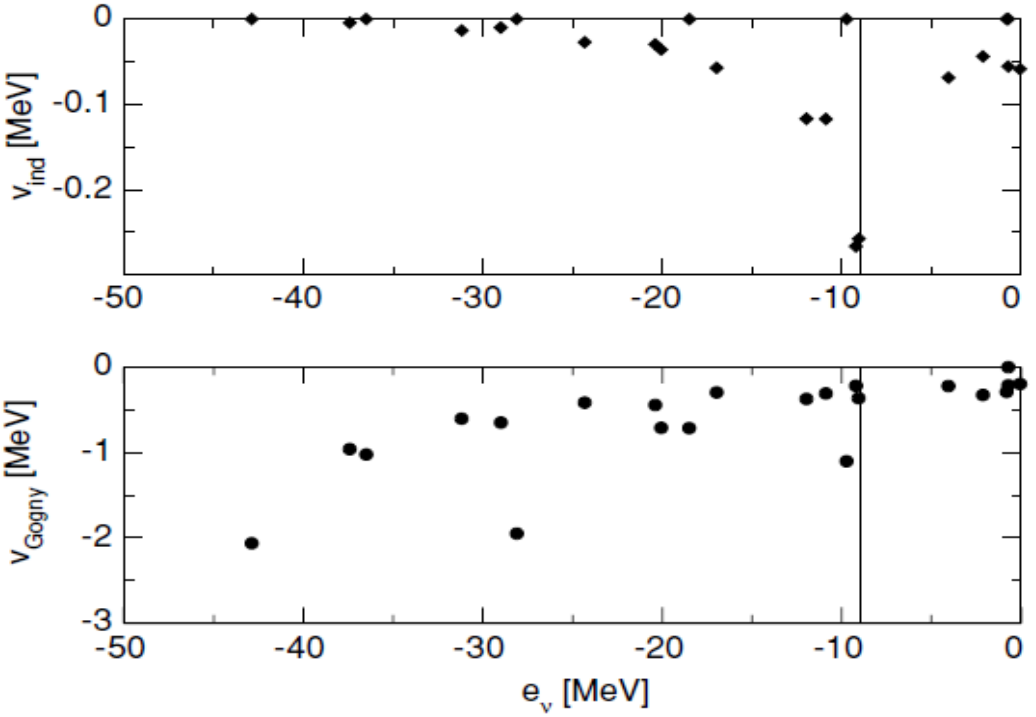

FIG. 1. The nucleus ^{120}Sn. Diagonal pairing matrix elements of the induced interaction (upper panel, solid diamonds) and of the Gogny force (lower panel, solid circles), displayed as a function of the single-particle energy, e_ν, of the state ν calculated using the bare nucleon mass and the single-particle wave functions of a Woods-Saxon potential with standard parameters (depth $V_0 = -49$ MeV, diffusivity $a = 0.65$ fm, and radius $R_0 = 6.16$ fm), including the spin-orbit term, parametrized according to Ref. [21]. Also shown by means of vertical lines is the position of the Fermi energy, $e_F = -9.1$ MeV. Note the different scale in the two figures.

Semiclassical (TF averaged) estimate of diagonal pairing matrix elements in 120Sn.

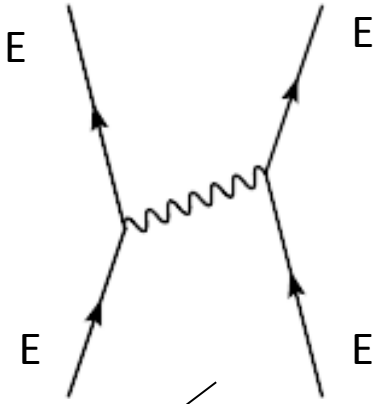

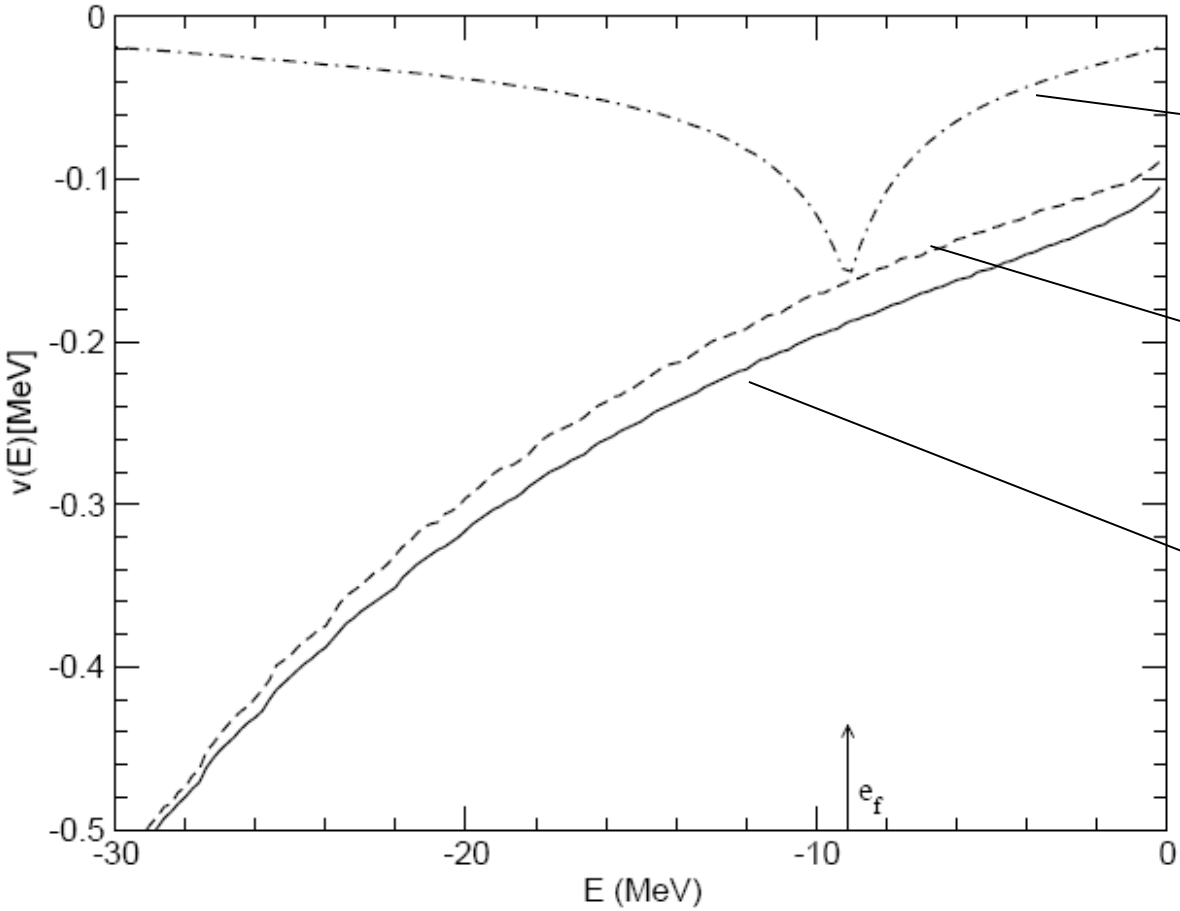

vind

vbare (vlow-k)
L=2fm**-1

vGogny

F. Barranco, P. Schuck et al., Phys. Rev. 72(2005)054314

COMBINING ARGONNE V14 AND INDUCED INTERACTION

The coupling with the phonons induces a surface-peaked interaction and pairing gap

$\Delta \approx Z(v14 + vind)\ \kappa$

A. Pastore et al., PRC 78(2008) 024315

But the pairing density k(r) is much less affected

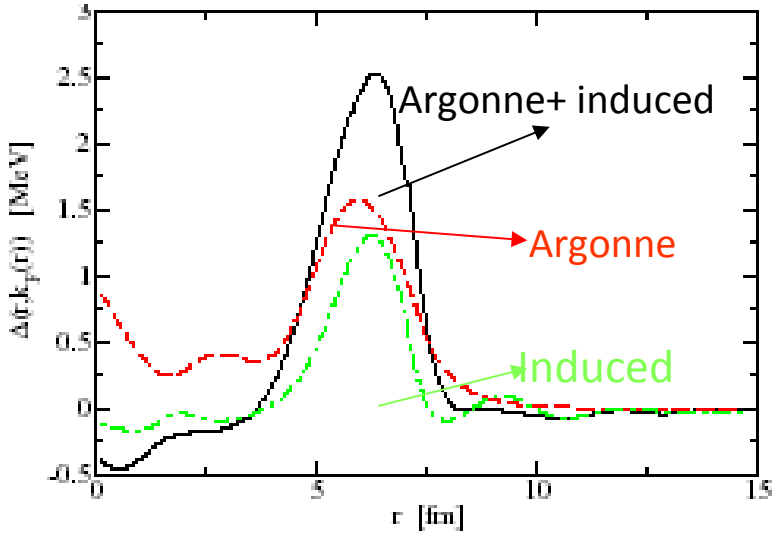

Density modes (surface): Attractive

Spin modes (volume); Repulsive !!

Equivalent DDDI parameters ***Volume Repulsive*** Interaction!!!

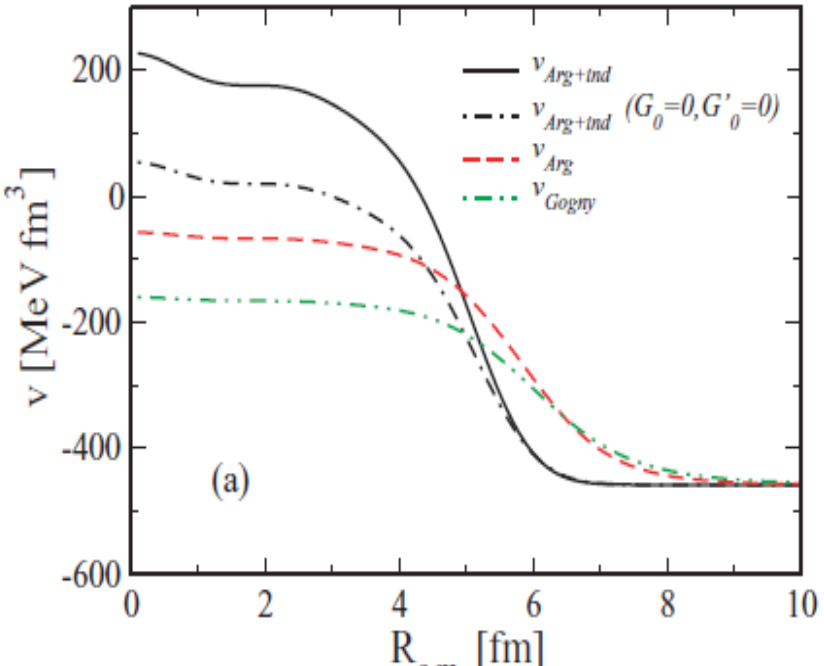

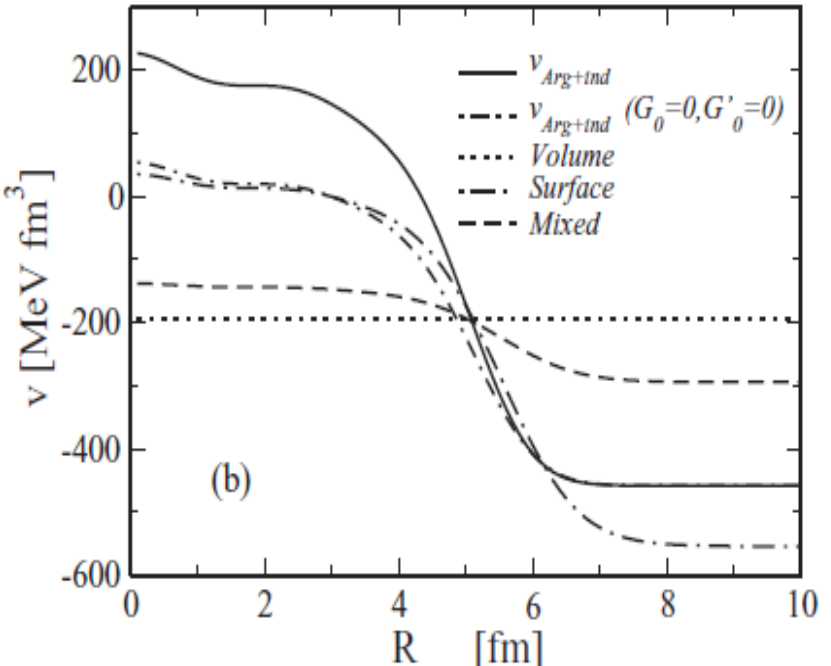

Induced Interaction in the Slab Model (Giovanardi, PRC65,041304(2002)):

Slab Model:Semi-infinte Nuclear Matter with realistic surface statical and dynamical properties (Esbensen&Bertsch Ann.Phys.(1984)

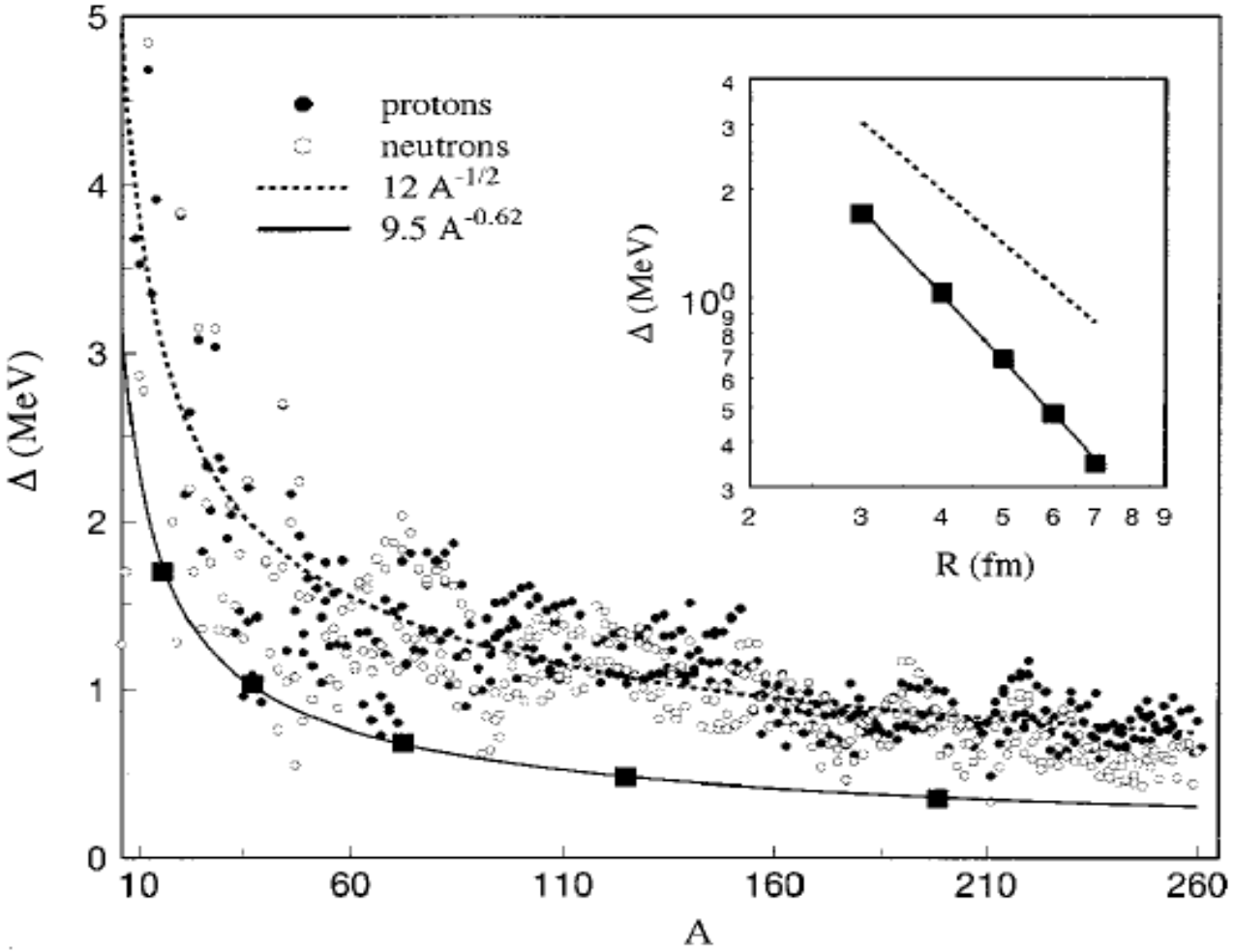

D. Microscopic description of superfluid nuclei beyond mean field:

Quasiparticle Vibration Coupling

(cf. Van der Sluys et al., NPA551(1993)210)

For each single-particle state $a = (q_a n_a l_a j_a)$ the equation-of-motion method leads to a system of linear equations of dimension $2(N+1)$ with N the dimension of the (1qp × phonon) space:

$$\begin{pmatrix} E_a & V(abJ\nu) & 0 & W(abJ\nu) \\ V(abJ\nu) & (E_{J\nu}+E_b) & W(abJ\nu) & 0 \\ 0 & W(abJ\nu) & -E_a & -V(abJ\nu) \\ W(abJ\nu) & 0 & -V(abJ\nu) & -(E_{J\nu}+E_b) \end{pmatrix} \begin{pmatrix} x_0 \\ C_{bJ\nu} \\ -y_0 \\ -D_{bJ\nu} \end{pmatrix} = \tilde{E}_a \begin{pmatrix} x_0 \\ C_{bJ\nu} \\ -y_0 \\ -D_{bJ\nu} \end{pmatrix}. \quad (23)$$

Neglecting the mutual interaction between the (1qp × phonon) states, it becomes easy to rewrite the secular equation (23) as a two-dimensional, hermitian and non-linear eigenvalue problem, by projecting onto the 1qp space:

$$\left[\begin{pmatrix} E_a & 0 \\ 0 & -E_a \end{pmatrix} + \begin{pmatrix} \Sigma_{11}(E) & \Sigma_{12}(E) \\ \Sigma_{12}(E) & \Sigma_{22}(E) \end{pmatrix} \right] \begin{pmatrix} x_0 \\ y_0 \end{pmatrix} = E \begin{pmatrix} x_0 \\ y_0 \end{pmatrix}. \quad (24)$$

The energy-dependent self-energy matrix elements $\Sigma_{ij}(E)$ stand for:

$$\Sigma_{11}(E) = \sum_{bJ\nu} \left(\frac{|V(abJ\nu)|^2}{E-(E_b+E_{J\nu})} + \frac{|W(abJ\nu)|^2}{E+(E_b+E_{J\nu})} \right),$$

$$\Sigma_{22}(E) = \sum_{bJ\nu} \left(\frac{|W(abJ\nu)|^2}{E-(E_b+E_{J\nu})} + \frac{|V(abJ\nu)|^2}{E+(E_b+E_{J\nu})} \right),$$

$$\Sigma_{12}(E) = -\sum_{bJ\nu} V(abJ\nu)\, W(abJ\nu) \left(\frac{1}{E-(E_b+E_{J\nu})} - \frac{1}{E+(E_b+E_{J\nu})} \right). \quad (25)$$

Correcting HFB/BCS Quasiparticles:
2 steps in calculating pairing properties

USED FORMALISM

(Idini, Barranco,Vigezzi,PRC85,014331(2012))

$$\begin{pmatrix} E_a + \Sigma_{11}(\tilde{E}_{a(n)}) & \Sigma_{12}(\tilde{E}_{a(n)}) \\ \Sigma_{12}(\tilde{E}_{a(n)}) & -E_a + \Sigma_{22}(\tilde{E}_{a(n)}) \end{pmatrix} \begin{pmatrix} x_{a(n)} \\ y_{a(n)} \end{pmatrix} = \tilde{E}_{a(n)} \begin{pmatrix} x_{a(n)} \\ y_{a(n)} \end{pmatrix} \quad (10)$$

where one has introduced the normal and abnormal self-energies $\Sigma_{11}(E)$ (being $\Sigma_{22}(E) = -\Sigma_{11}(-E)$) and $\Sigma_{12}(E)$, given by

$$\Sigma_{11} = \sum_{b,m,J,\nu} \frac{V^2(a(n)b(m)J\nu)}{\tilde{E}_{a(n)} - \tilde{E}_{b(m)} - \hbar\omega_{J\nu}} + \sum_{b,m,J,\nu} \frac{W^2(a(n)b(m)J\nu)}{\tilde{E}_{a(n)} + \tilde{E}_{b(m)} + \hbar\omega_{J\nu}} \quad (11)$$

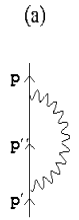

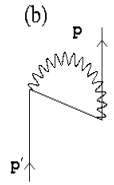

and

$$\Sigma_{12} = \Sigma^{pho}_{12} + \Sigma^{bare}_{12}$$

$$\Sigma^{pho}_{12} = -\sum_{b,m,J,\nu} V(a(n),b(m),J,\nu)W(a(n),b(m),J,\nu) \left[\frac{1}{\tilde{E}_a(n) - \tilde{E}_b(m) - \hbar\omega_{J,\nu}} - \frac{1}{E_a(n) + \tilde{E}_b(m) + \hbar\omega_{J,\nu}}\right].$$

$$\Sigma^{bare}_{12} = \pm \sum_{b,n} V_{bare}(a,b) \frac{(2j_b+1)}{2} \tilde{u}_{b(n)} \tilde{v}_{b(n)}.$$

Optional: 1 or 2 steps?

$V(jj'\lambda) = \beta\lambda(2\lambda+1)^{-1/2}\langle j||Ro\ dU/dr\ Y\lambda||j'\rangle\ (uj\ \tilde{u}j' - vj\ vj')\ (2j+1)^{-1/2}$

$W(jj'\lambda) = \beta\lambda(2\lambda+1)^{-1/2}\langle j||Ro\ dU/dr\ Y\lambda||j'\rangle\ (uj\ vj' + vj\ \tilde{u}j')\ (2j+1)^{-1/2}$

BCS-like rewriting

$$\begin{pmatrix} (\epsilon_{a(n)}-e_F)+\Sigma_{11}(a,E_{a(n)}) & \Sigma_{12}(a,E_{a(n)}) \\ \Sigma_{12}(a,E_{a(n)}) & -(\epsilon_{a(n)}-e_F)+\Sigma_{22}(a,E_{a(n)}) \end{pmatrix} \begin{pmatrix} u_{a(n)} \\ v_{a(n)} \end{pmatrix} = E_{a(n)} \begin{pmatrix} u_{a(n)} \\ v_{a(n)} \end{pmatrix}$$

multiply by $Z_{a(n)}=\left(1-\frac{\Sigma_{odd}(a,E_{a(n)})}{E_{a(n)}}\right)^{-1}$

$$\begin{pmatrix} (e_{a(n)}-e_F) & \Delta(a,E_{a(n)}) \\ \Delta(a,E_{a(n)}) & -(e_{a(n)}-e_F) \end{pmatrix} \begin{pmatrix} u_{a(n)} \\ v_{a(n)} \end{pmatrix} = E_{a(n)} \begin{pmatrix} u_{a(n)} \\ v_{a(n)} \end{pmatrix}$$

new single-particle energies

$$e_{a(n)}-e_F=Z_{a(n)}[(\epsilon_a-e_F)+\Sigma_{even}(a,E_{a(n)})]$$

effective gap

$$\Delta_{a(n)}=Z_{a(n)}(\Sigma_{12}^{bare}+\Sigma_{12}^{pho})\equiv\frac{2E_{a(n)}u_{a(n)}v_{a(n)}}{u_{a(n)}^2+v_{a(n)}^2}$$

where

$$\begin{cases} \Sigma_{odd}(a,E_{a(n)})=\dfrac{\Sigma_{11}(a,E_{a(n)})-\Sigma_{11}(a,-E_{a(n)})}{2} \\ \Sigma_{even}(a,E_{a(n)})=\dfrac{\Sigma_{11}(a,E_{a(n)})+\Sigma_{11}(a,-E_{a(n)})}{2} \end{cases}$$

Since self-energies are energy dependent many solutions are obtained: n=1,2,..
Each carrying a quasi-particle strength $u(a,n)^2+v(a,n)^2<1$
Closure requires Σ_n $u(a,n)^2+v(a,n)^2=1$

A generalized gap equation. Different versions

Expressing u*v as a function of sigma12, and reintroducing them in the sigma12 expression, a close expression for sigma is obtained

$$\Delta_{a(n)} = -Z_{a(n)} \sum_{b(m)} V_{eff}(a(n),b(m)) N_{b(m)} \frac{\Sigma_{12}(b(m),E_{b(m)})}{2\sqrt{(\epsilon_b - e_F + \Sigma_{even}(b(m),E_{b(m)}))^2 + \Sigma_{12}^2(b(m),E_{b(m)})}}$$

c.f.Baldo

where N is the proper quasi-particle normalization:

$$N_{b(m)} = \tilde{u}_{b(m)}^2 + \tilde{v}_{b(m)}^2 = \left(1 - \frac{\partial \Sigma_{11}(a,E_{a(n)})}{\partial E_{a(n)}} u_{b(m)}^2 - \frac{\partial \Sigma_{22}(a,E_{a(n)})}{\partial E_{a(n)}} v_{b(m)}^2 - 2\frac{\partial \Sigma_{12}(a,E_{a(n)})}{\partial E_{a(n)}} u_{b(m)} v_{b(m)}\right)^{-1} < 1$$

which gives the properly normalized u,v's starting from the normalized to 1 u,v's,

and where the effective interaction is

$$V_{eff}(a(n),b(m)) = V_{bare}(a,b) + \sum_{J,\nu} h^2(a,b,J,\nu)\left(\frac{1}{E_{an} - E_{bm} - \hbar\omega_{J,\nu}} - \frac{1}{E_{an} + E_{bm} + \hbar\omega_{J,\nu}}\right)$$

Reintroducing the Zb-factor

$$\Delta_{a(n)} = -Z_{a(n)} \sum_{b(m)} V_{eff}(a(n),b(m)) N_{b(m)} \frac{Z_{b(m)} \Sigma_{12}(b(m),E_{b(m)})}{2\sqrt{Z_{b(m)}^2 (\epsilon_b - e_F + \Sigma_{even}(b(m),E_{b(m)}))^2 + Z_{b(m)}^2 \Sigma_{12}^2(b(m),E_{b(m)})}}$$

$$\Delta_{a(n)} = -\sum_{b(m)} V_{eff}(a(n),b(m)) \frac{Z_{a(n)} \Delta_{b(m)} N_{b(m)}}{2\sqrt{(e_b - e_F)^2 + \Delta_{b(m)}^2}}$$

$$\Delta_{a(n)} = -\sum_{b(m)} V_{eff}(a(n),b(m)) \frac{Z_{a(n)} \Delta_{b(m)} N_{b(m)}}{2E_{b(m)}}$$

Generalized Gap Equation (schematic)

Z=1 free Fermi gas

Z<1 correlated Fermi system

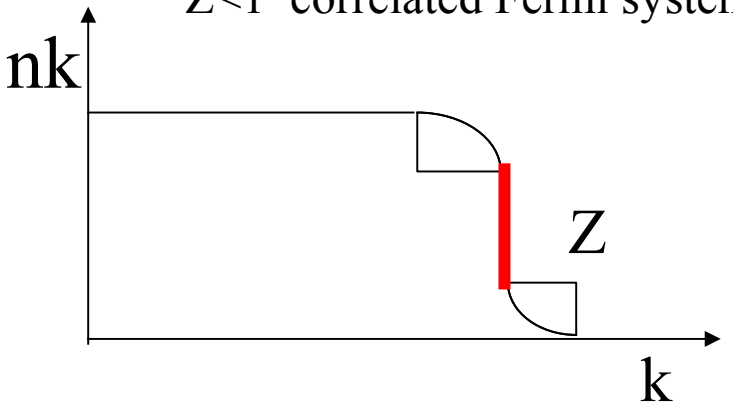

Quasiparticle strength <1

Bare+Induced interaction

$$\Delta_p = -\frac{1}{2}\int d^3p' \frac{Z_p V_{pp'} Z_{p'}}{\sqrt{(\tilde{\varepsilon}_{p'} - \varepsilon_F)^2 + \Delta_{p'}^2}} \Delta_{p'}$$

Renormalized s.p. energy

RENORMALIZING Argonne (on Sly4) pairing gaps
(2 steps calculation)

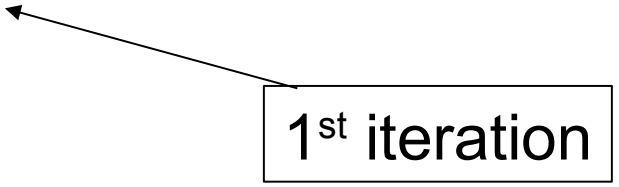

Experimental phonons were used for the density modes L=2,3,4,5
Spin modes not included in this results

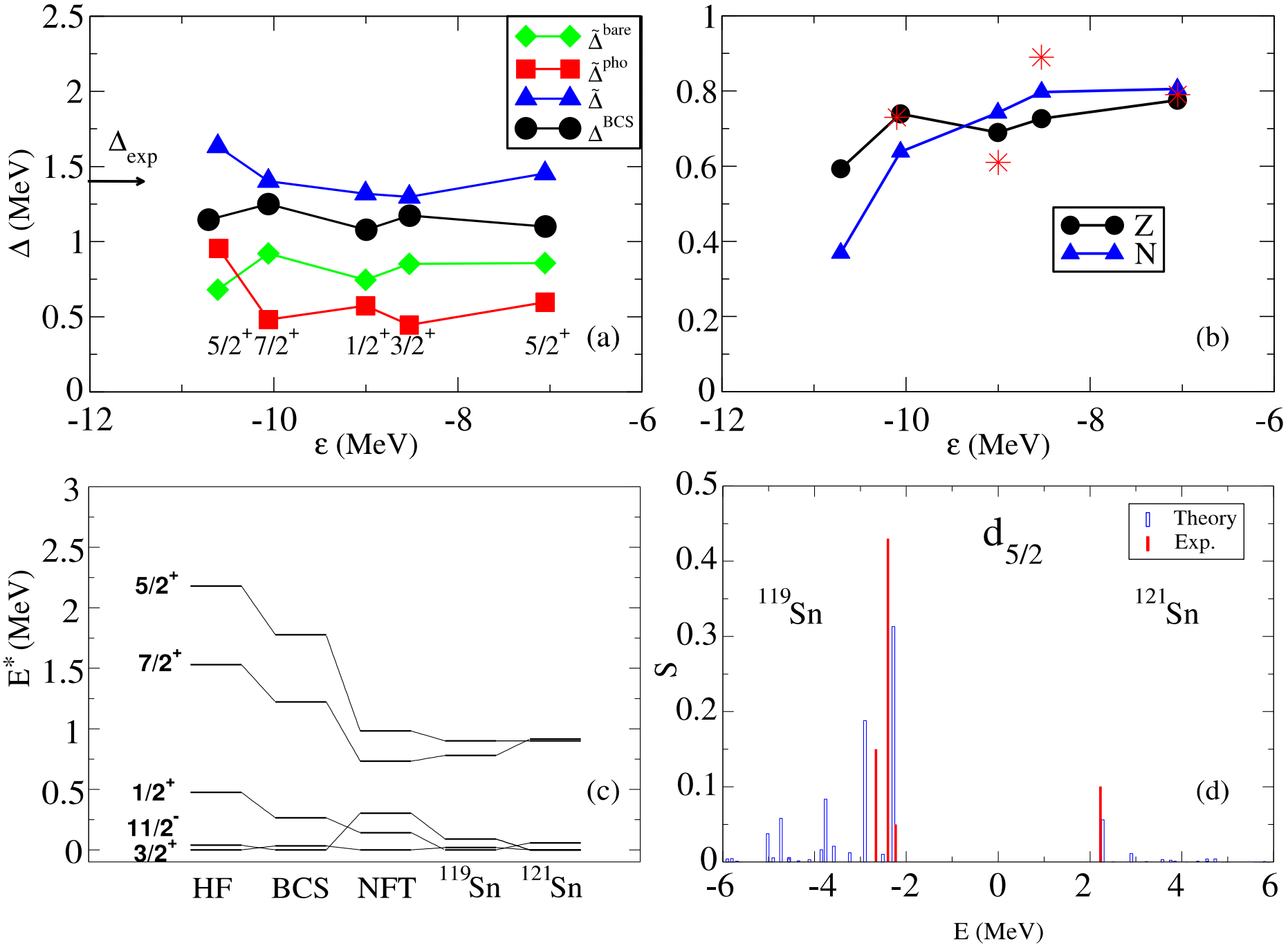
Δ (MeV)
ε (MeV)
Δ_exp
Δ̃^bare
Δ̃^pho
Δ̃
Δ^BCS
5/2+ 7/2+
1/2+ 3/2+
5/2+
(a)
Z
N
(b)
E* (MeV)
5/2+
7/2+
1/2+
11/2-
3/2+
HF
BCS
NFT
119Sn
121Sn
(c)
S
d5/2
Theory
Exp.
119Sn
121Sn
(d)
E (MeV)

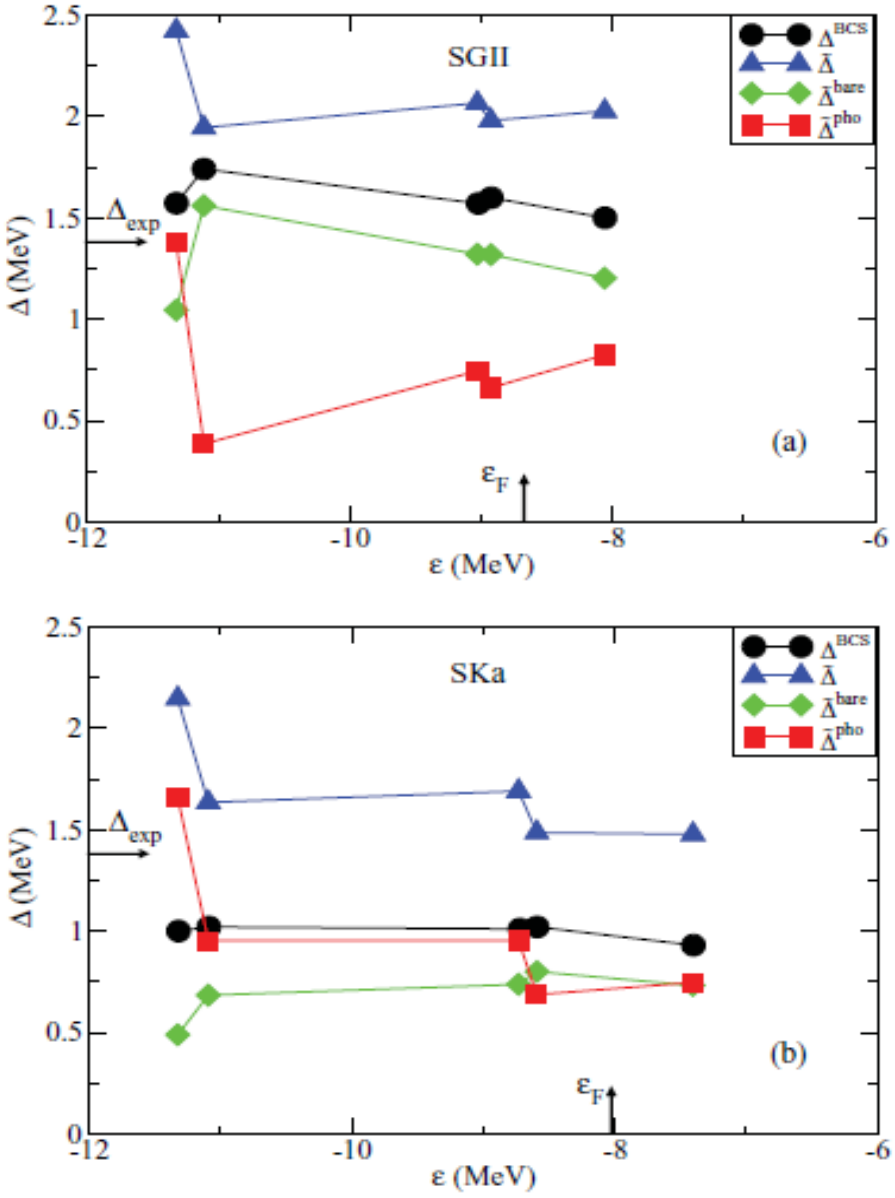

FIG. 17. (Color online) The state-dependent pairing gap Δ^{BCS} calculated in BCS with the bare v_{14} interaction is compared to the renormalized gap $\tilde{\Delta}$ [cf. Eq. (38)] obtained solving the Nambu-Gor'kov equations. We compare results obtained with a mean field

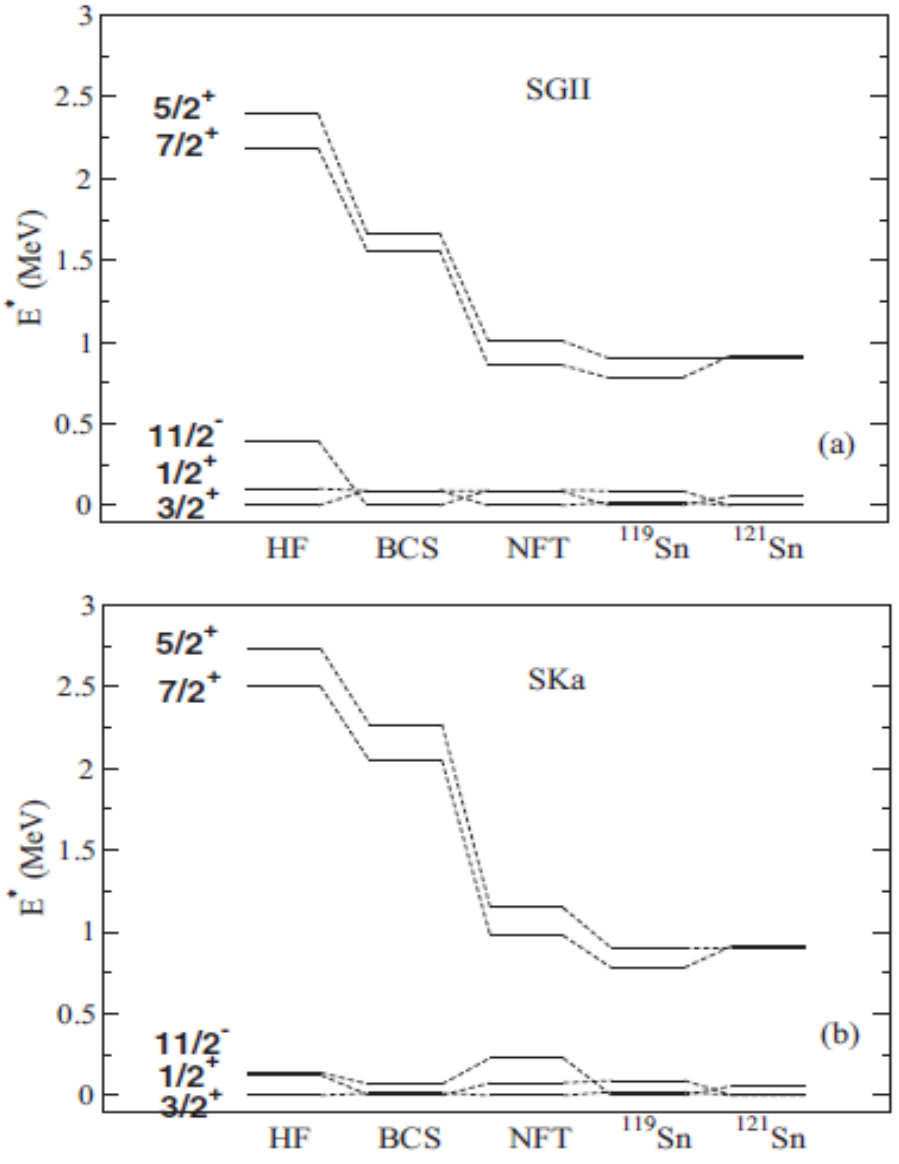

FIG. 18. The theoretical quasiparticle spectra obtained at the various steps of the calculation are compared to the experimental data. We compare results obtained with a mean field produced with the SGII interaction (a) and with the SKa interaction (b) (cf. Fig. 8 for the corresponding calculation with the SLy4 mean field).

Compare 1 and 2 step calculations
Using a simple monopole pairing force

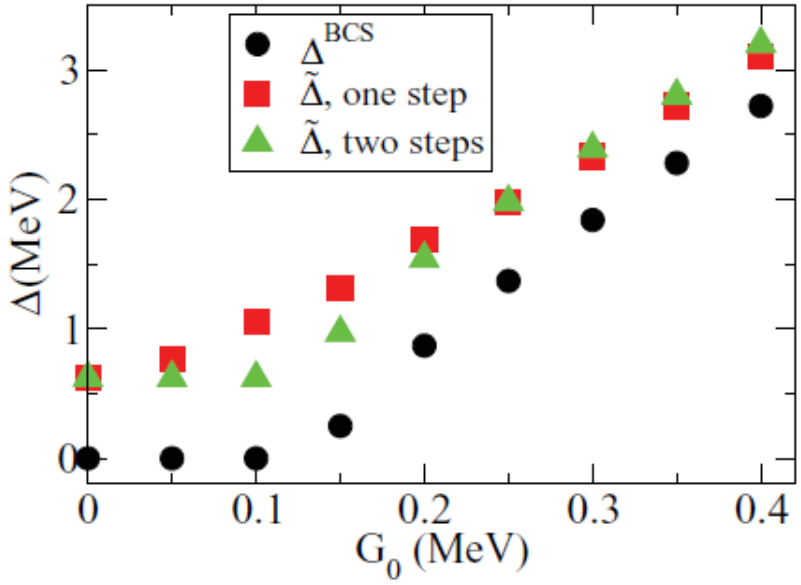

FIG. 26. (Color online) Renormalized gaps $\tilde{\Delta}$ obtained solving the Nambu Gor'kov equations in the one-step and the two-steps diagonalization schemes with the monopole pairing force as a function of the pairing constant G_0, averaged over the five valence orbitals. Also shown is the gap Δ^{BCS} obtained solving the BCS equation.

Full basis formulation,
A.Idini,Ph.D. Thesis,Milano 2013

Allows correcting r-dependence

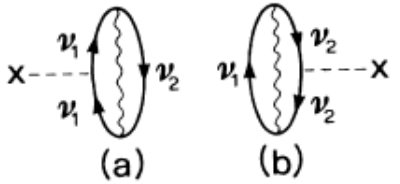

Barranco,Broglia,PRL29(1987)

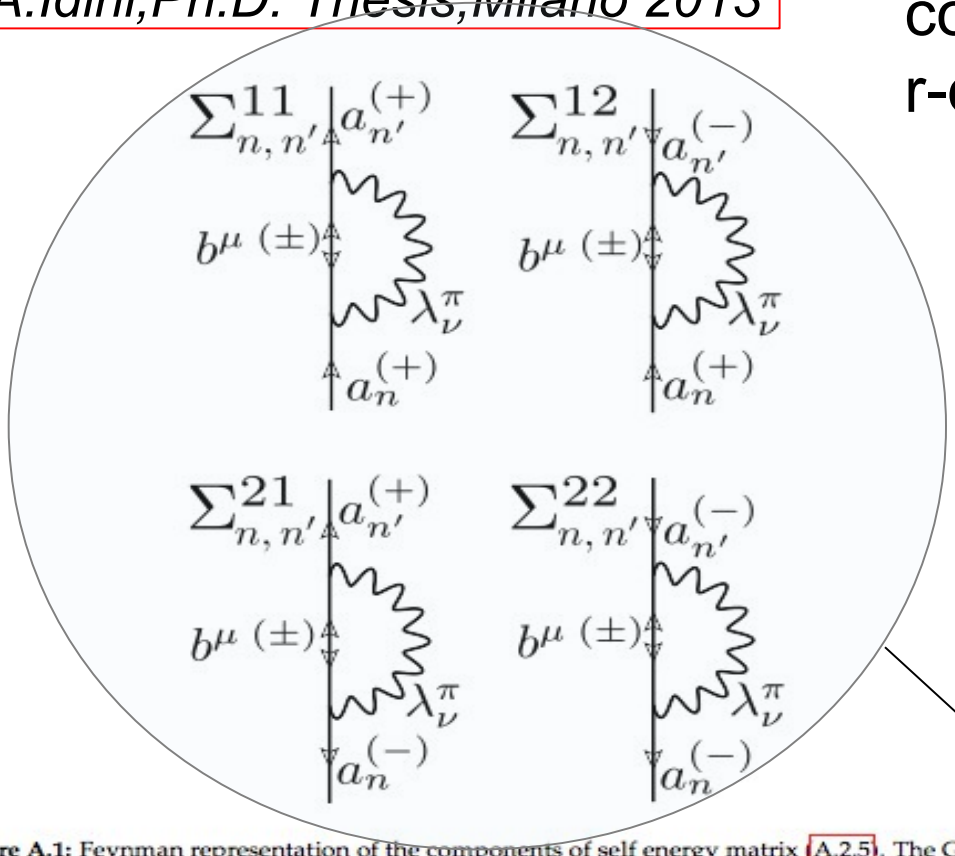

Figure A.1: Feynman representation of the components of self energy matrix (A.2.5). The Green's functions lines with the empty arrow represent respectively the positive and negative quasiparticle eigenvalue $^{(\pm)}$ of the basis (A.1.14)-(A.1.15).

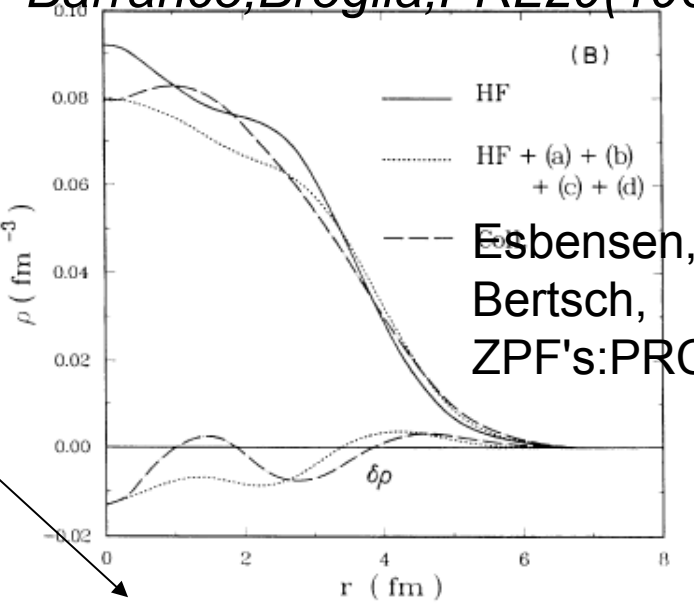

Esbensen, Bertsch, ZPF's:PRC28

$$\begin{pmatrix} -(\hat{T}+\hat{V}-\lambda)_{hh} & \hat{\Delta}^{t}_{ph} & -\Delta_{hh} & -(\hat{T}+\hat{V}-\lambda)_{hp} \\ \hat{\Delta}_{ph} & (\hat{T}+\hat{V}-\lambda)_{pp} & -(\hat{T}+\hat{V}-\lambda)_{ph} & \hat{\Delta}_{pp} \\ -\hat{\Delta}_{hh} & -(\hat{T}+\hat{V}-\lambda)_{hp} & (\hat{T}+\hat{V}-\lambda)_{hh} & -\hat{\Delta}_{hp} \\ -(\hat{T}+\hat{V}-\lambda)_{ph} & \hat{\Delta}^{t}_{pp} & -\Delta^{t}_{hp} & -(\hat{T}+\hat{V}-\lambda)_{pp} \end{pmatrix} + \begin{pmatrix} \Sigma^{11}_{hh} & \Sigma^{11}_{hp} & \Sigma^{12}_{hh} & \Sigma^{12}_{hp} \\ \Sigma^{11}_{ph} & \Sigma^{11}_{pp} & \Sigma^{12}_{ph} & \Sigma^{12}_{pp} \\ \Sigma^{21}_{hh} & \Sigma^{21}_{hp} & \Sigma^{22}_{hh} & \Sigma^{22}_{hp} \\ \Sigma^{21}_{ph} & \Sigma^{21}_{pp} & \Sigma^{22}_{ph} & \Sigma^{22}_{pp} \end{pmatrix}$$

Application to 10Li and 11Be: Talk by E. Vigezzi

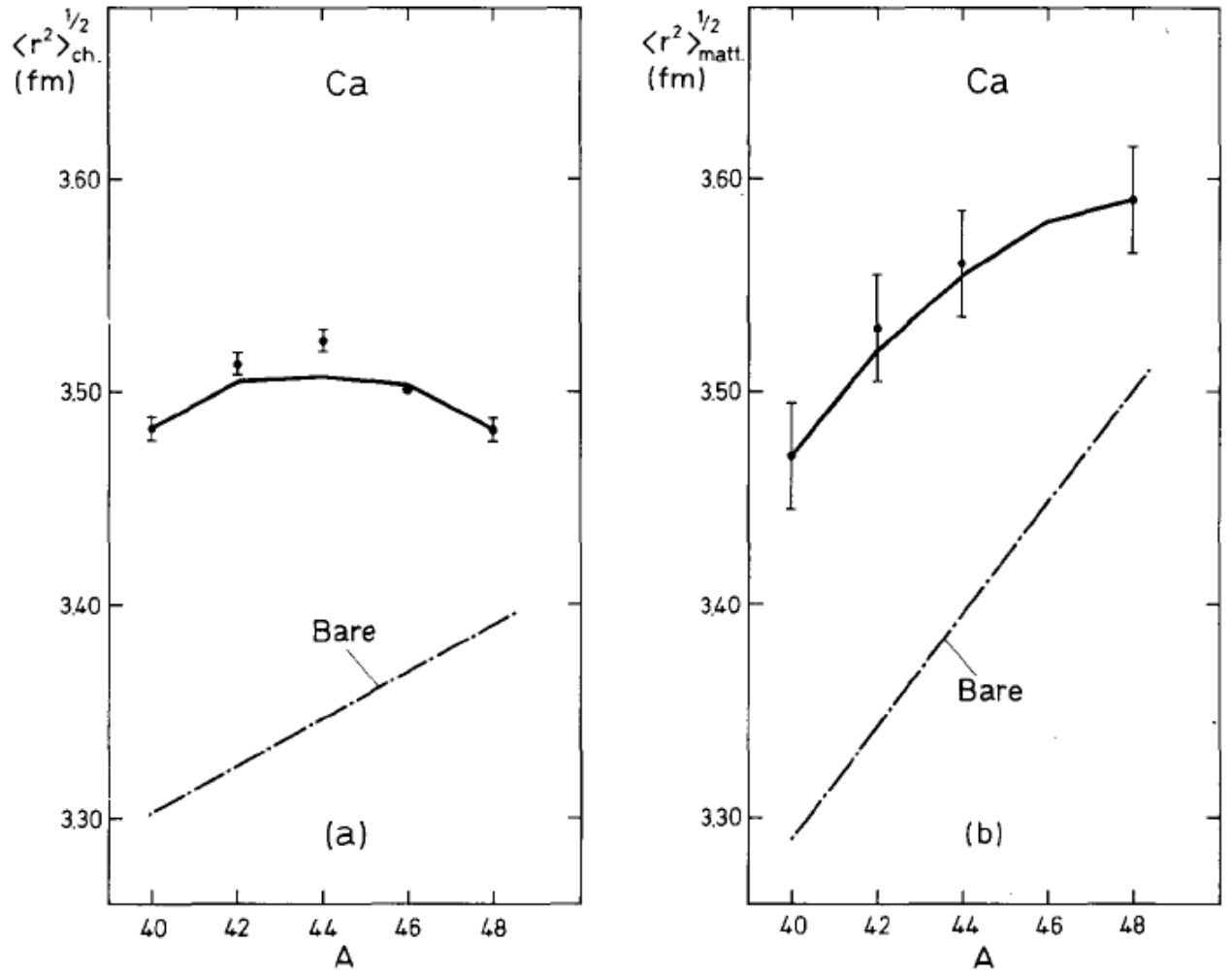

Fig. 1. Mean square radius of the Ca isotopes. In (a) the charge mean square radius is displayed as a function of the mass number [25–27]. The quantity $(\langle r^2 \rangle_0^{1/2})_{ch}$ was assumed to have a linear dependence with A. Its slope was fitted by requiring that the quantity (1) coincides with the experimental values for ^{40}Ca and ^{48}Ca making use of the values of $\Delta\sigma^2$ calculated through eqs. (2)–(4). These values are collected in table 1. The resulting values of $\langle r^2 \rangle_{ch}$ are displayed as a full drawn curve. In (b) the mass mean square radius is displayed [27]. The quantity $(\langle r^2 \rangle_0^{1/2})_{matt}$ was given an $A^{1/3}$ dependence, and its coefficient adjusted to get the best fit when use is made of eq. (1) and the quantities $\Delta\sigma^2$ (cf. table 1). The corresponding results are shown with a solid curve. The resulting bare mean square radius is $(\langle r^2 \rangle_0^{1/2})_{matt} = A^{1/3}\, 0.96$ fm.

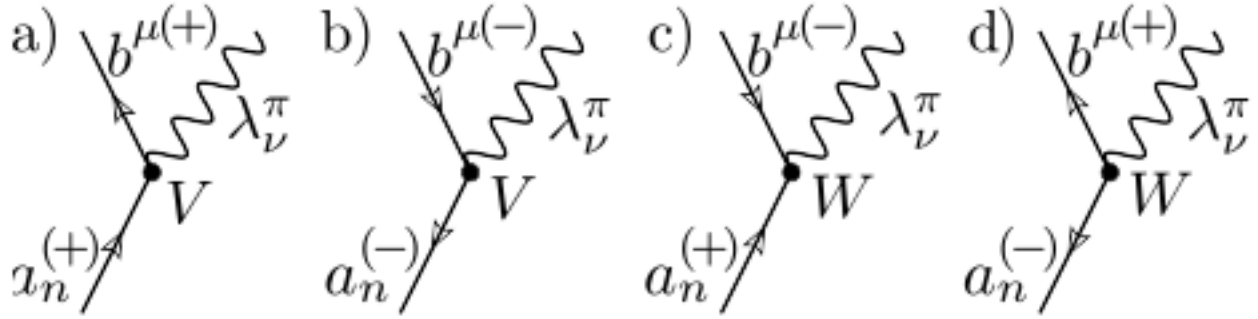

Figure A.2: Feynman representation of V and W vertices (A.2.8)-(A.2.11) for the case of particle a represented in the quasiparticle basis (A.1.14)-(A.1.15) $^{(\pm)}$ scattering into quasiparticle $b^{(\pm)}_{\mu}$ and a phonon λ^{π}_{ν}.

$$
\begin{aligned}
V(p_k^{(+)}, b^{\mu(+)}, \lambda_\nu^\pi) \equiv & \langle p_k^{(+)} | \hat{V_{res}} | b^{\mu(+)} \lambda_\nu^\pi \rangle = -\langle p_k^{(-)} | \hat{V_{res}} | b^{\mu(-)} \lambda_\nu^\pi \rangle \\
= & \langle 0 | a_{p_k} \hat{V_{res}} \alpha^\dagger_{b^\mu} \Gamma_{\lambda_\nu^\pi} | 0 \rangle = \langle 0 | a_{p_k} \hat{V} (\sum_l \widetilde{u}_{b^\mu,l} a^\dagger_{b_l} + \widetilde{v}_{b^\mu,l} a_{b_l}) \Gamma_{\lambda_\nu^\pi} | 0 \rangle \\
= & \sum_l (f+g)(p_k, b_l, \lambda_\nu^\pi) \widetilde{u}_{b^\mu,l} \qquad \text{cf. Fig. A.2(a)} \qquad (A.2.8) \\
V(h_k^{(+)}, b^{\mu(+)}, \lambda_\nu^\pi) \equiv & \langle h_k^{(+)} | \hat{V_{res}} | b^{\mu(+)} \lambda_\nu^\pi \rangle = -\langle h_k^{(-)} | \hat{V_{res}} | b^{\mu(-)} \lambda_\nu^\pi \rangle \\
= & \sum_l -\widetilde{v}_{b^\mu,l} (f-g)(h_k, b_l, \lambda_\nu^\pi) \qquad \text{cf. Fig. A.2(b),} \qquad (A.2.9) \\
W(p_k^{(+)}, b^{\mu(-)}, \lambda_\nu^\pi) \equiv & \langle p_k^{(+)} | \hat{V_{res}} | b^{\mu(-)} \lambda_\nu^\pi \rangle = \langle p_k^{(-)} | \hat{V_{res}} | b^{\mu(+)} \lambda_\nu^\pi \rangle \\
= & \sum_l \widetilde{v}_{b^\mu,l} (f-g)(p_k, b_l, \lambda_\nu^\pi) \qquad \text{cf. Fig. A.2(c),} \qquad (A.2.10) \\
W(h_k^{(+)}, b^{\mu(-)}, \lambda_\nu^\pi) \equiv & \langle h_k^{(+)} | \hat{V_{res}} | b^{\mu(-)} \lambda_n^\pi \rangle = \langle h_k^{(-)} | \hat{V_{res}} | b^{\mu(+)} \lambda_n^\pi \rangle \\
= & \sum_l \widetilde{u}_{b^\mu,l} (f+g)(h_k, b_l, \lambda_\nu^\pi) \qquad \text{cf. Fig. A.2(d).} \qquad (A.2.11)
\end{aligned}
$$

Similar developments (Soma,et.al,PRC87,011303(13)

Self-energy expansion

TECHNISCHE UNIVERSITÄT DARMSTADT

- Gorkov equations ⟶ energy *dependent* eigenvalue problem

$$\sum_b \begin{pmatrix} t_{ab} - \mu_{ab} + \Sigma^{11}_{ab}(\omega) & \Sigma^{12}_{ab}(\omega) \\ \Sigma^{21}_{ab}(\omega) & -t_{ab} + \mu_{ab} + \Sigma^{22}_{ab}(\omega) \end{pmatrix} \Bigg|_{\omega_k} \begin{pmatrix} \mathcal{U}^k_b \\ \mathcal{V}^k_b \end{pmatrix} = \omega_k \begin{pmatrix} \mathcal{U}^k_a \\ \mathcal{V}^k_a \end{pmatrix}$$

Ab Initio, and HF side, 2nd order

- 1st order ➟ energy-independent self-energy

$\Sigma^{11\,(1)}_{ab} =$ 

$\Sigma^{12\,(1)}_{ab} =$ 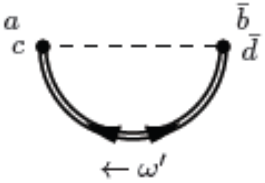

- 2nd order ➟ energy-dependent self-energy

$\Sigma^{11\,(2)}_{ab}(\omega) =$ 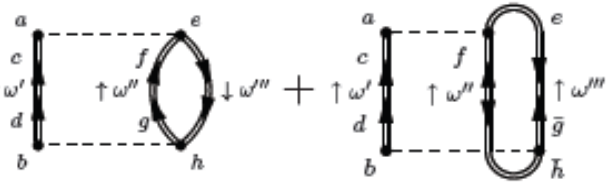

$\Sigma^{12\,(2)}_{ab}(\omega) =$ 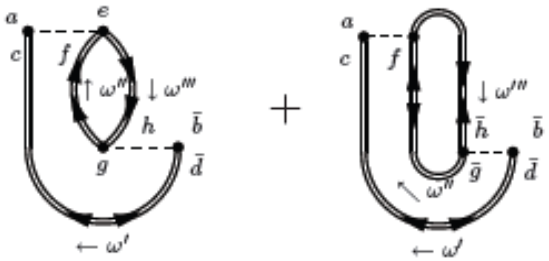

Scaling of Gorkov's problem

TECHNISCHE UNIVERSITÄT DARMSTADT

- Transformed into an energy *independent* eigenvalue problem

$$\begin{pmatrix} T-\mu+\Lambda & \tilde{h} & \mathcal{C} & -\mathcal{D}^\dagger \\ \tilde{h}^\dagger & -T+\mu-\Lambda & -\mathcal{D}^\dagger & \mathcal{C} \\ \mathcal{C}^\dagger & -\mathcal{D} & E & 0 \\ -\mathcal{D} & \mathcal{C}^\dagger & 0 & -E \end{pmatrix} \begin{pmatrix} \mathcal{U}^k \\ \mathcal{V}^k \\ \mathcal{W}_k \\ \mathcal{Z}_k \end{pmatrix} = \omega_k \begin{pmatrix} \mathcal{U}^k \\ \mathcal{V}^k \\ \mathcal{W}_k \\ \mathcal{Z}_k \end{pmatrix}$$

- Numerical scaling

$$m_{p,1} \approx \binom{N_b}{3} \propto \frac{N_b^3}{6}$$

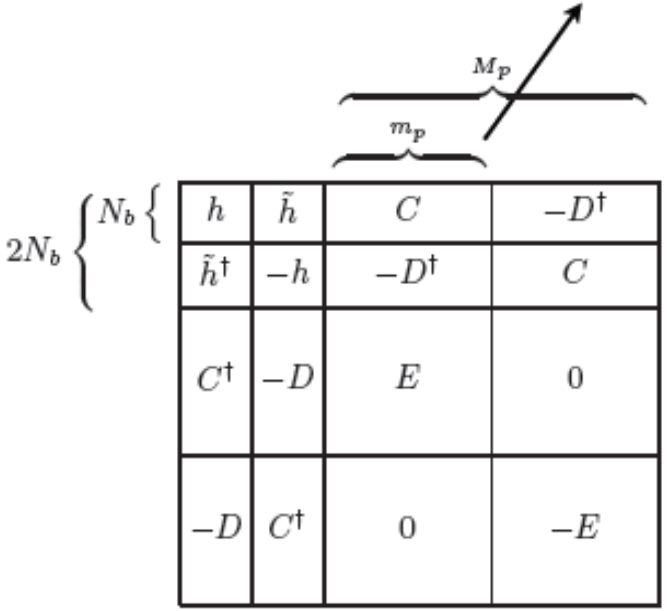

N_b → dimension of the s.p. basis

n → number of iterations

$$N_{tot,1} = 2N_b + M_{p,1} \approx N_b^3$$

$$\dots$$

$$N_{tot,n} = 2N_b + M_{p,n} \approx N_b^{3n}$$

Pairing gaps

TECHNISCHE UNIVERSITÄT DARMSTADT

- Three-point mass differences

$$\Delta_n^{(3)}(A) = \frac{(-1)^A}{2}[E_0^{A+1} - 2\,E_0^A + E_0^{A-1}]$$

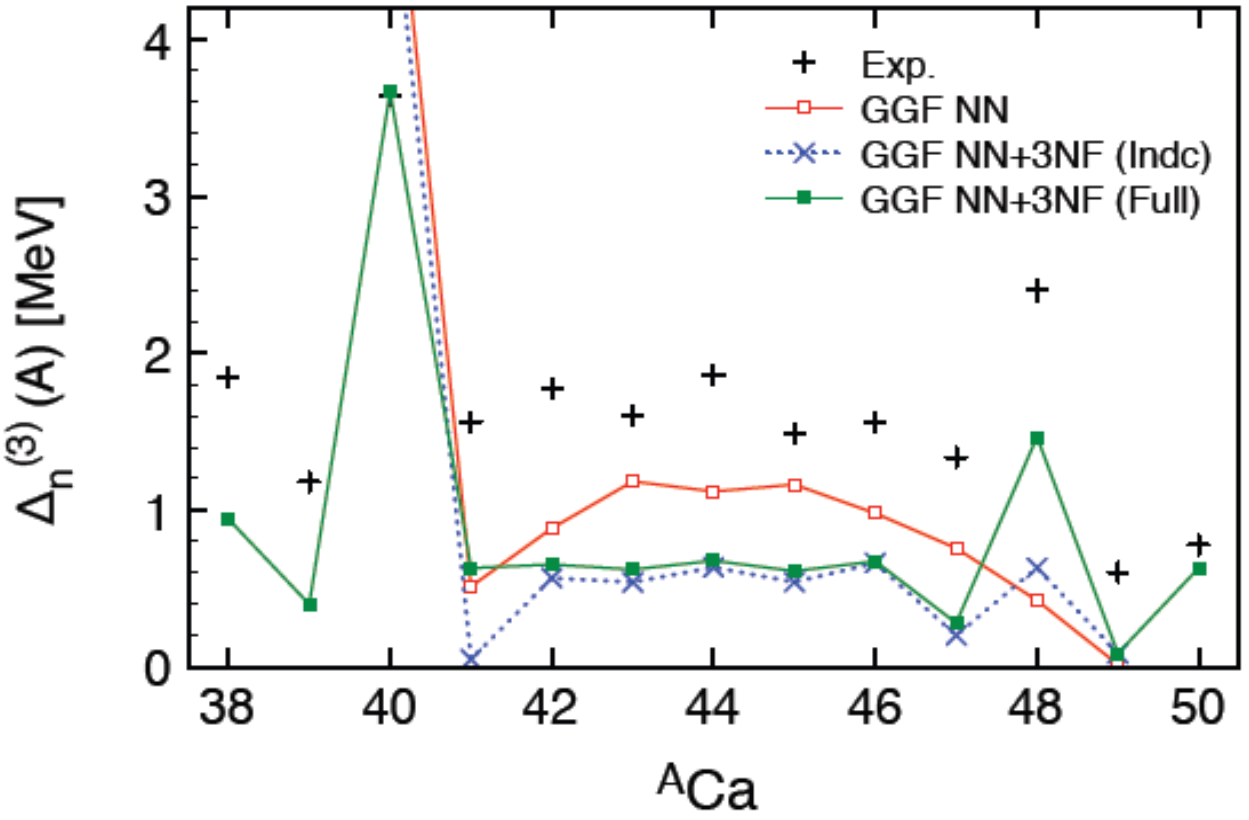

Shell Model Calculations

Holt, Menendez,Schwenk, arXiv1304.0434

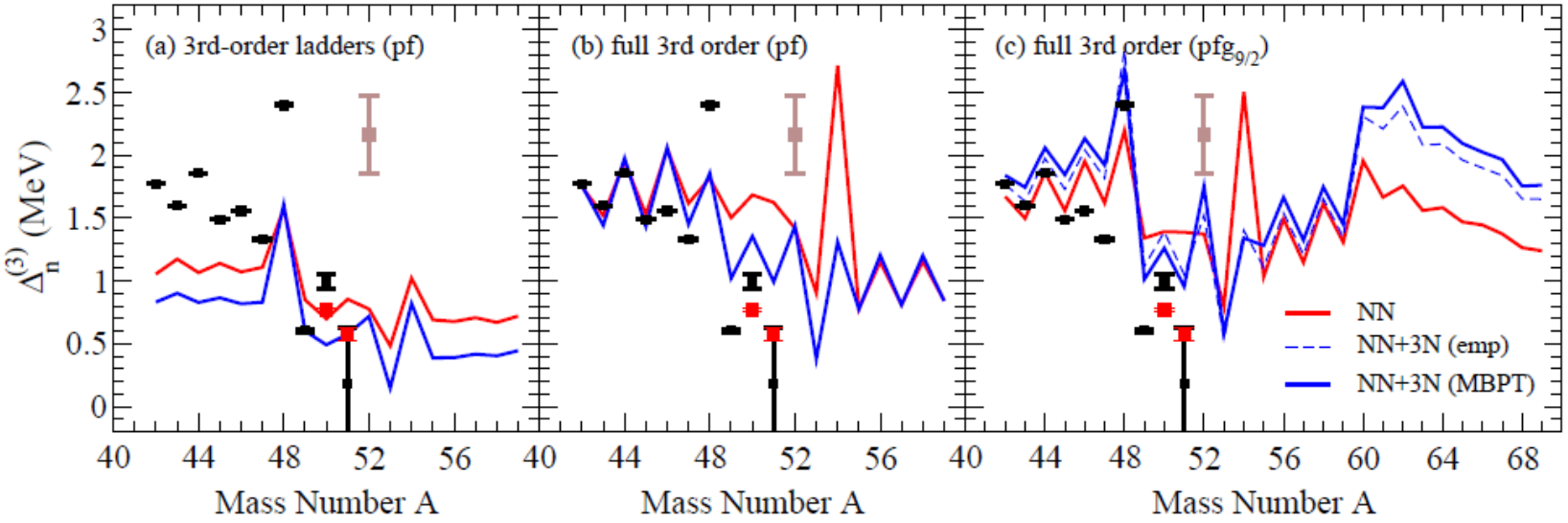

FIG. 3. (Color online) Three-point mass differences $\Delta_n^{(3)}$ in the calcium isotopes calculated to third order in MBPT with and without the leading chiral 3N forces, and in comparison with experiment [24, 67]. The legend is as in Fig. 1. Panel (a) shows the results of the third-order ladder contributions. Panels (b) and (c) include all MBPT diagrams to third order in the pf-shell and the extended $pfg_{9/2}$ valence space, respectively. The results in the pf-shell are with empirical SPEs. For the $pfg_{9/2}$ space, we show pairing gaps for both the MBPT and empirical SPEs.

When particle-hole contributions are included in a full third-order calculation, we find in Fig. 3 a clear improvement compared to including only ladder diagrams. In the pf-shell, the three-point mass differences are increased, leading to reasonable agreement with experimental data. This clearly demonstrates the importance of particle-hole many-body processes, such as core-polarization, on pairing in nuclei. Our results show that they can provide the missing pairing strength required to reproduce experiment on top of the direct NN+3N interactions. Analogously, the systematic differences between theoretical and experimental pairing gaps found in the EDF approach of Ref. [15] may be attributed to these effects.

Fadeev RPA,
Barbieri,Dickhoff;PRC63,034313(2001)

C. BARBIERI AND B. K. JENNINGS PRC72,014613(2005)

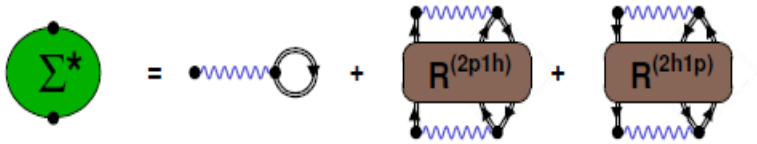

FIG. 1. (Color online) Feynman diagrams representation of the self energy. The first diagram on the right-hand side represents the Hartree-Fock–like contribution to the mean field. The remaining ones describe core polarization effects in the particle (2p1h) and hole (2h1p) part of the spectrum.

Combines
i)particle,
ii)ph-RPA and
iii)pp(hh)-RPA
consistently

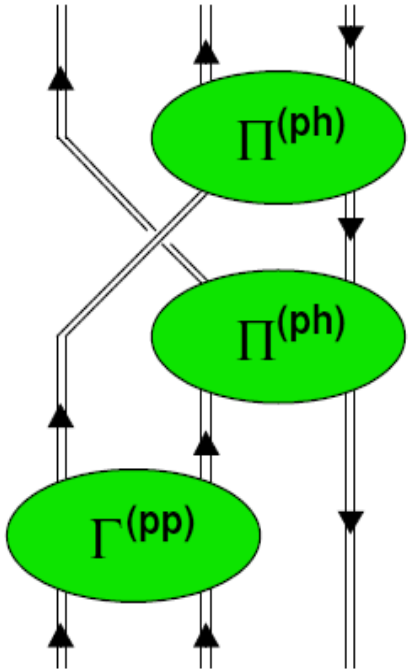

FIG. 2. (Color online) Example of a diagrammatic contribution included in the Faddeev expansion for $R^{(2p1h)}$ (see Fig. 1). A quasiparticle is coupled to the response function $\Pi^{(ph)}$ that describes the target nucleus. It can also participate in pairing processes, which are accounted for by the two-body propagator $g^{II,(pp)}$.

CONCLUSIONS

a. At mean field level surface pairing interaction prefered.
Bare Argonne tractable as pairing interaction.

b. Phonon Exchange Pairing Induced Interaction very
surface peaked. In volumen could be repulsive due
to spin modes.
Strong A-dependence from the Slab Model.

c. Close connection to self-energy effects from
Dyson Gorkov's eqs.: Quasi-particle Phonon Coupling:
Fragmentation and Dense Espectra<=> Induced Pairing Int.
Bare Argonne plus Induced Pairing good description of data.

d. Shell Model confirms relevance of surface phonons mediated
pairing interaction.

e. Multishell Self-energy: Full HFB renormalization.
Ab Initio calculations in progress (2^{nd} order).